Jørgen Tonning Buch

Control and Optimization of Ventilation in Zero Emission Buildings using IoT

June 2021

Master's thesis

Master's thesis

2021

Jørgen Tonning Buch

◼ NTNU
Norwegian University of
Science and Technology

NTNU
Norwegian University of
Science and Technology

Control and Optimization of Ventilation in Zero Emission Buildings using IoT

Jørgen Tonning Buch

Master Thesis

For

Student Jørgen Tonning Buch

Spring 2021

Control and Optimization of Ventilation in Zero Emission Buildings Using IoT

Regulering og optimalisering av ventilasjon i nullutslippsbygninger ved bruk av IoT

Background and objective

To obtain a zero emission building (ZEB), it is essential to reduce the energy use to a minimum. Demand controlled ventilation (DCV) is a widespread method to control the supply of fresh air and reduce energy use. Though seldom used in Norway, recirculation of exhaust air is a measure that can support energy savings for heating and, in some outdoor environments, be a protective measure from outdoor pollutants.

In previous work, students tested Arduino-based sensors and Raspberry Pi and used them to measure indoor air quality, mainly in classrooms. In this thesis, further work shall be completed to facilitate so that the sensors can be implemented in a DCV system in the laboratory.

The goal of this master thesis is to develop simulation models to test control strategies for DCV prepared for further testing in the laboratory. The simulations shall be based on the facility that is to be constructed in the laboratory. Another aim for this thesis work is to plan the construction of the facilities used in the laboratory.

The work is a continuation of previous project work conducted by the student.

The student will add to the work being developed on the Ph.D. work of Maria Justo Alonso. This Ph.D. is part of the Research Centre on Zero Emission Neighbourhoods in Smart Cities.

The following tasks are to be considered:

1. Conduct a literature review related to indoor air quality, demand controlled ventilation, control using low cost sensors, and new progress related to the project.

2. Evaluate modifications to be done in the laboratory setup and measurement technology.

3. Develop and plan a ventilation system that can be used to test DCV control strategies.

4. Development and investigation of control strategies for DCV.

Abbreviations

AHU	Air Handling Unit
CAV	Constant Air Volume
DCV	Demand Controlled Ventilation
DR	Draught Rate
FHI	The Norwegian Institute of Public Health
HCHO	Formaldehyde
IAQ	Indoor Air Quality
IEQ	Indoor Environmental Quality
LCS	Low Cost Sensors
MOx	Metal Oxide Sensors
NDIR	Non-Dispersive Infrared
OAF	Outdoor Air Fraction
PAQ	Perceived Air Quality
PM	Particulate Matter
PMV	Predicted Mean Vote
PPD	Predicted Percentage of Dissatisfied
RH	Relative Humidity
SBS	Sick Building Syndrome
SFP	Specific Fan Power
SPR	Static Pressure Reset
TVOC	Total Volatile Organic Compounds
VAV	Variable Air Volume
VOC	Volatile Organic Compounds
WHO	World Health Organization
ZEB	Zero Emission Building

Acknowledgement

This thesis is the culmination of the two-year master's program in Energy and Environmental Engineering at the Norwegian University of Science and Technology, NTNU. The work conducted extends over the last semester of the master's program. This thesis is a continuation of the project work, "Control and Optimization of Ventilation using Iot: A preliminary study" conducted in the previous semester.

I want to extend my sincere gratitude to my supervisors Hans Martin Mathisen and Maria Justo Alonso, for their guidance and support throughout this thesis and the last year of my studies. I would also like to thank all parties involved in constructing the full-scale model in the laboratory. Even though the DCV system could not be finalized in time to perform measurements, the construction phase in the laboratory helped shape this thesis.

Abstract

Ventilation accounts for a large amount of energy use in buildings. A large amount of a building's total energy consumption is related to heating, cooling, and ventilation. Demand Controlled Ventilation (DCV) can be used as means to achieve more energy-efficient buildings. In context with the progress surrounding DCV, low-cost Indoor Air Quality (IAQ) sensors are a subject of investigation. Low-cost sensors have shown improvement in the sensor's performance compared to recognized IAQ sensors and their relevance in controlling ventilation. This thesis further explores the possibilities of using low-cost IAQ sensors to control a DCV system based on IAQ measurements.

To facilitate the investigation of DCV control strategies, a provisional office area supplied with a DCV system was planned. The planned office area determined the framework for simulations. The simulation program CONTAM was used to compare the impact on IAQ and energy consumption for different DCV control strategies. Indoor air concentration of CO_2 or Formaldehyde (HCHO) or a combination of CO_2 and HCHO was the basis for the proposed DCV control cases. Five control cases were investigated and compared. In addition to supply air control, the CONTAM simulations contain an investigation of three control algorithms for recirculation of extract air. Indoor air concentration of HCHO, indoor air concentration of HCHO and CO_2, and indoor air concentration of particulate matter are the basis of the three recirculation controls.

Combining the DCV control strategies with the recirculation controls investigated in this thesis did not show promising results. The intent of implementing recirculation control was to lower the overall energy use. Simulations show that implementing recirculation control based on the same parameters as the supply airflow control did not work. The recirculation controls ended up being unstable and contradictory in terms of saving energy and achieving better IAQ.

The simulations in CONTAM show that ventilation controlled by the indoor concentration of CO_2 can keep HCHO below the recommended indoor threshold limit during working hours. But, pending on the base ventilation rate and pollutant generation rate, the level of HCHO exceeds the threshold limit outside working hours. The CONTAM simulation shows that a combined HCHO and CO_2 DCV control strategy prevents accumulation of HCHO and achieves better IAQ. Compared to Constant Air Volume (CAV), the DCV controls investigated will save energy related to heating and operation of fans. The DCV control based on CO_2 and HCHO saved a total of 31 % energy compared to CAV for the simulated week. Based on these results, the combined CO_2 and HCHO control is recommended for further investigation in the laboratory.

Sammendrag

En stor del av det totale energiforbruket i bygg kan knyttes til ventilasjon og bygningsklimatisering. Behovsstyrt ventilasjon (DCV) kan benyttes som et tiltak for å senke det totale energiforbruket. Som et ledd i utviklingen av DCV, har lav-kostnads sensorer som måler ulike inneklimaparametere blitt ett fokusområde. Både med tanke på muligheter til å måle inneklima sammenliknet med anerkjente sensorer, og hvorvidt de kan benyttes til å styre DCV. Denne oppgaven ser videre på muligheten til å benytte lav-kostnads sensorer til å kontrollere ventilasjon på bakgrunn av målinger av forskjellige inneklimaparametere.

For å tilrettelegge for videre testing av DCV strategier, ble et provisorisk kontorområde planlagt og påbegynt bygget i laboratoriet. Dette innebar prosjektering av et DCV anlegg samt selve byggingen av kontorområdet. Det planlagte kontorområdet i laboratoriet satte rammeverket for simuleringer som er gjennomført i CONTAM. CONTAM ble brukt til å undersøke innvirkningen til DCV på luftkvalitet og energiforbruk. Denne oppgaven tar for seg forskjellige kontrollstrategier for DCV basert på målinger av CO_2 og HCHO. Totalt ble fem DCV strategier analysert og sammenliknet gjennom simuleringer. I tillegg ble tre kontrollstrategier for styring av omluft undersøkt. De tre kontrollstrategiene for omluft er basert på målinger av CO_2, en kombinert løsning med måling av CO_2 og HCHO, og målinger av $PM_{2.5}$.

Implementering av omluft viste seg å være vanskelig uten å forstyrre kontrollen av tilluft. Siden reguleringen av omluft og tilluft er styrt av samme parametere, konkurrerer dem om autoritet. Dermed ble reguleringen ukontrollerbar. Med de forutsetninger som er satt i denne oppgaven, kan ikke omluftstyring anbefales som et ledd i å senke energiforbruket eller øke luftkvalitet.

Simuleringene viser at DCV kontrollert av CO_2 holder nivået av HCHO under anbefalte grenseverdier i arbeidstiden. Men, om emisjonsraten er for høy, kan HCHO akkumuleres og stige over anbefalte grenseverdier utenfor arbeidstid. Simuleringene viser at ventilasjon styrt av CO_2 og HCHO hindrer akkumuleringen av HCHO og sikrer bedre inneklima. Estimering av energiforbruk tilknyttet oppvarming og viftedrift viser stort potensiale til å spare energi sammenliknet med CAV. DCV styrt av CO_2 og HCHO sparer opp mot 31 % av energiforbruket sammenliknet med CAV for den simulerte uken. Basert på disse resultatene anbefales DCV styrt av CO_2 og HCHO for videre undersøkelser i laboratoriet.

Contents

List of Figures

List of Tables

Chapter 1

Introduction

1.1 Background

Overall strategies to monitor and collect data connected to the indoor climate quality are important issues to improve high-energy performance buildings (Stefano Paolo Corgnati 2011). In Norway, almost 40% of the energy consumption is related to buildings. Therefore, building more energy-efficient buildings is one of the most profitable measures to reduce greenhouse gases (*OM ZEB* n.d.). Lowering energy consumption in buildings is critical to fulfill the Paris agreement of being climate neutral by 2100. Even though the heating of buildings only accounts for 1,9% of the greenhouse gas emissions in Norway, further reducing greenhouse gas emissions should be a measure to strive for more energy-efficient buildings (Miljødirektoratet n.d.).

An increase in the ventilation system's performance may play a significant part in lowering the overall energy consumption (Jing et al. 2020). DCV can reduce the energy use for ventilation. Studies show the potential to save up to 70% compared to CAV (Krajčík et al. 2016). DCV completed correctly may reduce energy consumption while maintaining satisfactory IAQ. Therefore, good IAQ sensors are essential to get correct measurements as a basis for the control of the ventilation.

There has been significant progress on low-cost sensors that can monitor the IAQ. However, studies have shown variations in the performance of low-cost sensors, and there is room for further studies on long-term stability (Chojer et al. 2020). Studies show the possibilities of implementing low-cost sensors in ventilation systems to monitor and control the IAQ (Chiesa et al. 2019).

1.2 Scope and limitations

The work conducted in this thesis is the first step towards developing a strategy for DCV with the use of low-sensors assessed in previous work. The tasks to be considered in this master thesis were planned to be assessed in the laboratory. However, the construction of the full-scale model in the laboratory was delayed and could not be finalized in time. Due to the delays, it was not possible to conduct measurements to test the sensor's performance when coupled to a DCV system. Therefore, the scope for this thesis had to be altered.

This thesis aims to answer the tasks by developing control strategies for the specific DCV system under construction in the laboratory. These control strategies are to be investigated by simulations instead of measurements. Due to time limitations because the scope of the thesis had to be altered. The work conducted in this thesis is delimited to represent the full-scale laboratory model.

1.3 Research questions

The following research questions should be answered in this thesis.

- How are other pollutants affected when the DCV system is controlled based on CO2 concentration?

- How do formaldehyde perform compared to CO_2 in terms of controlling a DCV system?

- Will implementation of recirculation control save energy for heating of the supply air while achieving sufficient IAQ?

- Are CONTAM simulations adequate to investigate the impact of DCV?

- How do the proposed DCV control strategies perform compared to CAV in terms of energy use?

1.4 Previous work

This master thesis is a continuation of previous work conducted by Gram (Gram 2019) and Jørgensen (Jørgensen 2020) in addition to the preliminary project work performed by the author as a preparation towards this master thesis (Buch 2020). Since this thesis is a direct continuation of the project work, parts of the theory and literature review conducted in the project are adopted and used.

Low-cost Arduino sensors used for IAQ measurements have been assessed in previous work. The assessments of the Arduino sensor boards have been conducted by field testing in controlled environments in the laboratory and several schools in the Trondheim area. The previous work has shown some limitations for the low-cost sensors. However, they are deemed adequate for further implementation in a DCV system, with the end goal of using the sensors to control the ventilation.

Chapter 2

Theory and literature review

This chapter gives an overview of the relevant theory that sets the foundation for this thesis. The chapter revolves around the subjects of IAQ and DCV. The chapter is somehow limited to the relevant pollutants measured by the Arduino sensors in use. Some parts of this chapter are based on and gathered from the project work (Buch 2020).

2.1 Indoor Air Quality

IAQ can be defined as " an indicator of the types and amounts of pollutants in the air that might cause discomfort or risk of adverse effects on human or animal health, or damage to vegetation." (Stefano Paolo Corgnati 2011). Indoor air pollution is considered the second-highest killer globally and combined with the fact that people spend up to 90% of their time indoors (Ram 2019). Facilitating good IAQ is an essential aspect of people's general health.

IAQ has an impact on the Indoor Environmental Quality (IEQ). The main topics affecting the IEQ are IAQ and indoor pollutant source control, thermal comfort, lighting comfort, and acoustic comfort. The IAQ can be controlled by monitoring pollutant levels, assure adequate air change rates, limiting cracks that cause air pollution, minimizing microbiological contamination risk, and providing humidity control (Stefano Paolo Corgnati 2011). In order to achieve good IAQ, all the affecting factors must be addressed (Ram 2019).

In addition to affecting performance and work ability, poor IEQ can lead to discomfort and diseases. Even though the IEQ may not be the direct trigger to develop deceases, poor IEQ may worsen the condition, and controlling the IEQ is therefore essential for the public health (Folkehelseinstituttet 2015).

2.1.1 Norwegian regulations regarding IAQ

In Norway, there are several requirements regarding IAQ. The requirements are set by laws and regulations summarized in Table 2.1 and 2.2. To fulfill the laws and regulations some guidelines are recommended. These guidelines are not legally binding but should be used to ensure that buildings fulfill relevant requirements and ensure good IAQ.

Table 2.1: Laws concerning indoor climate (SINTEF Byggforsk 2005a).

Law	Content
The Working Environment Act	Obliges owners to ensure the facility is operated in accordance with regulations
Public Health Act	
The Education Act	
The Planning and Building Act	Regulates construction matters

Table 2.2: Regulations with requirements and recommendations for indoor climate (SINTEF Byggforsk 2005*a*).

Regulation	Content
The Workplace regulation	Obliges owners to ensure the facility is operated in accordance with regulations
Regulation on environmental health care	
Regulation on environmental health care in kindergartens and schools etc.	
Internal control regulations	Instructs companies to conduct systematic HSE work
The building code (TEK 17)	Requirements for indoor climate for new construction, change of use, and major alterations
	Requirements for FDV documentation

2.1.2 Indoor air pollutants

Knowledge of the indoor pollutants is necessary to classify the IAQ. Different pollutants have different effects on humans and various exposure over time. Both the The Norwegian Institute of Public Health (FHI) and the World Health Organization (WHO) have classified and provided limit guidelines for selected pollutants affecting the IAQ. Which of the pollutants that are most relevant to measure is still unknown (Wolkoff 2013). However, proposed priority compounds to monitor according to WHO is (Wolkoff 2013, WHO 2010):

- Benzene

- Formaldehyde

- Nitrogen

- Naphthalene

The IAQ sensors related to this thesis are restricted to measure the following compounds:

- CO_2

- Formaldehyde (HCHO)

- Total Volatile Organic Compounds (TVOC)

- Particulate Matter (PM)

- Relative Humidity (RH)

- Temperature

These pollutants were assessed in the preliminary project work (Buch 2020). An essential part of the following subsections concerning CO_2, VOC, PM, HCHO, RH and temperature are based on the preliminary work.

CO_2

CO_2 is directly connected to human presence and can be used to indicate the level of occupancy in a room. In addition to human presence, CO_2 is brought in from the outdoor air via ventilation. The main reason for increased CO_2 concentration indoors is human respiration (Siemens 2013). The CO_2 generation from people varies. Both the age, size, and activity level of a person impact

the amount of emitted CO_2. The CO_2 generation from one adult can be calculated according to Equation 2.1 (Mysen & Schild 2014).

$$\dot{V}_{CO_2} = 0.0042 \cdot M \tag{2.1}$$

Where:

$\dot{V}_{CO_2}$ Generated CO_2 from one person   [L/s]

M   Metabolism   [Met]

The typical level of CO_2 found indoors will not lead to any toxicological, physiological, psychological, or adaptive changes (Folkehelseinstituttet 2015). There are different views on which levels of CO_2 that affect the Perceived Air Quality (PAQ). Studies imply that exposure up to 5000 ppm does not harm the PAQ (Zhang et al. 2016). However, the relationship between Predicted Percentage of Dissatisfied (PPD) and CO_2 shown in Figure 2.1 presented by REHVA suggests that people are more affected by higher concentrations in rooms. The graph shows that concentrations up to 3000 ppm will lead to 50 % dissatisfaction with the IAQ. Studies by Wargocki on the relationships between classroom air quality and children's performance in school also show that lowering the CO_2 concentration from more than 2000 ppm to under 900 ppm will improve academic performance and increase children's attendance in school (Wargocki et al. 2020).
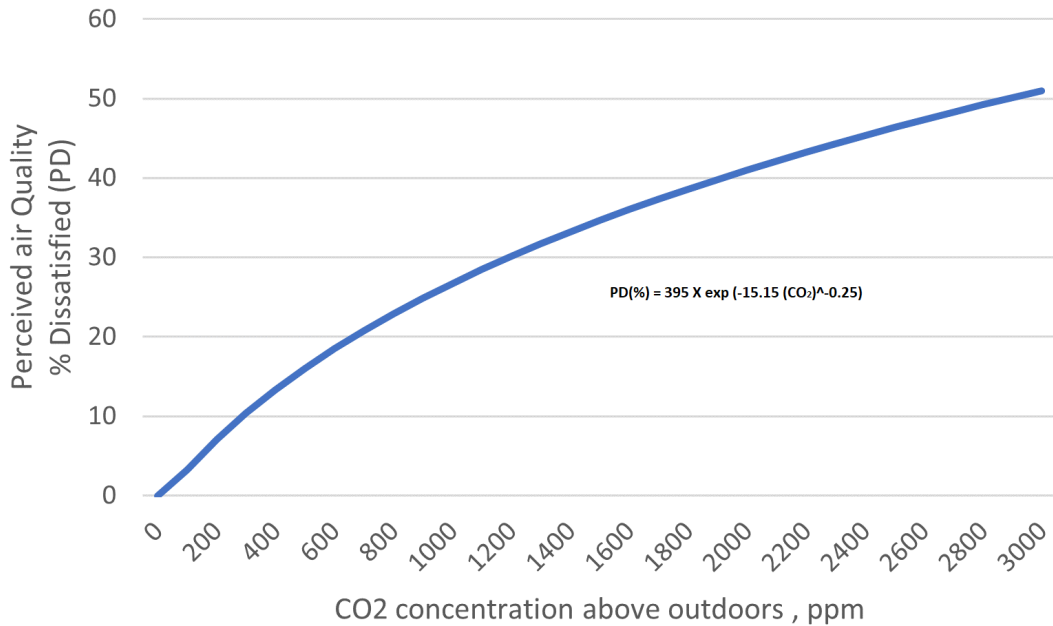
Figure 2.1: Perceived IAQ versus CO_2 (Stefano Paolo Corgnati 2011)

The threshold marker for an acceptable indoor concentration of CO_2 in Norway is 1000 ppm (*Veiledning, best.nr. 444: Klima og luftkvalitet på arbeidsplassen* 2016). 1000 ppm is also the recommended upper limit guideline proposed by the FHI (Folkehelseinstituttet 2015). A normal assumption is that the outdoor concentration of CO_2 is 400 ppm (Zhang et al. 2017). According to Figure 2.1, indoor concentration of 1000 ppm will lead to 18.5 % PPD.

Volatile Organic Compounds

VOC is a collective term for organic compounds with a lower boiling point of 50°C - 100°C and a higher boiling point of 240°C - 260°C. Most of the VOC's found indoors originates from indoor

sources such as emission from construction materials and because of people (Folkehelseinstituttet 2015). The general emission rate for VOC is decreasing during a building's lifetime. Therefore, new buildings may require higher ventilation rates during the "off-gassing" phase of the building. Studies imply that the off-gassing phase of a building may vary from two weeks up to two years (Holøs et al. 2019).

According to FHI, the negative health effects from exposure of VOC's can be divided into three categories(Folkehelseinstituttet 2015):

1. Mucosal irritation

2. Allergies, asthma, and related respiratory symptoms

3. Cancer

However, the levels of VOC found indoors in Norway do not impose significant health hazards (Folkehelseinstituttet 2015). Since common levels of VOCs in Norway are not directly connected to health hazards, it may be more interesting to investigate which levels may be disturbing in terms of PAQ. The guidelines provided by WHO and FHI do not assess this aspect of the pollutants. Wolkoff assessed the effects for different levels of VOC in terms of odor intensity. The odor threshold for VOC is much lower than the threshold for sensory irritation but has a significant impact on the IAQ and the immediately PAQ (Wolkoff 2013). However, the odor intensity is dependant on several factors, such as smoking status and previous olfactory experience (WHO 2010).

Because of the complexity, FHI has not set an upper limit threshold for exposure of VOC. Therefore, it is difficult to implement TVOC as a part of a DCV control strategy.

Formaldehyde

Formaldehyde (HCHO) is a volatile organic compound that primarily originates from indoor pollutant sources such as building materials. In recent years, the level of HCHO has decreased due to changes in the building materials used (Folkehelseinstituttet 2015). The indoor concentration of HCHO depends on several factors and local pollution sources such as smokers. The concentration varies according to the building's age, the temperature, the relative humidity, the air exchange rate, and the season (WHO 2010). Since the generation of HCHO primarily originates from indoor sources, ventilation can ensure that indoor concentration is kept at acceptable levels (Zhang et al. 2020).

As mentioned in the previous section, the odor threshold and the sensory irritation threshold are not the same. For HCHO, the odor threshold is 110 $[\mu g/m^3]$, while the threshold for sensory irritation is approximately 60 - 100 $[\mu g/m^3]$ (Wolkoff 2013). This is the same level as reported by WHO, which states that "A significant fraction of the population may perceive formaldehyde at or below 100 $[\mu g/m^3]$" (WHO 2010).

The upper limit threshold value for HCHO exposure is set to 100 $[\mu g/m^3]$ for a period of 30 minutes (Folkehelseinstituttet 2015, WHO 2010).

Particulate Matter

PM or airborne dust is a mixture of organic and inorganic components. Table 2.3 shows how PM is divided into fractions based on dynamic diameter. The fractions are classified with particle sizes from coarse particles with a dynamic diameter of $10\mu m$ to ultra-fine particles with a dynamic diameter $< 0{,}1\mu m$ (Folkehelseinstituttet 2015).

Table 2.3: Fractions of particulate matter.

Fraction	Dynamic diameter (d) [μm]
PM_{10}	<10
$PM_{10-2.5}$	2.5 <d <10
$PM_{2.5}$	<2.5
$PM_{0.1}$	<0.1

Different fractions impose different hazards to human health, depending on how deep in the human respiratory system they reach. Smaller fractions can travel further down in the system into the lungs. The respiratory filter system has the lowest effect for particles with a dynamic diameter between 1.0 and 0.1 μm (SINTEF Byggforsk 2005b). The origin of coarser particles >$PM_{2.5}$ is mainly from indoor sources, and smaller fractions mainly originate from outdoors (Goyal & Khare 2010). PM can be hazardous for humans directly by harming cells in the respiratory system or cause inflammation that can lead to further damage (Folkehelseinstituttet 2015). Studies conducted by the American heart association have concluded that especially long-term exposure of $PM_{2,5}$ increases the risk of cardiovascular morbidity and mortality (Brook et al. 2010). Therefore, any reduction of PM in the indoor environment will be beneficial for public health.

Particulate matter differs from other pollutants like VOC because its presence in the indoor air primarily originates from outdoor sources. The number of particles inside highly depends on the building's location and connection to roads with heavy traffic. Filters prevent PM from the outdoors from being transported into the building through ventilation. Based on their efficiency, filters are divided into classes. I.e., the percentage of particles that can break through the filter (SINTEF Byggforsk 2005b).

FHI has provided guidelines for exposure of $PM_{2.5}$ and PM_{10} that should not be exceeded for outdoor air. There is no guideline from FHI concerning lower fractions than $PM_{2.5}$ for indoor air. The recommended limit values from FHI are given in the Table 2.4 below (Folkehelseinstituttet 2015).

Table 2.4: Recommended guideline values for $PM_{2.5}$.

Limit values [$\mu g/m^3$]	Time span
15	24 hours mean value
8	1 year mean value

Relative humidity

RH can be classified as the third most important factor affecting IAQ after outdoor and indoor air temperature (Vellei et al. 2017). In cold climates, the relative humidity inside during winter may be as low as 10 %. Studies show that the best PAQ is expressed at medium levels with RH at 24%. Lower and higher levels of RH may lead people to feel too cold or too warm (Lind et al. 2019). In addition to affecting the PAQ, too high or too low RH may facilitate the growth of bacteria, viruses, fungi, mites, respiratory infections, allergic rhinitis and asthma, chemical interactions, and ozone production. The optimum level of RH found to prevent the mentioned issues is found to be 40 - 60 % (Alsmo & Alsmo 2014)

Temperature

As mentioned in 2.1.1, indoor air temperature greatly affects the PAQ. Studies show that temperature has an impact on other IAQ parameters. According to a study by Geng et al., a neutral or slightly cool thermal comfort sensation will be best to hinder loss in productivity (Geng et al. 2017). Another study examined the effect of poor IEQ with children's performance in school (Wargocki et al. 2007). The study concluded that the thermal environment has a major impact on children's

learning and performance, and therefore would improvements on the IEQ be cost-effective. However, the study was conducted in schools, and the effects of performance seem to be higher on children than for adults (Wargocki et al. 2007, Lan et al. 2011). The study does, however, show the impact the thermal environment can have on both long-term and short-term poor IEQ.

In the heating season, the indoor air temperature should be kept below 22°C. In general, the indoor air temperature in areas with light work such as offices should be kept between 19 and 26 °C (Direktoratet for byggkvalitet n.d.).

2.1.3 Health effects of poor indoor climate

Thermal comfort and the IAQ have effects on performance and learning. Thermal discomfort may distract the attention, lower arousal, and increase Sick Building Syndrome (SBS), lower manual dexterity, and reduce the perceived air quality (Stefano Paolo Corgnati 2011). In addition to health hazards due to exposure to pollutants, poor IAQ can lower performance in the daily work (Stefano Paolo Corgnati 2011). "Overall, evidence suggests that poor IEQ in schools is common and adversely influences the performance and attendance of students, primarily through health effects from indoor pollutants." (Mendell & Heath 2005). Mendell and Heath reviewed available research to investigate the relationship between poor IEQ and students' academic performance. Their review of the literature shows that there is a link. Low outdoor air ventilation can be connected to lower performance by students and adults, and that lower ventilation rates can be linked with decreased attendance.

2.1.4 Assessment of IAQ

One can differ between IAQ and IEQ. NS-EN 16798-1:2019 (Standard Norge 2019) provides a four-point scale categorization of expected IEQ shown in Table 2.5. For new buildings, it is common to aim for category II, medium.

Table 2.5: IEQ categories from NS - EN 16798-1:2019.

Category	Level of expectation
I	High
II	Medium
III	Moderate
IV	Low

The standard provides a set of default limits to achieve the desired category. To achieve category II, the following values should be met:

Table 2.6: Demands for the thermal environment from NS - EN 16798-1:2019.

Thermal environment	Limit value
PPD	<10
PMV	-0,5 <PMV <+0,5
Operative temperature	20 °C - 26 °C
DR	20 %
Vertical air temperature difference	3 K
Floor surface temperature	19 °C - 29 °C

The PPD is a measure of the general thermal comfort in a room and is used to determine how many people will be dissatisfied with the thermal environment in a room. The Predicted Mean Vote (PMV) can be used to calculate the PPD and is a 7 point scale ranging from -3 to +3, where

-3 represents cold, 0 represents thermal neutral, and + 3 represent hot. Equation 2.2 shows the calculation of the PPD based on the PMV (Ingebrigtsen 2015).

$$PPD = 100 - 95 \cdot e^{-(0,03353 \cdot PMV^4 + 0,2179 \cdot PMV^2)} \tag{2.2}$$

The correlation between PPD and PMV based on Equation 2.2 is shown in Figure 2.2. As the graph shows, the PPD level will never be below 5%.
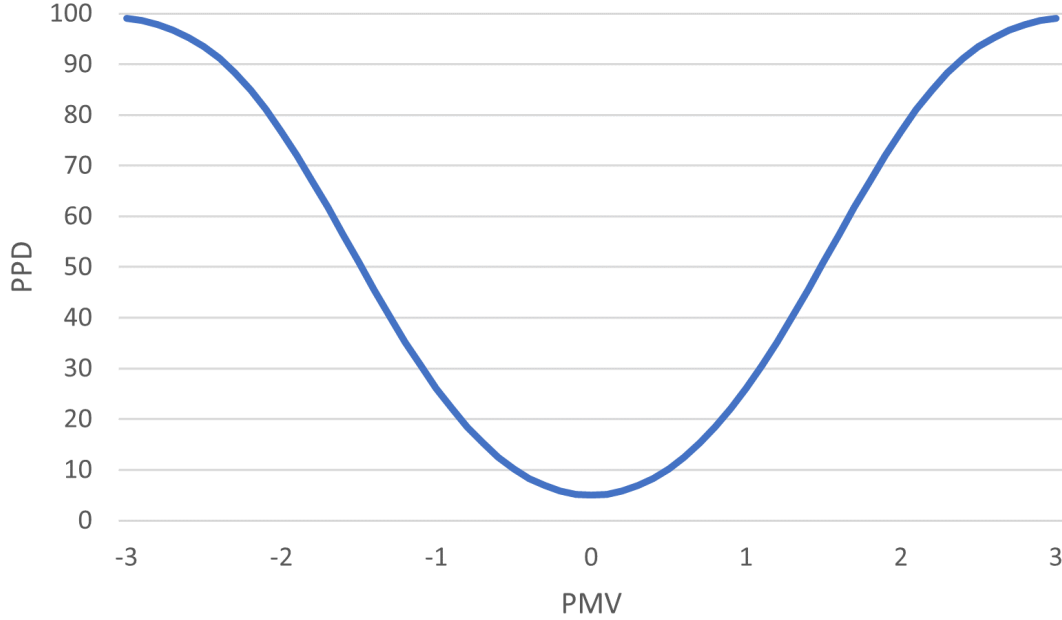
Figure 2.2: Correlation between PPD and PMV

The calculation of PMV and PPD is an expression of thermal dissatisfaction. In addition to these "global" parameters, Table 2.6 includes the local thermal comfort parameters of Draught Rate (DR) and vertical air temperature difference. The vertical air temperature difference is the temperature difference between head and ankles, and "Draught rate is defined as unwanted local cooling of the body due to air movement" (Stefano Paolo Corgnati 2011). The draught rate can be calculated by Equation 2.3 from NS-EN ISO 7730:2005 (Standard Norge 2005).

$$DR = (34 - t_{a,l})(\bar{v}_{a,l} - 0,05)^{0,62}(0,37 \cdot \bar{v}_{a,l} \cdot T_u + 3,14) \tag{2.3}$$

Where:

$t_{a,l}$	is the local air temperature between 20°C and 26°C	[°C]
$\bar{v}_{a,l}$	is the local mean air velocity, $< 0,5$ m/s	[m/s]
T_u	is the local turbulence intensity, 10% to 60%	[%]

There are three ways of evaluating the IAQ: directly by measuring the concentration of pollutants, indirectly by assessment of the consequences and effect on people, animals, or vegetation, and another indirect method by assessment of the ventilation (air exchange rate) (Stefano Paolo Corgnati 2011).

As mentioned, IAQ is a factor in deciding the IEQ. A review on the factors used to assess the quality of the IEQ showed that the IAQ accounted for 34 % of the overall IEQ (Wei et al. 2020). Of the four factors investigated in the study, IAQ was deemed the most important.

In addition to the measured levels of pollutants, the IAQ can be classified by the PAQ. Investigation of the PAQ can be conducted by surveys. PAQ is categorized by the scale in Table 2.7 (Stefano Paolo Corgnati 2011).

Table 2.7: Scale for PAQ.

+1	Clearly acceptable
0	Just acceptable
0	Just unacceptable
-1	Clearly unacceptable

2.2   Ventilation

Ventilation should contribute to a healthy IAQ. However, controll of mechanical ventilation requires energy. Measurements indicate that energy use related ventilation fans requires 15-20 % of the total energy demand for modern office buildings in Norway (SINTEF Byggforsk 2000). Therefore, a well-functioning ventilation system is essential to cut overall energy and ensure good IAQ.

2.2.1   Ventilation Requirements

The ventilation demand for a room is calculated based on the expected occupancy level of the room. The required fresh air demand is decided by the expected personal load, emissions from building materials, and pollutants from other processes. The largest amount from either personal load and emission from building materials or pollutants from other processes is the dimensioning factor (Ingebrigtsen 2015).

Table 2.8: Minimum airflow rates for ventilation in public buildings.

Category	TEK 17	444
Airflow rate due to personal load	26 m^3/h*person	7 l/s*person
Min. airflow rate due to emission during operating hours	2.5 m^3/h*m^2	2 l/s*m^2
Min. airflow rate due to emission outside operating hours	0,7 m^3/h*m^2	-

Table 2.8 gives an overview of the requirements for the fresh air supply demands set by the building code (Direktoratet for byggkvalitet n.d.) and the Norwegian labor inspector (444).

2.2.2   Ventilation strategies

Ingebrigtsen describes four main principles used for ventilation in buildings (Ingebrigtsen 2015):

- Natural ventilation

- Exhaust ventilation

- Balanced ventilation

- Hybrid ventilation

Balanced ventilation is the most common principle. The principle of balanced ventilation is that every room is equipped with supply and extract diffusers. The supply and extract air is controlled by an AHU consisting of filters, fans, heat recovery unit, and heating coil (Ingebrigtsen 2015).

Within the term of balanced ventilation, one can differ between three principles:

- CAV

- VAV

- DCV

CAV is a strategy where the airflow rate in a system or separate rooms/zones is kept constant. VAV is a common term for ventilation systems with variable air volume, without any thought of how the air volume is controlled. DCV differs from VAV by the fact that the airflow is controlled by a measured demand in the room/zone. Therefore, DCV can be classified as VAV, but VAV can not be classified as DCV. (Ingebrigtsen 2016)

2.3 Demand-Controlled Ventilation

DCV is used to lower the overall energy use and maintain the comfort level. By reducing the airflow rate in periods with lower demands, energy use is reduced. The comfort levels are increased or maintained by adapting the airflow rate to the actual demand in the room. DCV is suitable if the use of a room varies and if the variable use is possible to measure. The variations can for instance be measured by a CO_2 sensor (Ingebrigtsen 2016).

The principles of DCV were assessed in the preliminary project work (Buch 2020). The following sections concerning balancing strategies for DCV are somehow based on the literature review conducted in the previous project work. In general, the information given on DCV in this section is based on information by Mysen and Schild (Mysen & Schild 2014), and Ingebrigtsen (Ingebrigtsen 2016).

2.3.1 Control of DCV

In order to control the airflow rate in the system, DCV/VAV dampers are used. Based on measurements in the room, the designated damper changes the angle to get the correct airflow rate (SINTEF Byggforsk 2016b). In order to control the airflow rate through the damper according to the desired set-point value, DCV dampers can measure either the airflow velocity or the pressure drop (Mysen & Schild 2014).
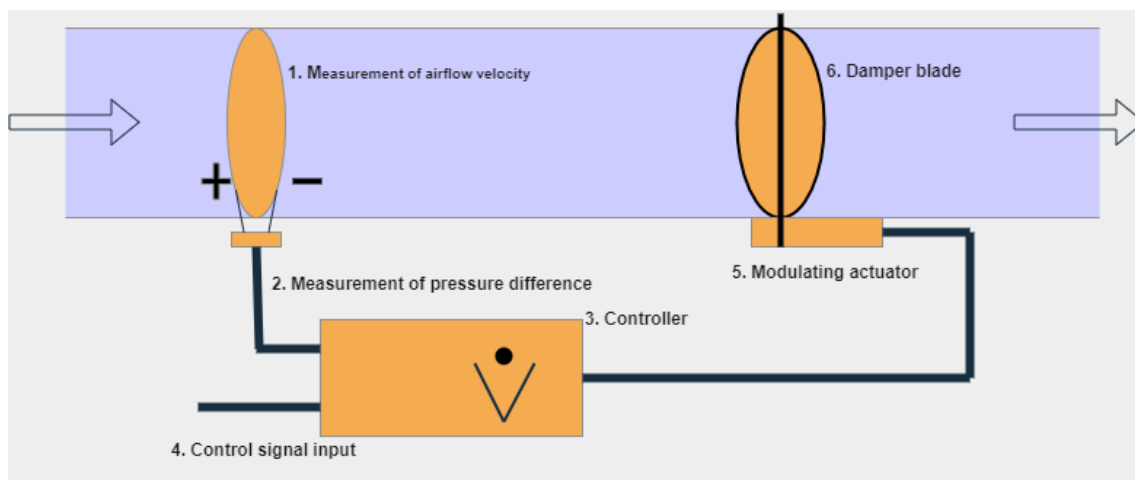
Figure 2.3: Principle setup for a DCV damper with inspiration from (Ingebrigtsen 2016).

Figure 2.3 shows the basic principle build-up of a DCV damper. The figure shows how the damper blade is controlled to open or close based on the measured airflow rate.

Some considerations must be done when placing traditional DCV-dampers. In order to get correct airflow rate measurements, the damper must not be placed too close to any junctions. Junctions may cause disturbances in the airflow. Therefore, DCV-dampers should be placed at a distance of a minimum of five times the diameter of the duct (Mysen & Schild 2014). However, new DCV-dampers on the marked can, by ultra-sound, measure the airflow rate in the duct. The five times the diameter "rule" will therefore no longer be critical for placement of the DCV damper (*Optivent Ultra VAV* n.d.). In addition to placement, the DCV dampers must be suitable for the design airflow rates. The recommended work area for DCV dampers is between 30 and 80 % opening for the DCV damper blade. This control area should ensure sufficient authority for the DCV damper (SINTEF Byggforsk 2016*b*).

In traditional CAV ventilation systems, fixed dampers are used to throttle and balance zones. The balancing is done to get the correct projected airflow rates in each zone (Ingebrigtsen 2016). With the use of DCV, the balancing of the system is done automatically. Mysen and Schild distinguish between four principles for balancing of DCV: pressure-controlled DCV, Static Pressure Reset DCV, Damper-optimized DCV, and Variable Supply Air diffuser DCV (Mysen & Schild 2014). According to SINTEF, the two primary principles of control are pressure control and damper-optimized control (SINTEF Byggforsk 2016*a*).

Pressure control

The most common principle of balancing control of a DCV system is the constant static pressure principle (Mysen & Schild 2014). The principle of pressure control is to maintain a constant static pressure at a reference point in the ducts. A pressure sensor provides feedback to the fan-control to increase or decrease the pressure in the duct (SINTEF Byggforsk 2016*a*). The placement of the pressure sensor has a direct impact on energy use. The sensor should be placed as far out in the ductwork as possible to ensure the lowest possible energy consumption at reduced simultaneity (Ingebrigtsen 2016). If the pressure sensor is placed close to the fan, the pressure increase will be higher than necessary (Ingebrigtsen 2016). Figure 2.4 shows the principle for a pressure controlled DCV system. Balancing for pressure-controlled DCV is performed by the control unit. The control unit controls the supply and extract fan in the AHU to keep a constant pressure at the pressure sensors (Mysen & Schild 2014).
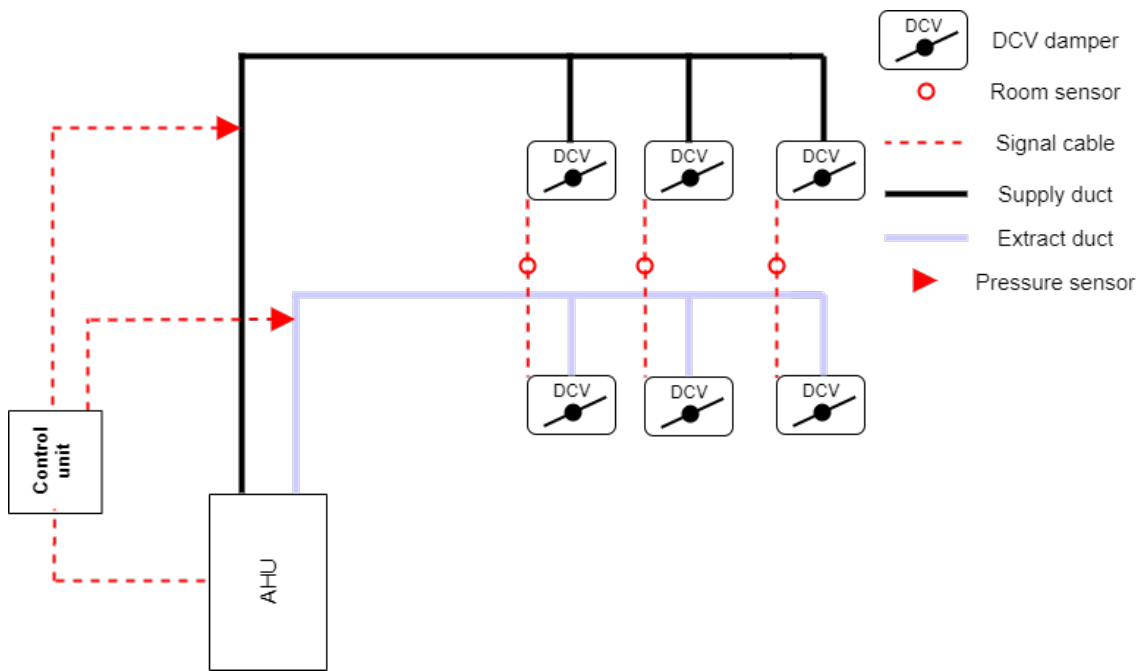
Figure 2.4: Pressure controlled DCV. Made with inspiration from (Mysen & Schild 2014).

Figure 2.5 shows how the necessary pressure increase is lower when the pressure sensor is placed far out in the main duct. If the sensor is placed too close to the AHU, a decrease in airflow rate may not be registered correctly by the pressure sensor. In the other case, with the pressure sensor placed further away from the AHU, a reduction in the airflow rate lead to less required pressure increase over the fan. This will further lead to reduced energy consumption (Ingebrigtsen 2016). (Ingebrigtsen 2016).
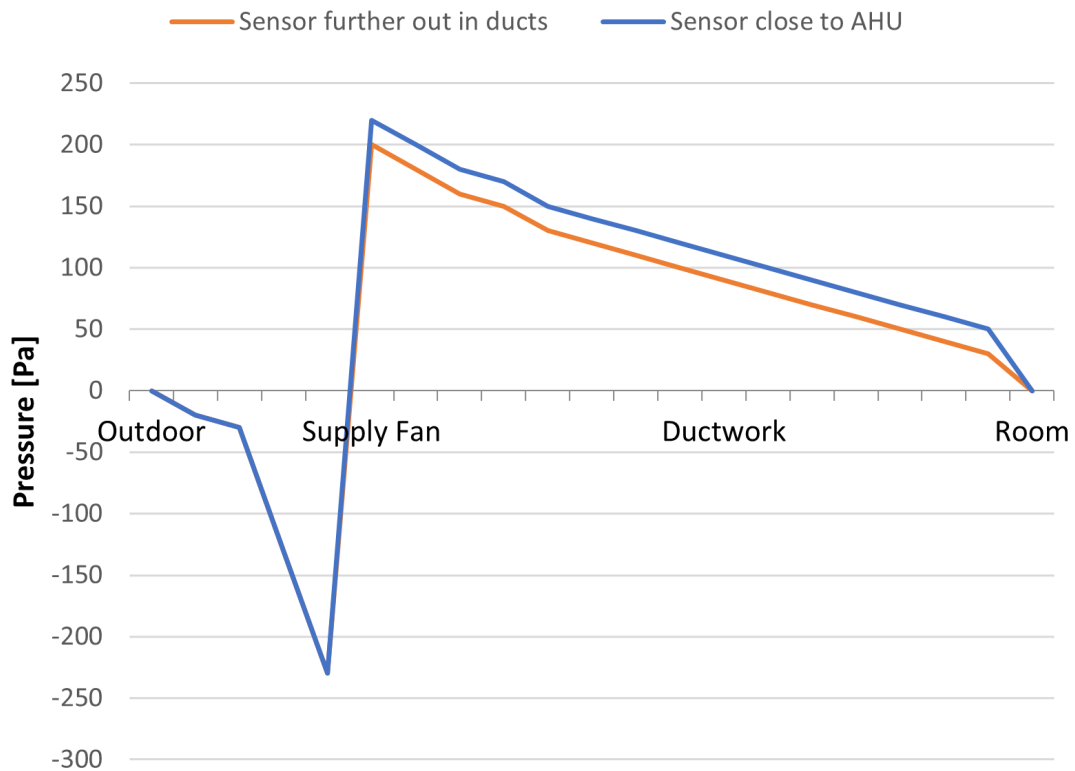
Figure 2.5: Difference in energy use for supply fan, based on the placement of the pressure sensor. Made with inspiration from (Ingebrigtsen 2016).

Damper-optimized control

Another balancing method for DCV is a damper-optimized control. Damper-optimized control will strive to maintain one damper in a fully open position. The aim of damper optimized control is to lower energy consumption by always keeping the critical pathway in the ductwork open (Mysen & Schild 2014). The required pressure increase will be lower for a damper-optimized system than for a pressure-controlled system (Ingebrigtsen 2016). Figure 2.6 shows how every DCV damper is connected to the control unit instead of one pressure sensor.
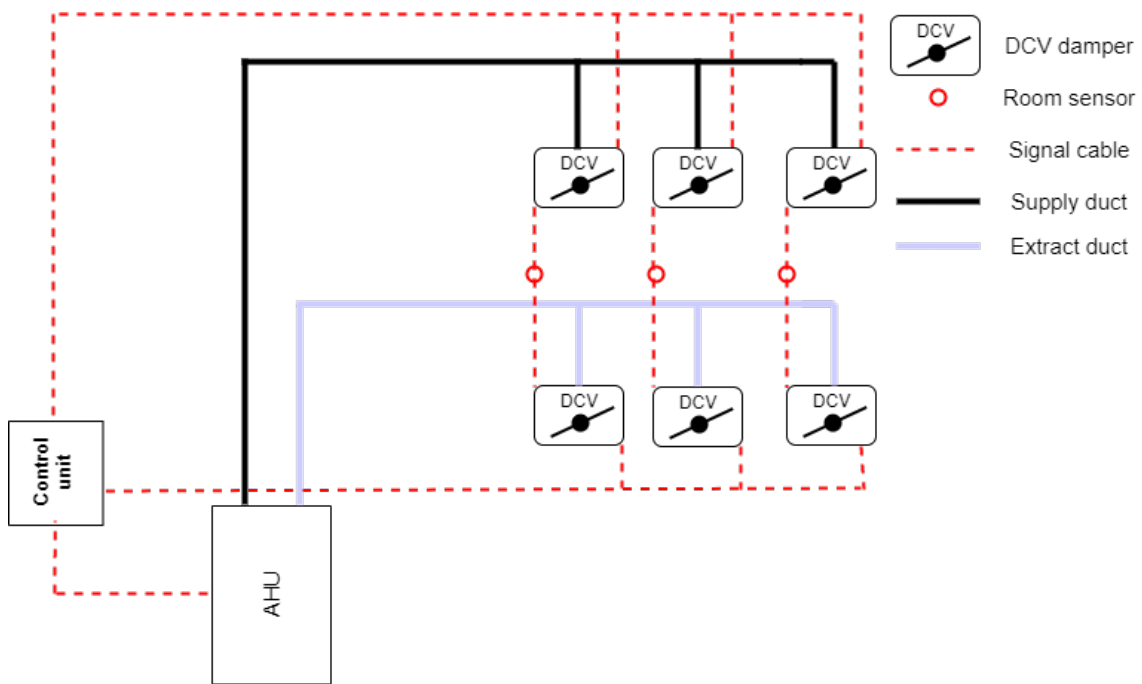
Figure 2.6: Damper-optimized control. Made with inspiration from (Mysen & Schild 2014).

Static Pressure Reset DCV

Static Pressure Reset (SPR) DCV is a combination of damper-optimized control and pressure control. The principle is to control the dampers so that one is always in an open position. The control is done by varying the pressure set point in the duct accordingly. One of the significant advantages of static pressure reset control is that the solution ensures that the static pressure in the duct will be as low as possible. This will minimize the energy used by the fan (Mysen & Schild 2014).

Balancing by SPR DCV will perform better in terms of saving energy and providing accurate airflow rates compared to pressure-controlled DCV. The investment cost of SPR DCV is higher, since it will require more components to control the system (Mysen & Schild 2011). A pressure control would only require a pressure sensor as shown in Figure 2.4, whereas SPR DCV will require a pressure sensor in addition to the signal cables from the VAV/DCV dampers as shown in Figure 2.6 in addition to a more advanced controller than a simple ΔP control.

Control strategy

If the desired airflow rate is to be decided by the CO_2 concentration in the room, the maximum allowed CO_2 concentration allowed should be set lower than the norm of 1000 ppm. The airflow rate should gradually be increased with increasing CO_2 concentration until a limit value is reached. When the specified limit value is reached, the airflow rate should be at maximum (Mysen & Schild 2014).

The airflow rate may also be controlled with a combined control strategy. A combined control strategy of temperature and CO_2 is the recommended strategy proposed by Mysen and Schild (Mysen & Schild 2014).

Other control strategies can be based on control by non-occupant-pollutants. Studies conducted in Hong Kong show that DCV purely controlled by CO_2, may have problems maintaining acceptable levels of non-occupant-related pollution, such as VOC and formaldehyde (Chao & Hu 2004). Their study suggests a control strategy with CO_2 in combination with the dominating non-occupant-related pollution. Therefore, the dominant pollutant should be identified by site measurements.

The strategy proposed by Chao et al. is based on two strategies, one with and one without people. CO_2 measurements can be used to determine the occupancy. If the level of CO_2 inside is noticeably higher than outdoors, there are people in the room. Their proposed ventilation strategy, without people, was classified into purging sequences. These sequences should be designed to dilute the pollution level in the room, with maximum airflow rate.(Chao & Hu 2004).

Steady state VS non-stationary conditions

It is essential to differentiate between stationary and non-stationary conditions when calculating supply air demand because of pollutants. If there is a noticeable delay from exposure of the pollutant until there is a clear impact in the room, it would be incorrect to calculate the required fresh air supply with stationary conditions (Ingebrigtsen 2015).
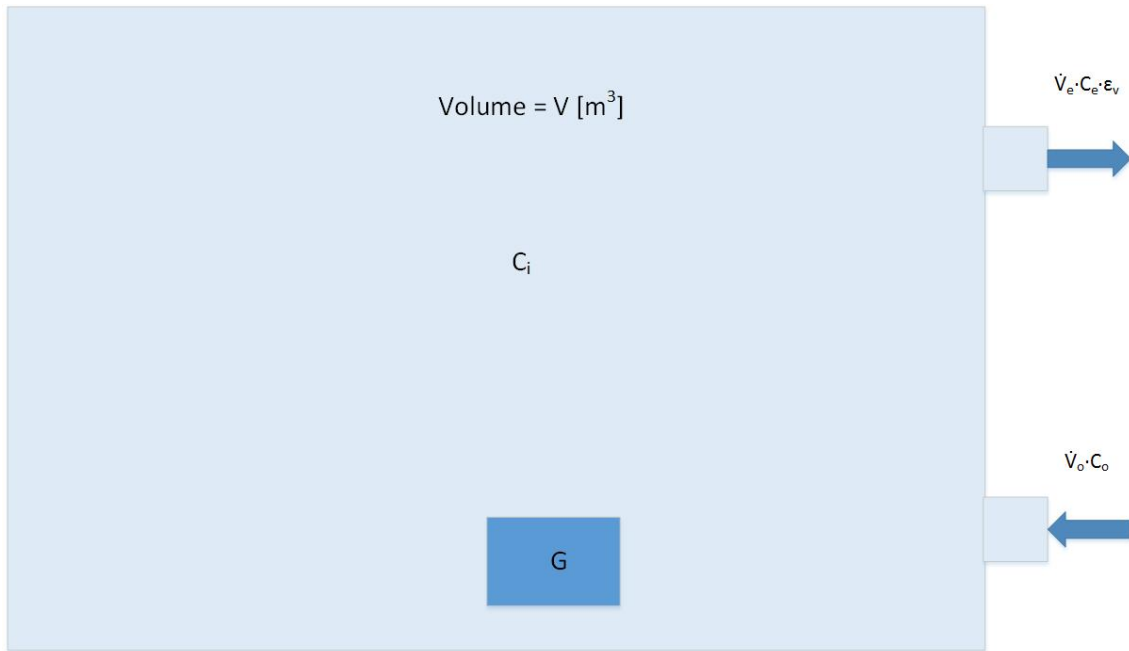
Figure 2.7: Volume-flow balance in a room, neglecting infiltration and exfiltration. Made with inspiration from (Ingebrigtsen 2015).

Figure 2.7 shows the factors affecting the volume-flow of a room (neglecting infiltration, exfiltration, and the effect of filtration on the supply). Where V is the volume of the room $[m^3]$, G is the generation of pollution inside $[mg/h]$, C_i is the concentration of pollution indoors$[mg/m^3]$, C

V	Volume of the room	$[m^3]$
G	Indoor generation rate of the pollutant	$[mg/h]$
C_i	Pollution load of the given substance indoors	$[mg/m^3]$
C_o	Pollution load of the given substance outdoors	$[mg/m^3]$
C_e	Pollution load of the given substance in the extract	$[mg/m^3]$
$\dot{V}_e$	Airflow rate in the extract	$[m^3/h]$
$\dot{V}_o$	Airflow rate in the supply	$[m^3/h]$
ϵ_v	Ventilation efficiency	$[-]$

With Figure 2.7 as foundation Ingebrigsten shows how Equation 2.4 is developed and used to

determine the pollution load in a room (Ingebrigtsen 2015).

$$C_i = C_0 \cdot e^{-(\frac{\dot{V}}{V} \cdot t)} + C_o \cdot (1 - e^{-(\frac{\dot{V}}{V} \cdot t)}) + \frac{G}{\dot{V}} \cdot (1 - e^{-(\frac{\dot{V}}{V} \cdot t)}) \tag{2.4}$$

Where:

G	Indoor generation rate of pollutant	[m³/h]
C_i	Pollution load of the given substance indoors	[mg/m³]
C_0	Pollution load of the given substance indoors at t=0	[mg/m³]
C_o	Pollution load of the given substance outdoors	[mg/m³]
$\dot{V}$	Airflow rate for ventilation	[m³/h]
V	Volume of the zone/room	[m³]
t	Ventilation time	[h]

If the conditions are steady state, Equation 2.4 and the required fresh air demand $\dot{V}$ can be simplified to Equation 2.5.

$$\dot{V} = \frac{G}{C_i - C_o} \cdot \frac{1}{\epsilon_v} \tag{2.5}$$

If the temperature is a decisive factor for the airflow rate, Equation 2.6 is used to calculate the required fresh air demand.

$$\dot{V} = \frac{\Phi_o \cdot 3600}{C_{pl} \cdot \rho \cdot (T_i - T_s)} \tag{2.6}$$

Where:

$\dot{V}$	Required airflow rate	[m³/h]
Φ_o	Excess heat in the room	[W]
C_{pl}	Specific heat capacity of air	[J/(kg $\cdot K$)]
ρ	Density of air	[kg/m³]
T_i	Indoor air temperature	[°C]
T_s	Supply air temperature	[°C]

2.3.2 Energy use related to DCV

DCV can reduce the overall energy consumption of a building by reducing the electricity consumption (Delwati et al. 2018). The main reason for using DCV is to save energy, not to improve the IAQ (Siemens 2013). The airflow rate in a DCV system is often controlled by varying the fan speed to maintain a constant static pressure in the ducts (Zhang et al. 2015). By varying the airflow rate, the energy demand for ventilation in a DCV system may be significantly lower than for a system with CAV.

According to Ingebrigtsen, three main points will lead to energy saving by using DCV (Ingebrigtsen 2016):

- Fan operation

- Heating of the ventilation air

- Space heating

Energy used to operate the fan will be lower because the airflow rate and the required pressure increase will be lower for most operating hours. With lower airflow rates, there will be less air volume that needs to be heated in the AHU. DCV can prevent rooms that are not in use from being ventilated and thus save energy required for space heating.

Equation 2.7 from NS3031:2014 (Standard Norge 2014) calculates the energy demand for fans in a DCV system.

$$E_{fan} = \frac{\dot{V}_{on} \cdot SFP_{on} \cdot t_{on} + \dot{V}_{red} \cdot SFP_{red} \cdot t_{red}}{3600} \tag{2.7}$$

Where:

E_{fan}	Total energy use for fans	[kWh/year]
SFP_{on}	Specific fan power during working hours	$[kW/(m^3/s)]$
SFP_{red}	Specific fan power outside working hours	$[kW/(m^3/s)]$
t_{red}	number of hours outside working hours	$[h]$
t_{on}	number of working hours	$[h]$
$\dot{V}_{on}$	Average ventilation rate during working hours	$[m^3/h]$
$\dot{V}_{red}$	Average ventilation rate outside working hours	$[m^3/h]$

SFP_{on} is calculated according to Equation 2.8.

$$SFP_{on} = \frac{3600 \cdot \sum P_{v,on}}{\dot{V}_{on}} \tag{2.8}$$

Where:

$\sum P_{v,on}$	Power supply of the fan at $\dot{V}_{on}$	$[kW]$

And the SFP at reduced ventilation rate is calculated according to Equation 2.9.

$$SFP_{red} = SFP_{on} \cdot (1.6 \cdot r^2 - r + 0.6) \tag{2.9}$$

Where:

$$r = \frac{\dot{V}_{red}}{\dot{V}_{on}} \tag{2.10}$$

Simultaneity

If the factor of simultaneity is expected to be below a particular value during the operating hours, smaller duct dimensions can be used. The ducts must be planned to deliver the required airflow rates at the highest expected simultaneity with a safety margin (Ingebrigtsen 2016). The impact of the factor of simultaneity for the required airflow rate is shown with Equation 2.11

$$\dot{V}_{DCV} = S \cdot \dot{V}_{CAV} \tag{2.11}$$

Where:

$\dot{V}_{DCV}$	Airflow rate for a system with DCV	[m³/h]
S	Factor of simultaneity	[-]
$\dot{V}_{CAV}$	Airflow rate for a system with	[m³/h]

The average factor of simultaneity should not be used as a criterion when dimensioning a ventilation system but strictly for calculating energy savings. For dimensioning purposes, one should use the maximum expected simultaneous use of the rooms connected to the ventilation system as a criterion.

Energy saving potential

It is difficult to generalize the potential in energy saving due to DCV. Energy saving is highly dependent on factors such as building type, type of room, and system build-up (Ingebrigtsen 2016). The different control strategies for DCV have different potential in energy savings. Delwati et al. conducted studies including simulation and measurements on the energy-saving on different DCV control strategies compared to CAV (Delwati et al. 2018). Their work indicated an energy-saving potential of 64 % to 84 % for traditional constant static pressure set-point (CPSP) DCV compared to CAV, and up to 10 % additional energy saving with the use of variable static pressure set-point (VPSP) as a control strategy. However, measurements in their laboratory show that there are challenges connected to the VAV-dampers that could lead to higher energy consumption than strictly necessary.

Summed up, DCV may lower the energy use significantly. However, it must be planned and built correctly. In order to get an energy-efficient ventilation system, the efficiency of the fans must be close to maximum in the normal operating area. The Specific Fan Power (SFP) should be controlled at the average pressure drop in the system. In addition, one of the DCV-dampers should be in an open position (Mysen & Schild 2013). A DCV system will be most cost-effective in energy saving on single-supply systems for large spaces with variable occupancy such as meeting rooms and lecture auditoriums (Siemens 2013).

2.3.3   Recirculation of air

Recirculation of air is about sending the exhaust air back as supply air. The concept of using recirculated air is seldom used in Norway. The Norwegian Labor Inspection Authority states that "Energy saving by recirculation should, as a general rule, not be accepted" (*Veiledning, best.nr. 444: Klima og luftkvalitet på arbeidsplassen* 2016). Recirculated air can save energy by reducing the energy demand for heating the supply air. Recirculated air may also be used to prevent outdoor pollutants from entering indoors via ventilation. However, reducing the ventilation rate should not be done without countermeasures that can prevent the accumulation of pollutants (Fisk et al. 2011).

Some of the consequences of reducing the ventilation rate without countermeasures are shown in Table 2.9.

Table 2.9: Consequences of reducing the ventilation rate (Fisk et al. 2011).

Pollutant	Exposure changes
Outodoor air pollutants	No change or decrease
Indoor generated VOCs	Increased
Indoor generated airbonre particles	Small increase
Indoor combustion - produced gaseous pollutants	Increase
Semi-volatile organic compounds	Not much change

The main principle with ventilation is to provide acceptable IAQ. Therefore, if recirculation of air

is used, it should not be used at the expense of the IAQ to save energy. Some studies and scientific evidence conclude that air filtration and air cleaning can replace outdoor air ventilation (Wargocki et al. 2015). Recirculation will reduce the exposure of contaminants generated outdoors but may increase the exposure of pollutants generated indoors.

Dampers are used to control recirculation and OAF. A study on the effect of reverse airflow through the exhaust air damper in an AHU described the traditional operating strategies for VAV AHU. It proposed a new strategy for controlling the supply, extract, and recirculation damper in an AHU (Seem et al. 2000).
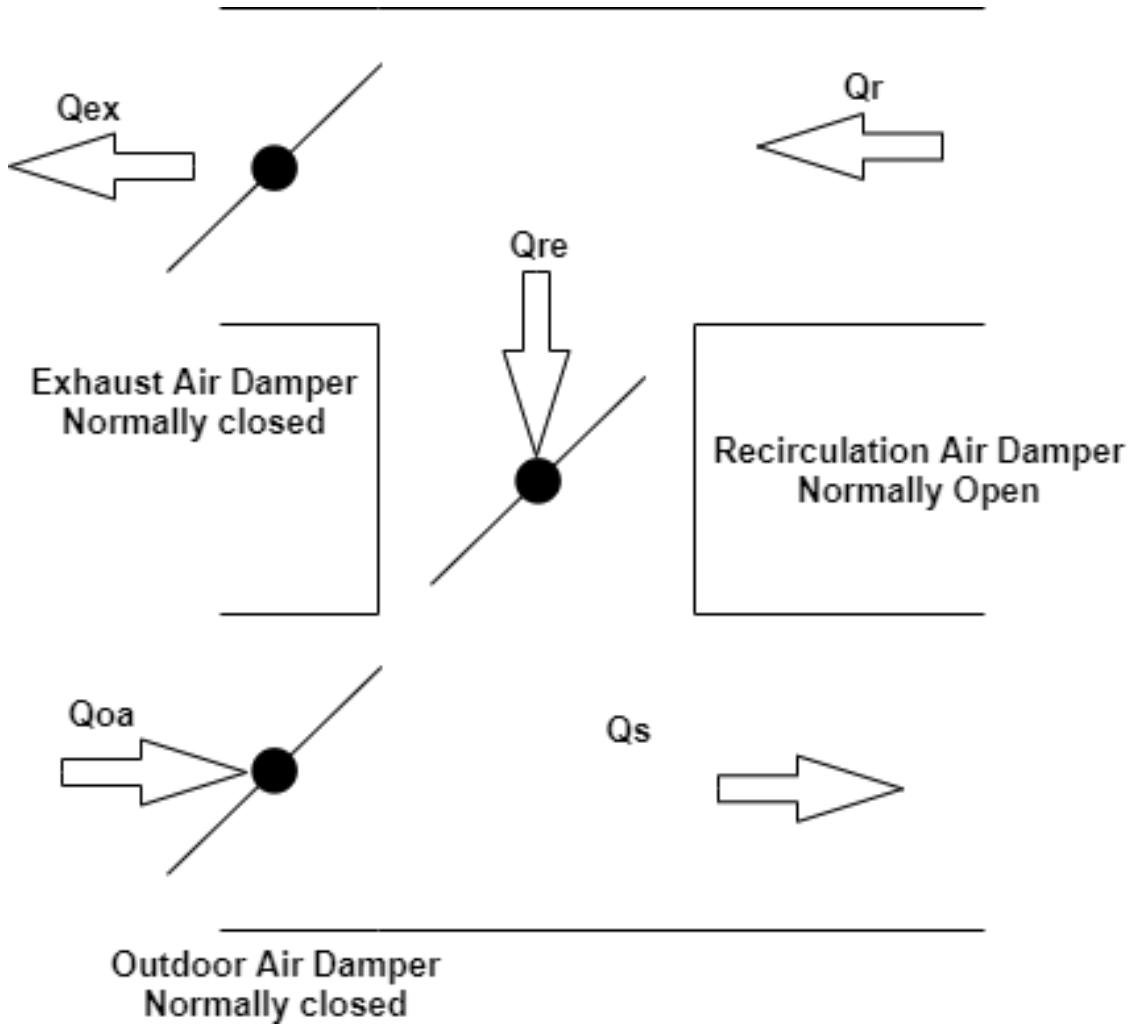
Figure 2.8: VAV recirculation dampers in an AHU (Seem et al. 2000).

If outdoor air enters the AHU through the exhaust air damper, the air may pass through the unit without sufficient filtration. The study by Seem concluded with a new proposed AHU damper control system where the exhaust air damper should be linked with the recirculation air damper according to the following equation:

$$\Theta_{re} = 1 - \Theta_{ex} \tag{2.12}$$

According to their study, this control strategy will, in most cases, prevent reverse airflow through the extract damper.

2.4 Low-cost sensors - Principals and limitations

IAQ sensors are used to measure the IAQ in a building by measuring one or several parameters affecting the IAQ. There are many studies on IAQ-sensors that are classified as Low Cost Sensors (LCS) in their respective study. It can be challenging to distinguish what we can classify as low-cost. In this thesis, LCS are meant to be sensors that are commercially available at a reasonable price. Some studies define low-cost to a few 10's of US dollars for the sensor (100 US dollars for sensing kits/nodes/platforms) (Chojer et al. 2020, Rai et al. 2017), whereas others set a more comprehensive frame where all sensors costing below 100 US dollars is included (Chojer et al. 2020, Morawska et al. 2018).

A considerable number of low-cost sensors are now available for monitoring indoor air quality. The sensors enable the possibility of placing multiple sensors in a room and provide more data to evaluate the IAQ in a room. However, this relies on the fact that the low-cost sensors measure correct values for the selected pollutant. The correct placement of IAQ sensors is further assessed in Section 2.4.1.

In general, the major issue with LCS is the lack of data reliability and the lack of studies conducted on the long-term stability and cross-sensitivity (Chojer et al. 2020). There are several studies on LCS, and a major part of them focus on one specific type of sensor (Metal Oxide Sensors (MOx) for VOC measurements, PM sensors etc.) (Morawska et al. 2018). The LCS technology and its limitations for the parameters relevant in this thesis are reviewed in the following subsections.

CO_2 sensors

A typical low-cost option to measure CO_2 is by the use of Non-Dispersive Infrared (NDIR) sensors. The NDIR sensor may be used in ventilation control, agricultural and industrial application and can be found within the price range of 100 - 200 US dollars (Martin et al. 2017). Martin et al. did an assessment of the accuracy compared to the information given by the manufacturer on one NDIR sensor (Martin et al. 2017). The study concluded that the assessed sensor had a low root mean square error. The CO_2 measurements were accurate. Other studies on the NDIR show promising results and imply that the sensors should be able to measure with acceptable accuracy (Yasuda et al. 2012). This is in line with the previous work related to this thesis, where another NDIR sensor (Sensirion SCD30) was assessed and showed promising results for measurements of CO_2 compared to validated equipment (Buch 2020).

VOC and formaldehyde sensors

Several technologies can be used to measure the level of VOC in the indoor air. The most common way to monitor VOC is by using expensive laboratory gas chromatography-mass spectrometry and not commercially available electronic sensors (Yurko et al. 2019). Gas chromatography is both expensive and time-consuming (Spinelle et al. 2017). Spinelle et al. reviewed the literature on commercially available sensors and methods. The commercial sensor working principles can be divided into six and is summarized in Table 2.10

Table 2.10: The six most common principles of operation for commercial VOC sensors (Spinelle et al. 2017)

Method	Comments
Photo-ionization detectors (PID)	Both portable handheld instrument and Original Equipment Manufacturers (OEMs)
OEM electrochemical sensor	Amperomethic or potetiometric type
OEM metal oxide sensors (MOx)	Change of conductivity instead of chemical reaction
Optical sensors	Including UV portable spectrometers
Portable or micro-gas chromatograph (μGC)	Combines micro column with MOx or PID OEM as detectors
Electronic noses and sensor-arrays	

Several studies conducted on low-cost VOC sensors show significant advantages from an economic point of view. However, the sensors often show a lack in performance in detection and selectivity (Spinelle et al. 2017). A study investigating the performance of low-cost sensors for formaldehyde and TVOC measurements found differences in performance based on the target group of the sensors. The sensors targeted at the public performed worse than the more expensive sensors targeted towards professionals (Goletto et al. 2020). The sensor that measures VOC related to this thesis work is an SGP30 from Sensirion. This type of sensor is a MOx. The operating principle of MOx sensors is the change of the electrical properties of the metal oxide in the sensors when it is exposed to different ambient gases. In order to specify the amount of a specified VOC, one measures the change in resistance or conductivity (Spinelle et al. 2017). Studies conducted on MOx sensor show that commercial sensors suffer from a lack of reliability and that MOx sensors need individual calibrating to target hydrocarbons (Yurko et al. 2019).

PM

The most common measurement technology for low-cost PM sensors is the utilization of light-scattering to detect particles with aerodynamic diameters between 0.3 - 10 μm (Bulot et al. 2019). As for the gaseous pollutants, LCS are developed to measure PM. However, the development of low-cost PM-sensors can be seen as more comprehensive than low-cost gaseous sensors. This is due to particulate matter mainly measured by counting particles or measuring the mass (Lowther et al. 2019).

LCS's have proven to be selective in their performance in measuring PM. In studies, the SPS 30 sensor has had significant problems with coarser particles (Kuula et al. 2020). These findings are in line with previous measurements related to this project where the SPS 30 sensor shows the inaccuracy towards coarser particles (Jørgensen 2020, Gram 2019). Possible reasoning for the inaccuracy is that low-cost PM sensors are often based on laser scattering. Laser scattering converts the readings into mass concentration (Karagulian et al. 2019). Other studies suggest that low-cost PM sensors may have variable accuracy at low concentrations of PM and that they may be affected differently at varying temperature and humidity (Bulot et al. 2019). These studies imply that the sensor should be calibrated and validated in the environment they are meant to operate.

Temperature and RH

A review of 35 studies on the development of low-cost IAQ sensors (whereas 33 on temperature and 32 on RH) found that thermistors and capacitive sensors were the most common choice of technology to measure temperature and RH (Chojer et al. 2020). Martin-Garin et al. conducted a study on the use of LCS in a building environmental monitoring system (Martín-Garín et al. 2018). In the study, sensors was calibrated and compared to reference equipment. Their measurements show that the LCS performed in compliance with the deviation given by the manufacturer. Their measurements show an accuracy of $\pm$ 1°C. For RH, the sensors did not perform as well. However,

after calibration, the sensors measured consistent results. Their study shows that LCS are not necessarily calibrated correct from the manufacturer and that validation and calibration should be done before trusting the measurements completely.

2.4.1 Sensor placement

If sensors are to be used in order to control DCV, the sensors must be able to give a correct overview of the IAQ in the room. The ventilation efficiency in a room is not always as good as planned. Therefore, the correct placement of sensors is essential to ensure valid measurements. Sensor placement strategies can be divided into engineering/heuristic methods and optimization methods (Fontanini et al. 2016).

An example of an optimization method is developing an algorithm that calculates the best placement of IAQ based on CFD simulations (Fontanini et al. 2016). Fontanini developed an algorithm that calculates the optimum placement of sensors. The algorithm tended to place sensors in regions with low airspeed. Previous measurements conducted in the preliminary work with sensors placed in the extract duct showed that high airspeed impacted the sensors and caused a clear drift in the measurements (Buch 2020). The drifts show that sensor placement can lead to unstable ventilation control. CO_2 sensors are often placed in the main extract duct to save costs (Taal & Itard 2020). This can, however, impose difficulties in controlling the system correctly. If the ventilation efficiency is low, CO_2 measurements in the extract would not represent the room's concentration. The ventilation principle in the rooms has an impact on the preferred placement of the IAQ-sensors. In rooms with mixing ventilation, the sensor should be placed in the occupant zone, preferably at 1 to 1.7 meters above the floor (Ingebrigtsen 2016).

In theory, if the ventilation efficiency in a room is 100 %. The conditions and IAQ should be uniform. However, this is seldom the case. Placement of sensors around doors, windows, and areas where people are expected to vacate often, should be avoided (Siemens 2013). The combination of LCS and the use of IoT enables a more freely placement of sensors. Since the sensors do not can communicate wireless, the best placement can be found when the rooms are in use.

Chapter 3

Methodology

This chapter presents the methodology used in this thesis. First, the planning and reasoning for the construction of the office areas in the laboratory are reviewed. Then, a description of how the CONTAM simulation models are set up. Lastly, the control algorithms for DCV and recirculation control are described.

3.1 Full-scale laboratory model

A full-scale model is under construction in the laboratory. The model shall be used to investigate different control strategies for DCV. The office area is a 21 m^2 rectangular enclosed box containing three cell offices of 7 m^2 each. The ceiling and outer walls consist of EPS insulation plates with a metal cover on the inside and outside of the main chamber. The inner walls consist of EPS insulation plates (Glava EPS S 80).

The first step in developing the DCV system was to establish the framework. The DCV system is to be set up with a UNI 2 AHU. More info on the AHU is found in Appendix C.1. In order to decide the size and specs for the necessary equipment, a simulation was conducted in the energy simulation program SIMIEN. The simulation was set up so that the operative temperature in the offices should not exceed 26°C for more than 50 hours a year. This complies with guidelines from the Norwegian Labor Inspection Authority (*Veiledning, best.nr. 444: Klima og luftkvalitet på arbeidsplassen* 2016).

The complete results from the simulation with all input values are found in Appendix A.1. Even though the DCV system is planned to be set up in the laboratory, the SIMIEN simulation was conducted with one exposed facade. The simulation was conducted with one exposed facade facilitating investigation of higher airflow rate's impact on indoor air temperature. The results from the simulation show that the heat load from the sun has a significant impact on the indoor air temperature during summertime. The system was chosen to be prepared for higher airflow rates than the requirements set in TEK 17 (Direktoratet for byggkvalitet n.d.). The possibility of higher airflow rates facilitates further testing of ventilation strategies other than those explored in this thesis. The design maximum airflow rate was set to 84 m^3/h for every room. The reason for oversizing the system was to facilitate for further investigation of DCV strategies not included in this thesis. Appendix A.1 shows the results from the SIMIEN simulation.

The velocity method described by Ingebrigtsen was used to decide the required diameter of the ductwork (Ingebrigtsen 2016). The desired airflow rate was set to 3-5 m/s for the main duct and 1-3 m/s for the supply ducts. The calculation of the required duct sizes is shown in Table 3.1.

Table 3.1: The calculated diameters for the ductwork.

Selected u [m/s]	Airflow [m3/h]	Calculated d [mm]	Standard d [mm]	Actual u [m/s]
3	252	172	160	3.5
2	84	122	125	1.9

The floor plan of the ventilation is shown in Figure 3.1. The ductwork is to be placed on the roof. The main ducts have a diameter of 160 mm. The supply and extract ducts connected to each office diffuser have a diameter of 125 mm. The supply is marked in blue and the extract in red. The damper positions are marked MD and are placed to fulfill the common demand of a distance greater than five times the diameter from branching. Information about the LVC dampers placed in the extract and the ORION-LØV supply diffusers are found in Appendix C.2 and C.3.

Figure 3.1: Ventilation floor plan.

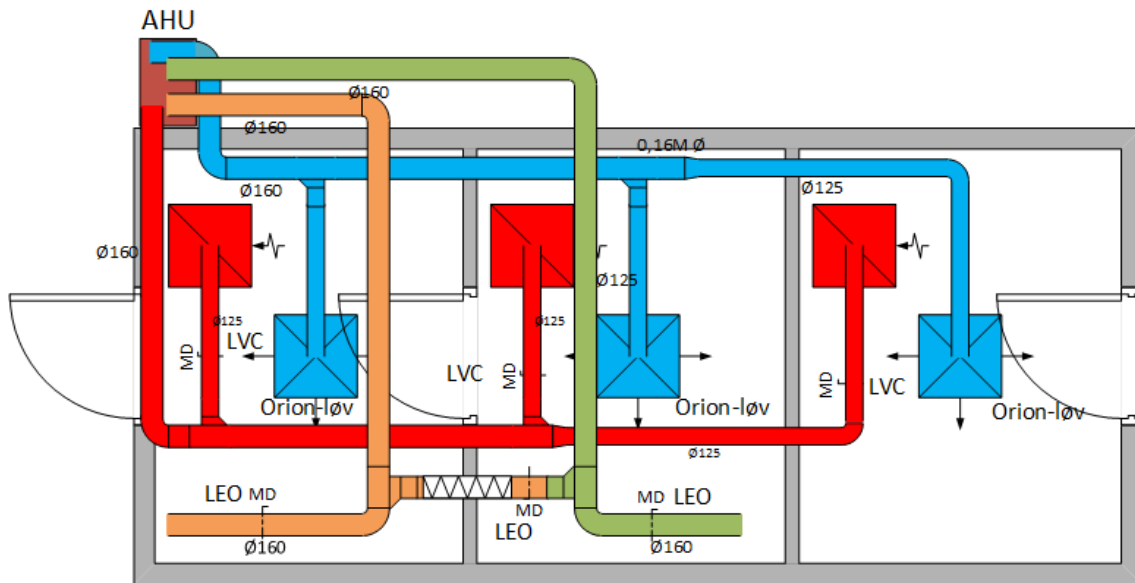As seen in Figure 3.1, a system to control air recirculation is implemented. The green duct is the intake, and the orange duct is the exhaust. The exhaust and intake are connected by a duct equipped with an F9 filter. The specific filter is a HFGX-F9-287/287/520-5 shown in Appendix C.4. Three dampers marked LEO are placed in the exhaust, intake, and recirculation ducts to control the OAF fraction.
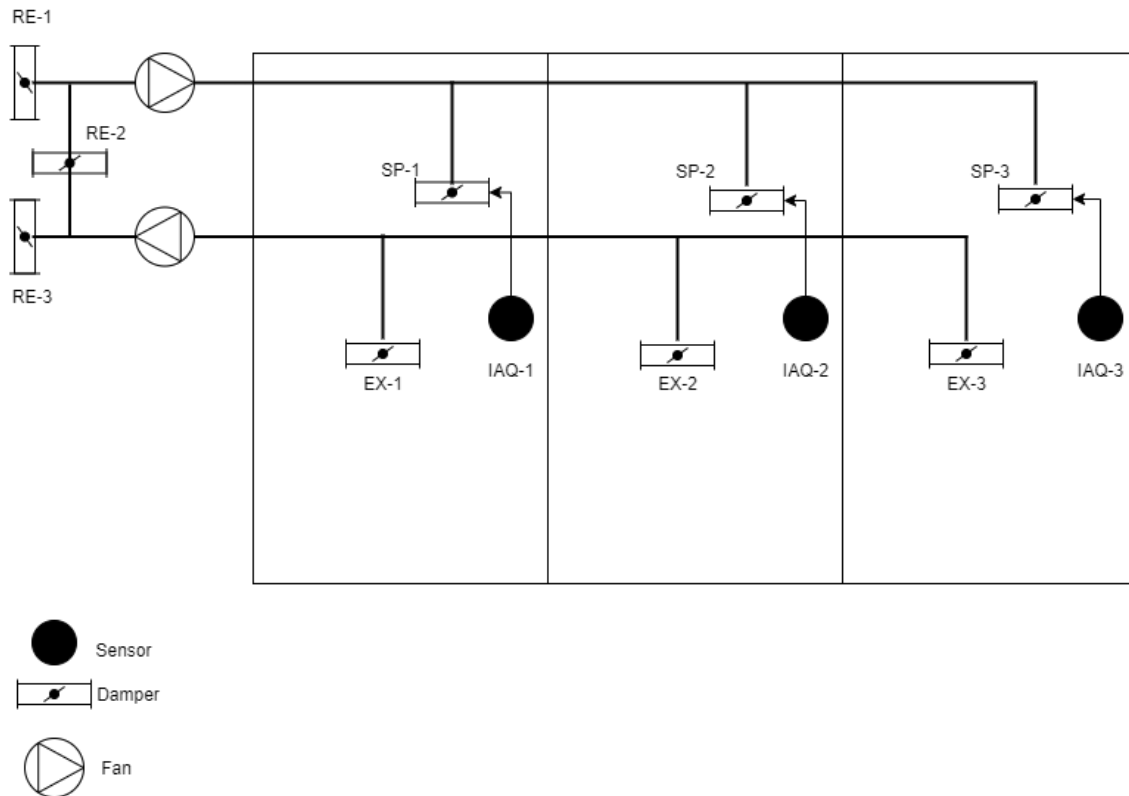
Figure 3.2: System overview for the DCV control.

Figure 3.2 is a system overview of how the parts in the system should be controlled. One IAQ sensor should be placed in every office to control the required airflow rate in that specific office area. The recirculation dampers are to be controlled in line with Equation 2.12. This means that RE-2 and RE-3 are complementary to one another. The supply damper (SP-1,2,3) and the extract damper (EX-1,2,3) are controlled equally for all the rooms. This should ensure balanced ventilation in each room. In addition, a pressure sensor is to be placed out in the ductwork to facilitate for static pressure reset DCV control as described in Section 2.3.1.

3.2 CONTAM model

The multizone IAQ and ventilation analysis program CONTAM developed by NIST were used to develop and analyze DCV control strategies. CONTAM can calculate airflows due to infiltration, exfiltration, and mechanical-, buoyancy, and wind pressure-driven airflows. In addition, CONTAM can calculate the concentration of specified pollutants (NIST n.d.).

Because of detailed descriptions of the control algorithm of the ventilation system, CONTAM was chosen. In addition, CONTAM is free to download software. There are some limitations with CONTAM. CONTAM operates with the assumption of well-mixed zones, where each zone is treated as a node with uniform conditions in the zone. There are possibilities of defining non-uniform areas in a zone, but this option is not explored further and, therefore, not implemented in this thesis.

3.2.1 General build-up of simulation model

The model was set up to represent the physical office areas in the laboratory. Therefore the simulation model is split into three zones called room 1, 2, and 3. Each room has an area of 7m^2,

where room 1 and 3 have doorways to the outside, and room 2 is accessible through room 1 by an interior door as seen by the floor plan in Figure 3.1.

The leakage areas for the offices were calculated assuming that the doors are mainly closed, and the rest of the leakages in the offices were simplified in one path-flow representing the total leakage area of the room. The doors are calculated with a leakage area of 1.7 cm^2/m^2 based on values from chapter 26 in The 2001 ASHRAE Handbook (*2001 ASHRAE handbook : fundamentals* 2001).
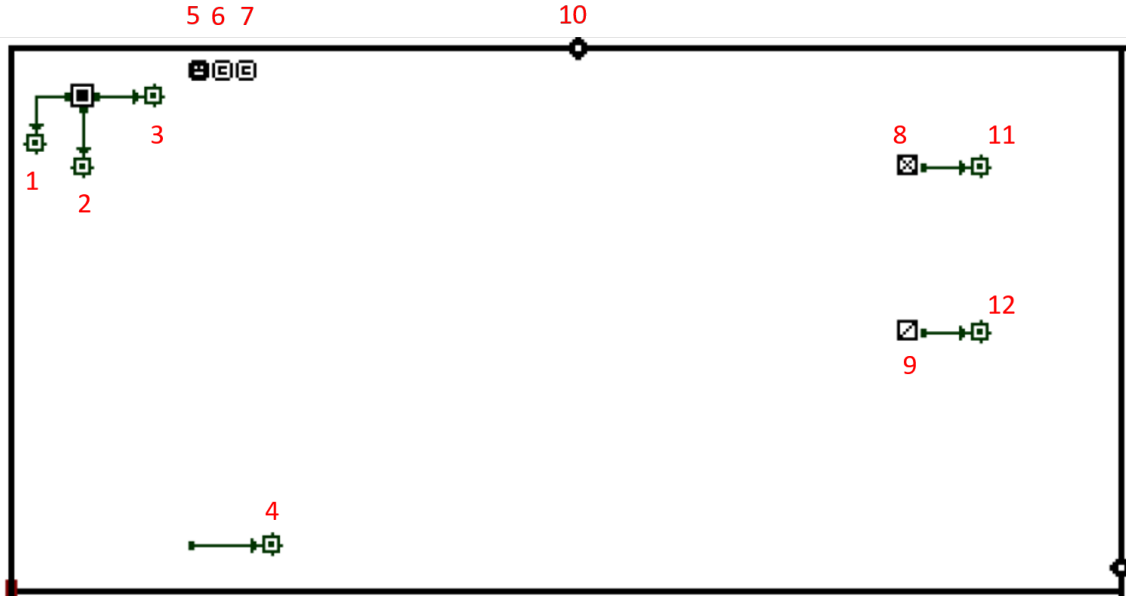
Figure 3.3: Basic room setup for the CONTAM model.

Figure 3.3 shows the general setup of each room in the simulation. The elements marked 1-4 report the room concentration of CO_2, HCHO, $PM_{2.5}$, and the temperature. Element 5 represents the generation of CO_2 due to occupancy. Element 6 and 7 are pollution sources which include the emission rate of HCHO and $PM_{2.5}$. Elements 8 and 9 represent the supply and extract diffuser, and element 10 represents the doors' leakage area. Element 11 and 12 report the supply and extract airflow rate during the simulation.

3.2.2 AHU

The AHU implemented in the CONTAM model was a simplified unit with the ability to control the OAF and specify filters with defined filter efficiency. The AHU that are to be used in the laboratory is a UNI 2 unit. The unit contains two filters classified as F7 grade, one for supply and one for the return air. According to NS-EN 779 (Standard Norge 2012), F7 filters should have an average efficiency of 80 - 90 % for particles with the size of 0.4 μm. Therefore, the filter efficiency is set to 90% in the simulations. The recirculation filter to be used in the laboratory is an F9 filter. This filter should have an efficiency of 95% for particles with the size of 0.4 μm (SINTEF Byggforsk 2005*b*).

3.2.3 Occupancy

In Norway, the standard working week is five days a week with a total working load of 37 - 38 hours a week. According to a survey from 2006, 71.1% of Norwegian workers reported their working hours to be between 06.00 and 18.00 (Sterud 2009). In order to get some variations in the occupancy load of the office areas, three different schedules were implemented in the simulation. The schedules are summarized as CO_2 generation rate in Figure 3.4.
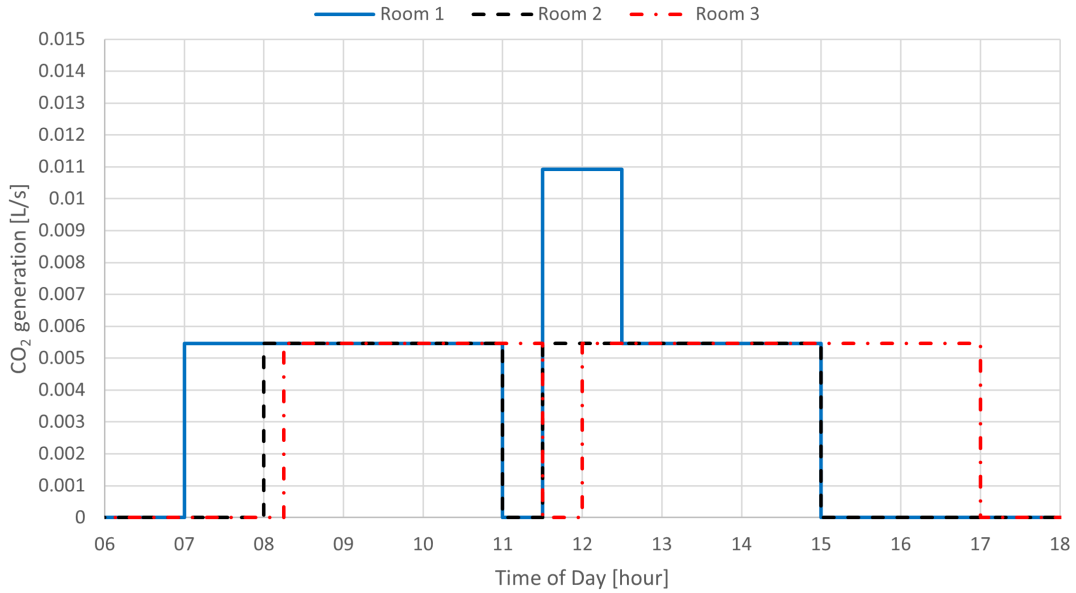
Figure 3.4: Generation rate for CO_2 during occupied hours.

As seen in Figure 3.4, the rooms are normally occupied by one person resulting in a generation rate of 0.00546 L/s of CO_2. To impose some variations in the pollution load, two persons are present in room one every day from 11:30 to 12:30. The extra person represents a short meeting after lunchtime. Since there are people present from 07.00 - 17.00, this time-span represents the "working hours" in this thesis.

3.2.4 Pollutants and emission rate

The CO_2 generation in the rooms is assumed to be from people with a low activity level. The metabolic rate from a seated person reading, writing, and/or typing can be set to 1.3 MET (Persily & Jonge 2017). With the use of Equation 2.1, the CO_2 generation from one person is set to 0.00546 L/s.

If a building is to be classified as low polluting, the generation rate of HCHO should be lower than 0.05 $[mg/(m^2 \cdot h)]$ (Ingebrigtsen 2015, Standard Norge 2007). The office areas in the full-scale laboratory model are 7 m^2. In order to be classified as low polluting, the HCHO emission rate shall be lower than 0.35 mg/h = 350 μg/h.

A study on HCHO in the indoor environment compared different studies on the emission rate of HCHO from different materials (Salthammer et al. 2010). In the study, the mean emission rate for new walls was 7 μg/(m²·h), the mean emission rate for ceilings in new buildings was 42 μg/(m²·h), and wood-based floor coverings were 31 μg/(m²·h). The simulations in CONTAM were set up before the office areas were built. Instead of actual measurements of the HCHO emission rate, the values from Salthammer were used to calculate the emission rate of HCHO for the simulation. The calculation of the HCHO emission rate is shown in Table 3.2.

Table 3.2: Calculation of HCHO emission rate.

Unit	Area [m2]	Emission rate $[\mu g/m^2 \cdot h]$	Emission rate $[\mu g/h]$
Walls	25.584	7	179.088
Floor	7	31	217
Ceiling	7	42	294
Total	-	-	690.088

These values are used as the emission rate of HCHO in the CONTAM simulations. The reason for choosing these values in the CONTAM simulations is to use "reasonable" emission rates and to be able to investigate the impact of higher emission rates than low polluting buildings classified by NS-EN-ISO-15251 (Standard Norge 2007). To compare, both emission rates were used in the same simulation in different rooms with the same ventilation strategy.

The generation of PM is divided into outdoor and indoor sources. A transient contaminant data file with measured values from Elgseter in Trondheim was used to get accurate values for outdoor particulate matter. The outdoor concentration of $PM_{2.5}$ from the contaminant file is shown in Figure 3.5.
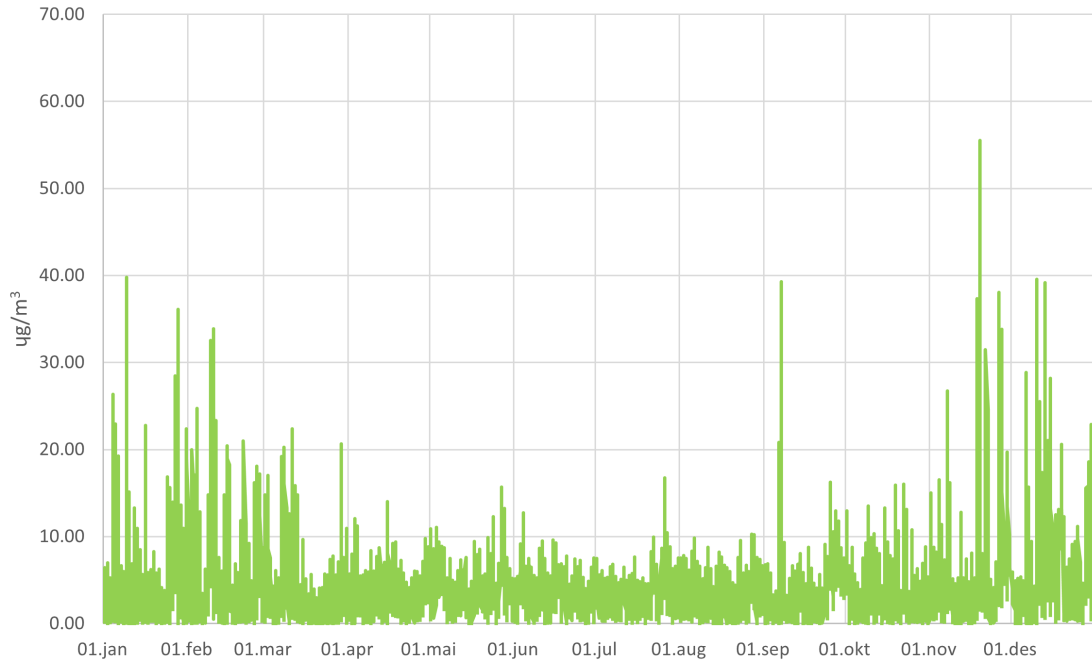
Figure 3.5: Outdoor concentration of $PM_{2.5}$ from contaminant file.

As for the level of HCHO, the actual generation rate of PM is not measured for the laboratory office areas. Since 50 % of the indoor PM originates from outdoor sources (National Academies of Sciences et al. 2016), the indoor generation of $PM_{2.5}$ were adapted to equal 50 % of the indoor air concentration in the simulations. Therefore, the generation rate for $PM_{2.5}$ was set to 15 $\mu g/h$ for each room.

Table 3.3: Generation rate for pollutants in the CONTAM simulation.

Pollutant	Room generation rate
CO2	0.00546 [L/s]
HCHO	690 [$\mu g/h$]
PM2.5	15 [$\mu g/h$]

To get the most significant variations in $PM_{2.5}$ pollution load, the CONTAM simulation was set to the last week of the year.

3.2.5   Outdoor air temperature

A weather file for the Trondheim area was implemented to get realistic simulations. The weather file contains relevant data such as outdoor temperature, pressure, wind speed and direction, and absolute air humidity throughout the year.

The outdoor air temperature from the weather file is graphically displayed in Figure 3.6.
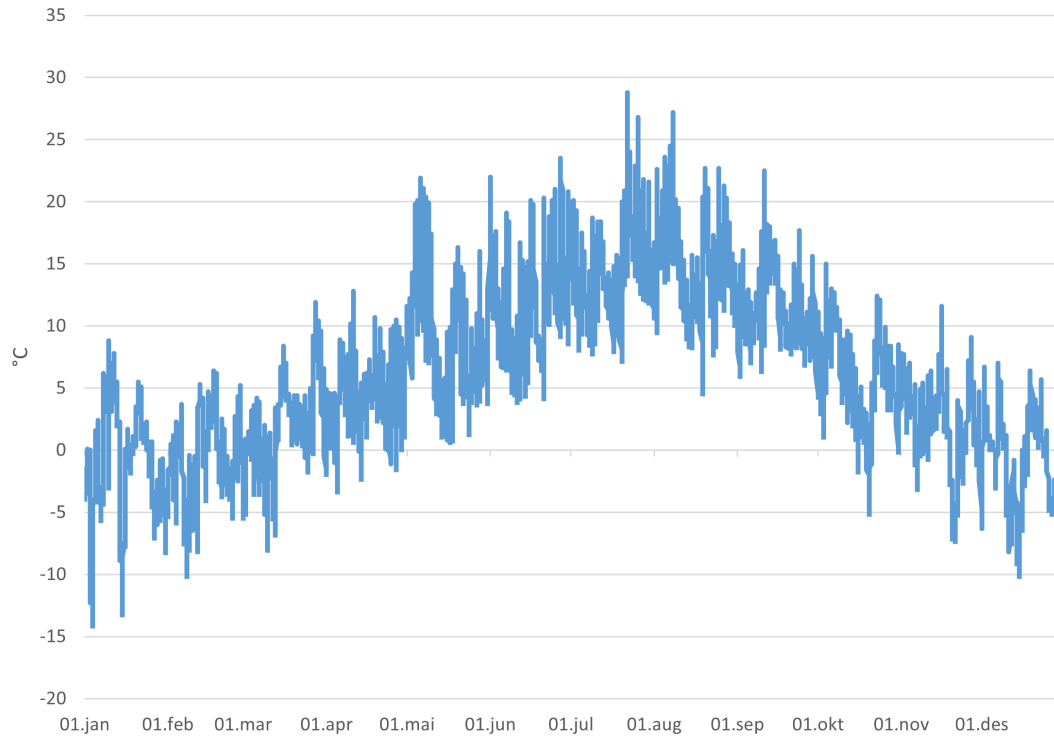
Figure 3.6: Outdoor air temperature from weather file.

3.2.6   Indoor air temperature

A typical control strategy for DCV is a control based on indoor air concentration of CO_2 and indoor air temperature. Since the CONTAM simulation does not correctly calculate indoor air temperature variations, the temperature was constructed based on a SIMIEN simulation. The SIMIEN simulation was set up to keep the indoor air temperature below 23 °C and the concentration of CO_2 below 1000 ppm. The heat load, personal load, and ventilation rate from the SIMIEN simulation were copied to CONTAM as pollutant sources. This simplified way of constructing the indoor air temperature was deemed good enough for a weekly simulation. In the SIMIEN simulation, the internal heat load from one person was set to 105 W (SINTEF Byggforsk, 1990). More info on the SIMIEN simulation is found in Appendix A.2.

The resulting heat load for one room in SIMIEN is shown in Figure 3.7.
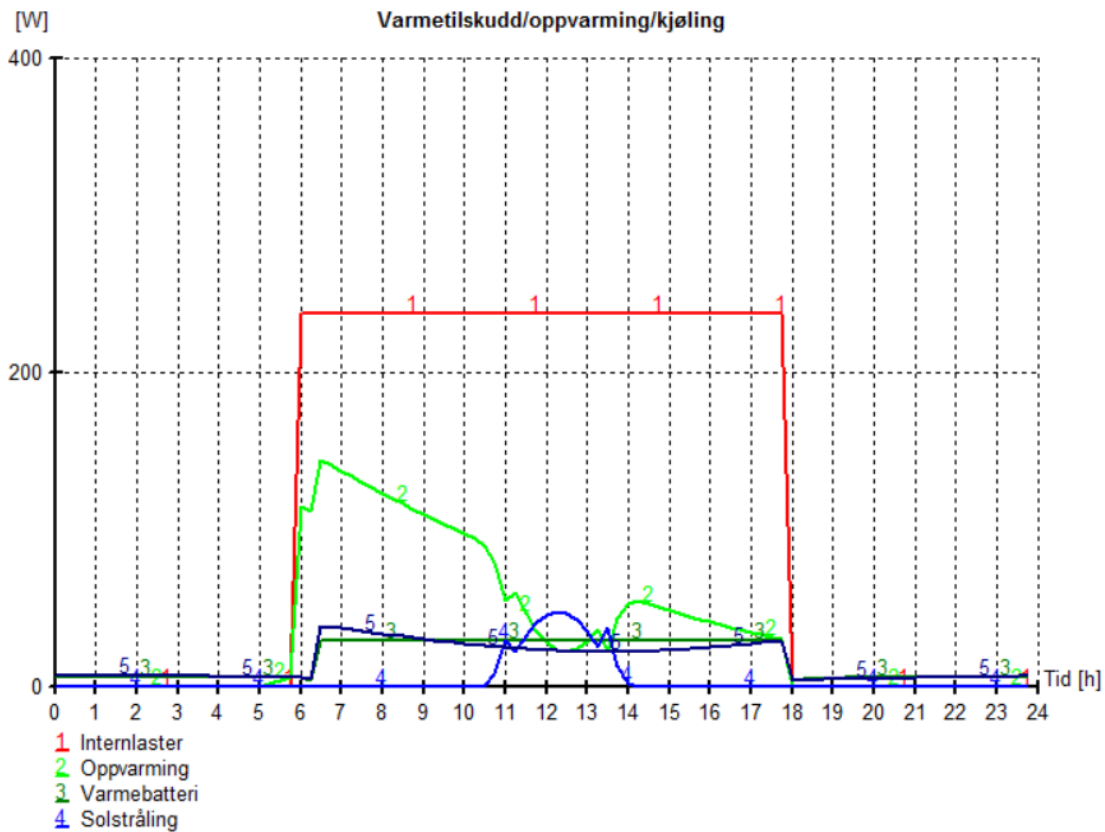
Figure 3.7: Heat loads used in SIMIEN simulation.

To copy the heat loads from SIMIEN to CONTAM, the heat loads from Figure 3.7 were used. The pollution load from each of the temperature sources is set equal to the specified heat loads. The temperature contaminants are constructed as constant-coefficient sources with a constant generation rate of 11 #/h. The general contaminant date used to specify the temperature pollution in CONTAM is shown in Figure 3.8.

Figure 3.8: Input values for the temperature contaminant in CONTAM.

Figures 3.9a and 3.9b shows the pollution load schedules for heat loads implemented in the CONTAM simulation model. In addition, the heat load due to personal load was constructed according to the occupancy schedule shown in Figure 3.4.
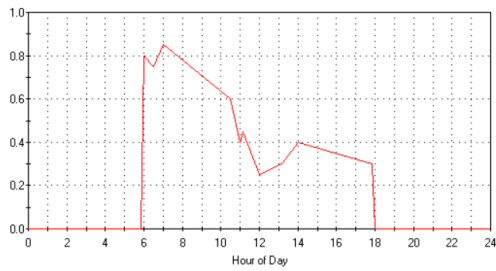
(a) CONTAM schedule for heating.
(b) CONTAM schedule for solar heat load.
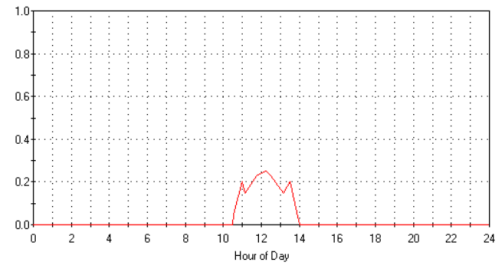
Figure 3.9: Schedules for heat loads implemented in CONTAM.

The temperature output from the SIMIEN simulation is shown in Figure 3.10. Graph 2 represents the indoor air temperature, and graph 4 represents the supply air temperature.
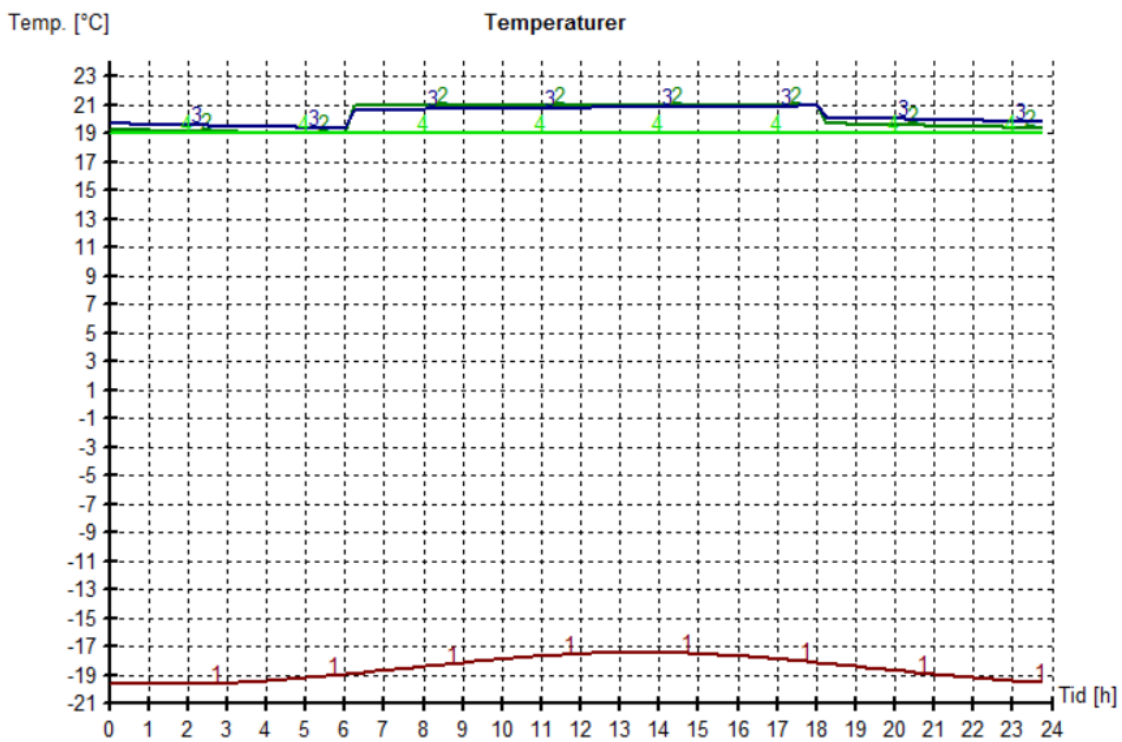
Figure 3.10: Temperature output from the SIMIEN simulation.

As Figure 3.8 shows, the default concentration is set to 19 $\mu g/kg$. This represents the constant supply air temperature of 19 °C shown in Figure 3.10. Figure 3.11 shows the resulting concentration of the "improvised" temperature contaminant in CONTAM when the heat loads are exact copies from the SIMIEN simulation. As the graph shows, the output is similar to the SIMIEN output in Figure3.10. Therefore, the constructed CONTAM temperature was deemed adequate to be used in the DCV simulations.
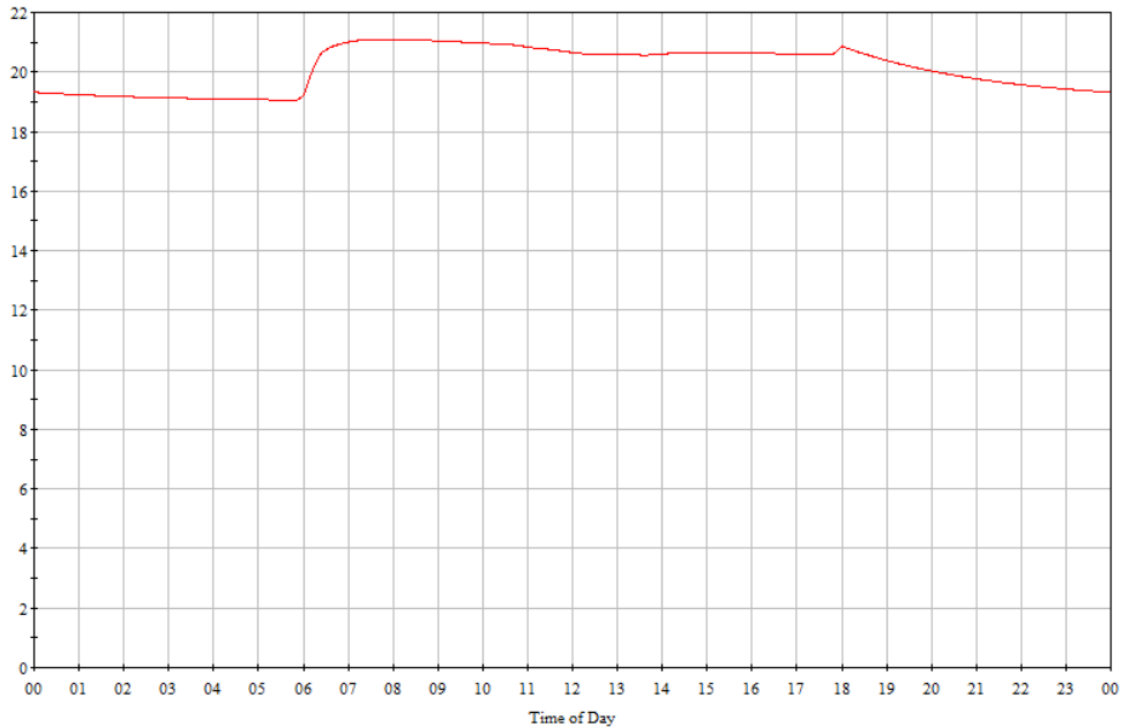
Figure 3.11: Temperature in CONTAM simulation.

3.3 DCV controls

In order to test different scenarios, different control systems were simulated. In total, five cases were set up and are further described in the following subsections. Two simple controls based on CO_2 and HCHO concentrations were set up with the intent of validating the CONTAM model and the physical lab.

To facilitate for comparison between each DCV control, the duration for every simulation was one week. Based on the outdoor concentration of $PM_{2.5}$ from Figure 3.5, week 52 was chosen because this is the week with the highest overall concentration of outdoor $PM_{2.5}$.

In the thesis by Gram (Gram 2019), it was concluded that HCHO should be implemented in DCV control to assure good IAQ. Therefore, the proposed controls in the following sections are investigated with the intent of comparing occupant-related and non-occupant related DCV controls.

3.3.1 CAV model

To compare energy use for the different control strategies, a basic CAV model was simulated in CONTAM. The airflow rates in the CAV model are based on the demands set by TEK 17 (Direktoratet for byggkvalitet n.d.). This gives a design airflow rate of 43.5 m³/h during working hours and 4.9 m³/h outside working hours. Working hours were set from 07.00 - 17.00 every weekday. Figure 3.12 shows the schedule for the CAV control in CONTAM. In the diagram, 0.5 equals 42 m^3/h and 0.06 equals 4.9 m^3/h. The ventilation rate was set to 4.9 m^3/h during the weekend.
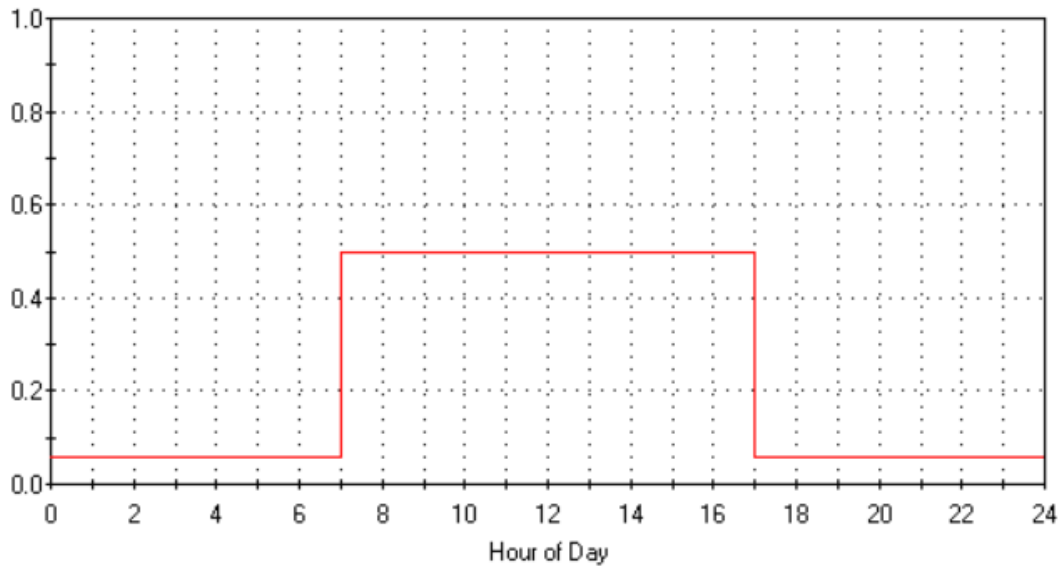
Figure 3.12: CAV - Supply and extract airflow rate schedule for a weekday.

3.3.2   Case 1 - CO$_2$ upper limit control

This CO$_2$ control was simulated and developed with the primary goal of developing a simple control strategy that could be used to test the control in the laboratory. The logic behind the control algorithm implemented in CONTAM is shown in Figure 3.13.
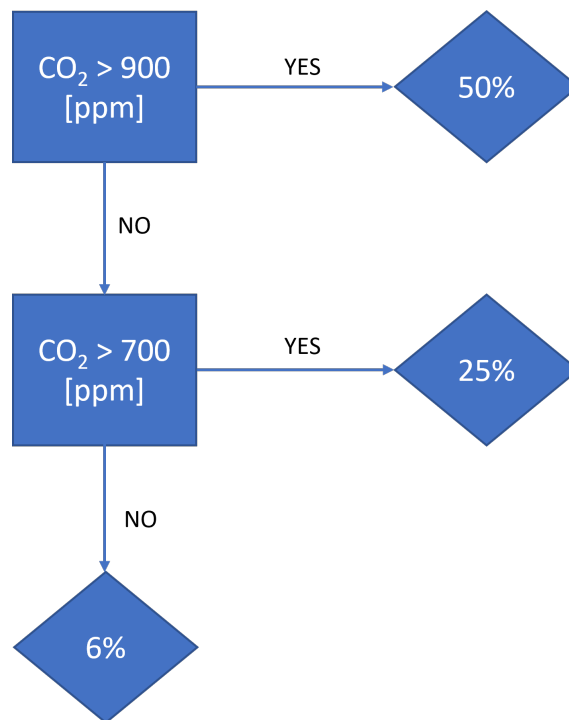
Figure 3.13: Case 1 - Control algorithm for upper limit control based on CO$_2$ measurements.

The maximum ventilation rate used in the simulation is 50 % capacity of the design airflow rate of 84 m^3/h. A maximum ventilation rate of 42% complies with the required airflow rate from TEK 17 (Direktoratet for byggkvalitet n.d.). The calculation of time steps in the simulation was set to

30 minutes to avoid fluctuations. This was considered the most accurate way of representing how it can be done in the actual laboratory measurements.

Figure 3.14: Case 1 - Control network in CONTAM.

Figure 3.14 shows the control network in CONTAM. Elements 1-3 represent zone measurements of CO_2. Elements 4 and 5 are upper limit constants connected to upper limit switches (7, 8). Element 9 is a lower limit switch connected to a lower limit constant. Modifiers (10 - 12) give the signal output as 50, 25, or 6 % pending on the measured CO_2 concentration in the room. A maximum switch (13) selects the highest input signal from the modifiers. The signal output from the maximum switch is sent to a signal split(14), sending the signal to the supply and extract diffusers to set the airflow rates according to the measured CO_2 concentration.

3.3.3   Case 2 - HCHO upper limit control

As for Case 1, this control was mainly developed to test the control of dampers in the laboratory. This case consists solely of HCHO control. The idea was to investigate the impact on other indoor pollutants. The control logic is shown in Figure 3.15.
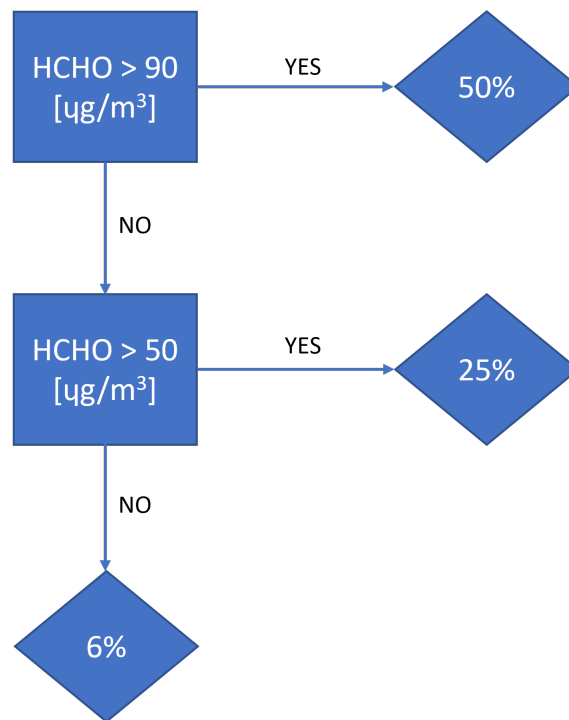
Figure 3.15: Case 2 - Control algorithm for upper limit control based on HCHO measurements

The control network in CONTAM is similar to the control shown in Figure 3.14 for case 1. The difference between the cases is that elements 1-3 measure the concentration of HCHO instead of CO_2, and the upper limit switches are adapted to the values shown in Figure 3.15. The maximum ventilation rate used in this case was 42 m^3/h (50%). The time between each calculation of HCHO concentration in the rooms was set to 30 minutes to avoid fluctuations.

3.3.4 Case 3 - CO_2 proportional and HCHO upper limit control

This control was constructed to keep the level of CO_2 below 1000 ppm to comply with the guidelines described in Section 2.1.2. Figure 3.16 shows the logic of the control based on CO_2 and HCHO measurements. The upper limit value for the control was set to 900 ppm to ensure that the CO_2 level in the zone should not exceed 1000 ppm. In other words, the proportional control was set to increase the supply airflow accordingly so that the level of CO_2 is as close as possible to 900 ppm. Measurements conducted by Gram (Gram 2019), Jørgensen (Jørgensen 2020) and Buch (Buch 2020), showed that HCHO concentration could be higher than recommended guidelines from WHO. Since HCHO is a specific VOC with given guidelines of acceptable exposure, it is possible to set an upper limit value that should not be exceeded. The guideline value from WHO is that the level of formaldehyde should not exceed 100 μg/m^3 for 30 minutes (WHO 2010).
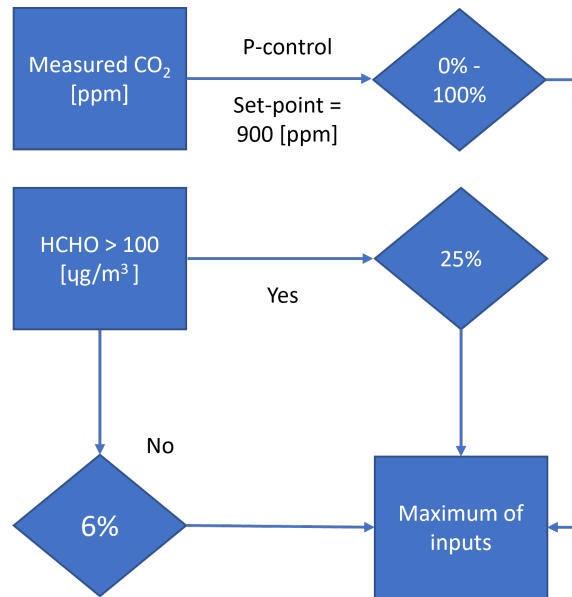
Figure 3.16: Case 3 - Control algorithm for proportional CO_2 control and upper limit HCHO control.
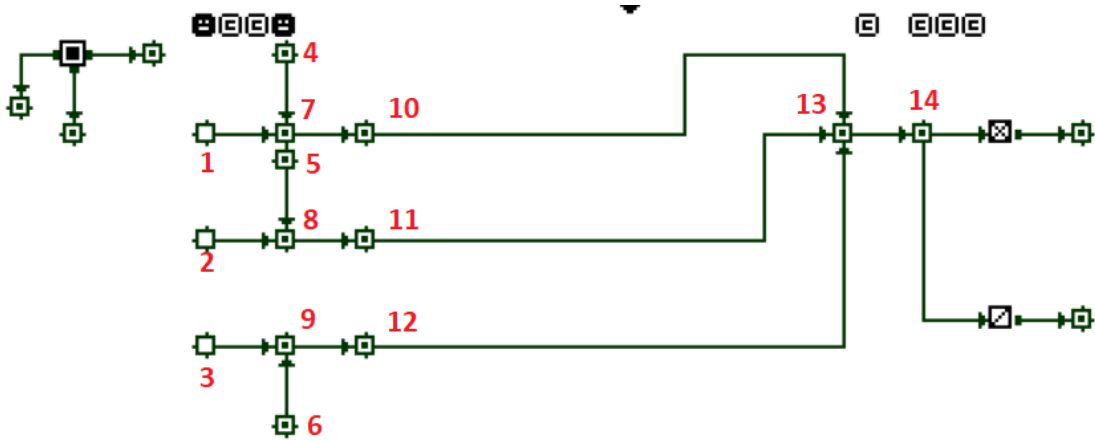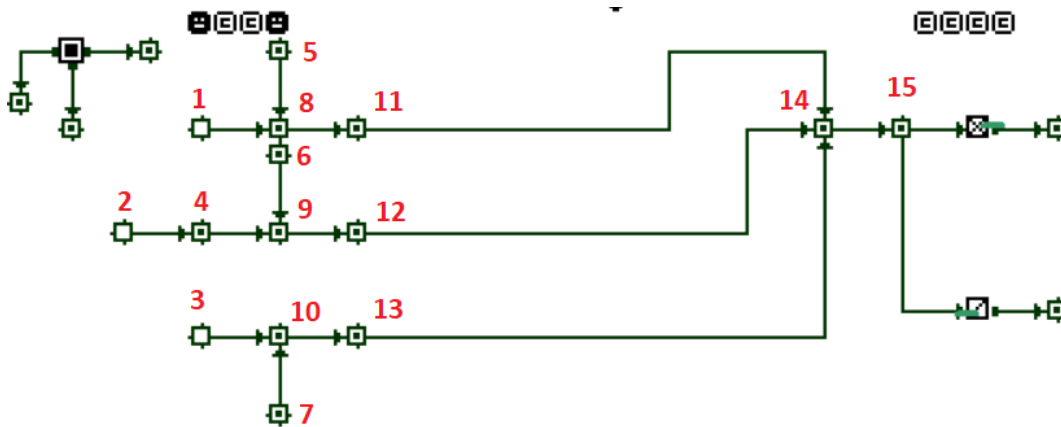

Figure 3.17: Case 3 - Control network in CONTAM

Figure 3.17 shows the control network in CONTAM. Elements 1 and 3 represent the CO_2 measurements. Element 2 performs HCHO measurements, with element 4 being a 30-minute running average. The running average assures the output of the measured HCHO level is in line with the limit guideline set by WHO. Elements 5 - 7 are constants representing the upper limit thresholds described in the control algorithm in Figure 3.16.

The two lower network branches are similar to the ones used in cases 1 and 2. The bottom one is a lower limit switch control that assures a minimum airflow rate of 6 % (5 m^3/h). The middle one is an upper limit switch control that increases the airflow rate to 25 % if the measured level of HCHO is higher than 100 $\mu g/m^3$.

The upper branch is the proportional CO_2 control. A subtract (8) calculates the deviation between the CO_2 measurement (1) and the upper limit constant (5). The deviation is sent to a proportional controller (11). The proportional constant $K_p = 0.01$ was found to be the best adaption. The K_p value was found by running a series of simulations and choosing the value that prevented fluctuations.

A maximum switch (14) compares the input signal from the three branches and selects the highest signal (highest required airflow rate). The control signal from the maximum switch is sent to a

signal split (15). The signal split sends the same control signal to the extract and supply control in the room.

3.3.5 Case 4 - HCHO proportional and CO_2 upper limit control

This control was designed with the same principles as case 3. The algorithm is based on HCHO measurements used to control the ventilation rate proportionally, and CO_2 measurements are used as an upper limit control to prevent CO_2 concentration from exceeding 1000 ppm. The logic of the control algorithm implemented in CONTAM is shown in Figure 3.18.
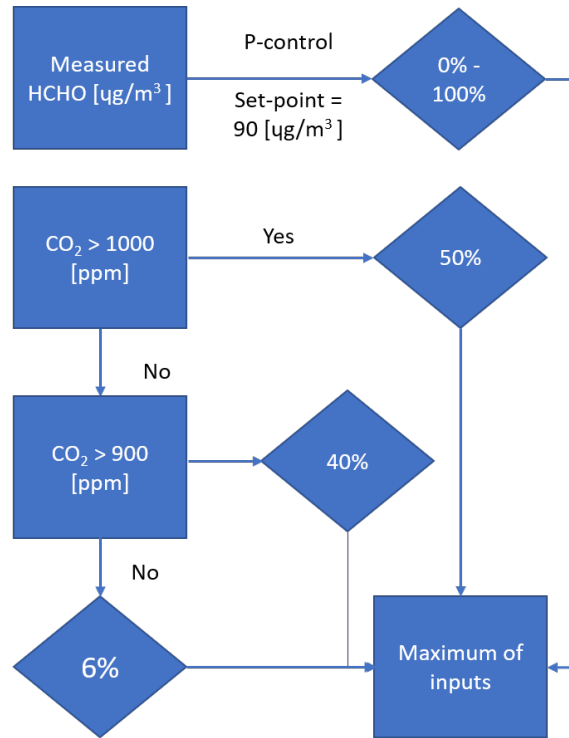
Figure 3.18: Case 4 - Control algorithm for proportional HCHO control and CO_2 upper limit.

The time step for the simulation was set to 1 minute. Based on Equation 2.5, with extract air concentration of 1000 ppm, outdoor concentration of 400 ppm, and a generation rate of 0.00546 L/s, the resulting required airflow rate is 33 m^3/h. Therefore, when indoor CO_2 concentration exceeds 900ppm, the airflow rate is set to 33 m^3/h (40% of the maximum design airflow rate). To comply with the demands in TEK 17, if the concentration of CO_2 is higher than 1000 ppm, the supply airflow rate is set to 42 m^3/h.
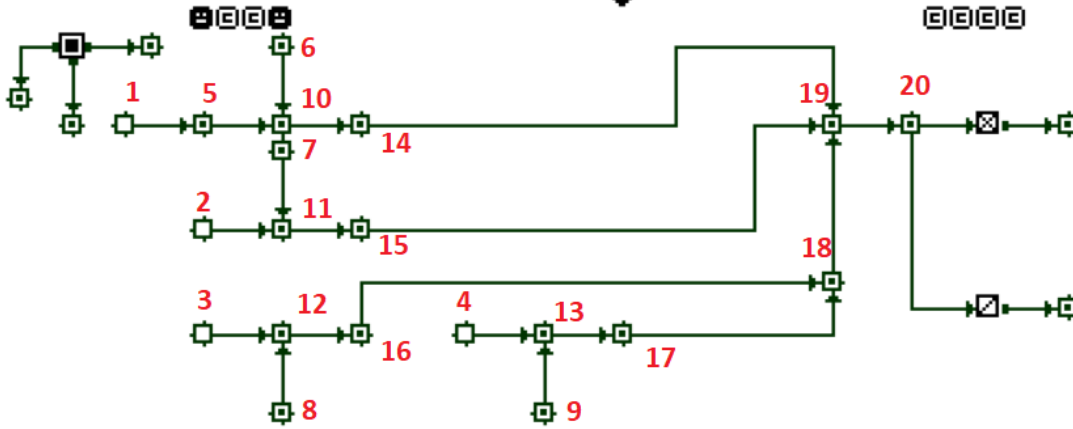
Figure 3.19: Case 4 - Control network in CONTAM

Figure 3.19 shows the control network implemented in CONTAM. This control was designed similar to case 3. The major difference is that the proportional controller is controlled by HCHO measurements instead of CO_2 measurements.

The upper branch was designed with measurements of HCHO concentration (1) which is transformed to a 30 minute averaged value (5). The measured HCHO concentration value is subtracted (10) from the constant upper limit value of 90 $\mu g/m^3$ (6). The deviation is sent to a proportional controller (14) with the proportional constant $K_p = 0.01$. As for case 3, the proportional constant was found by running a series of simulations.

The middle branch is the CO_2 upper limit control that measures CO_2 (2). The signal is sent to the upper limit switch (11), comparing the value to the upper limit constant of 900 ppm (7). The upper limit switch transmits a signal = 1 if the measured value is above 900 ppm and 0 if the value is below 900 ppm. A modifier (15) transforms the signal to 40 % if the upper limit switch is activated.

The two lower branches consist of an upper limit witch control and a lower limit switch control. The upper limit switch control set the airflow rate to 50 % ($42m^3/h$) if the measured CO_2 concentration is higher than 1000 ppm.

The lower limit switch control ensures a minimum airflow rate of 6 % (5 m^3/h). The indoor concentration of CO_2 is measured by element 3. The lower limit constant (8) is set to 1 ppm, assuring that the lower limit switch is always "true". Therefore, the modifier (12) transmits a signal of 6 % at all times. A maximum switch only has three possible inputs. Therefore, an additional maximum switch (18) is used to compare the two lower control branches.

As for the other controls, a maximum switch (19) transmits the highest value from the branches to be sent on to control the supply and extract airflow rate.

3.3.6 Case 5 - CO_2 proportional and temperature upper limit control

Figure 3.20 shows the temperature and CO_2 control. As for case 3, proportional control is set to prevent the concentration of CO_2 from exceeding 1000 ppm. In addition, an upper limit control is set to prevent the temperature from exceeding 23 °C.
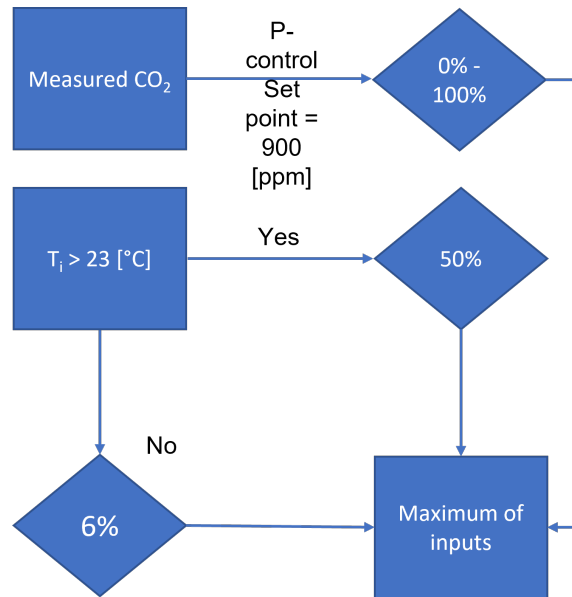
Figure 3.20: Case 5 - Control algorithm for proportional CO_2 and upper limit indoor air temperature (T_i) control.

Since the indoor air temperature is a part of the control strategy for case 5, the case was not suitable to be simulated with other recirculation strategies than the base case with 100 % OAF.
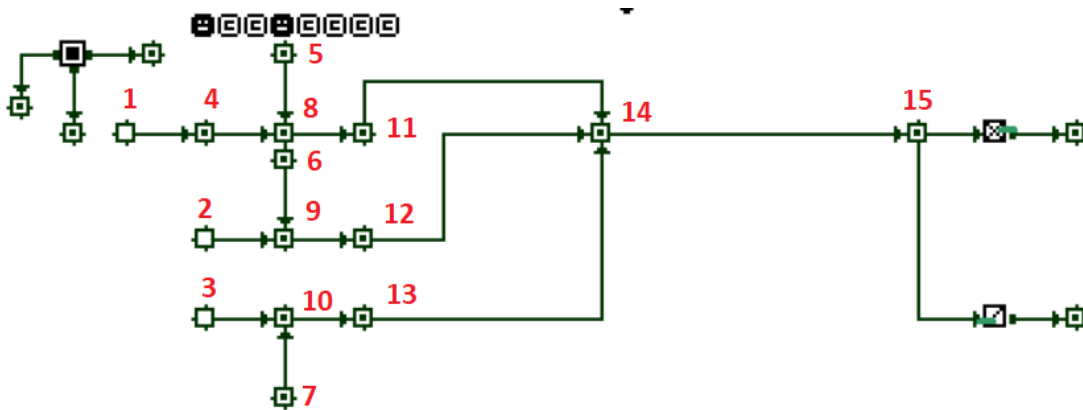
Figure 3.21: Case 5 - Control network in CONTAM

Figure 3.21 shows how the control network was constructed in CONTAM. As for the other cases, elements 1-3 represent measurements of pollutants, where 1 measures temperature and the others measure CO_2. The upper branch of the control network is the temperature control. Element 4 calculates the 30 min average to avoid fluctuations. The signal is then sent to an upper limit switch (8). The upper limit switch transmits "true" if the measured value is higher than the upper limit constant (5) of 23 °C. Then, the signal is sent to a modifier (11). If the upper limit switch is "true", the modifier alters the signal to be 50 %.

The middle branch of the network is the CO_2 proportional control. The measured concentration (2) of CO_2 is subtracted (9) from the upper limit constant (6). The deviation is sent to a proportional controller (12). The proportional constant K_p is set to 0.01. The procedure for selecting the correct K_p was the same as for cases 3 and 4.

The lower branch is a lower limit switch control to ensure a minimum airflow rate of 5 m^3/h. The lower limit control branch is a copy of the one used in case 4.

3.3.7 Recirculation control A - CO_2

This control is based on indoor CO_2 measurements in each room. The room with the highest amount of CO_2 concentration is the decisive parameter in the simulation. The logic of the control is shown in Figure 3.22. As shown, the base OAF for this control is 20 %. Based on indoor concentration of CO_2 the OAF will rise to 50 and ultimately 100 %.
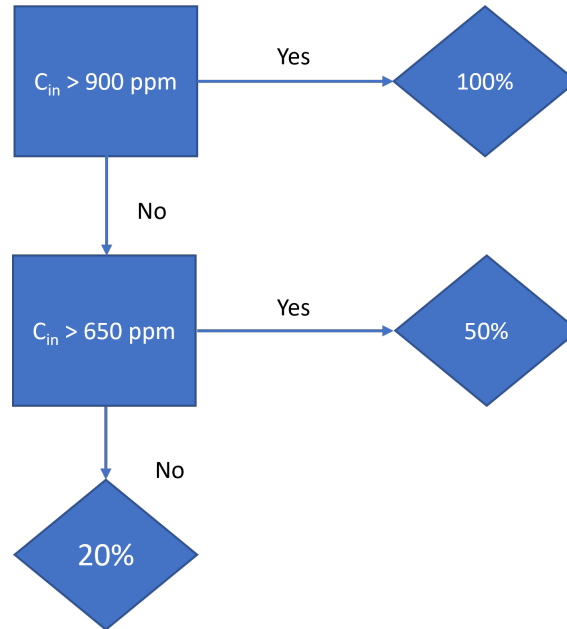
Figure 3.22: Recirculation control A - Control strategy based on CO_2 measurements.

Figure 3.23 shows how the control network was set up in CONTAM. Elements 1-3 represent the CO_2 measurements. Elements 4 and 5 are upper limit switches that are activated if the CO_2 concentration is higher than the upper limit constant of 900 ppm (7) or 650 ppm (8). If an upper limit switch is activated, the signal is modified by elements 10 or 11 to 100 % or 50 %. The lower branch is a lower limit switch (6) connected to a modifier (12) that transmits a 20 % signal at all times. All the signals from the modifiers are sent to a maximum switch (13). The maximum switch transmits the highest value to be sent further. This control is equal for all three rooms connected to the AHU. The highest measured CO_2 concentration from the three rooms decides the OAF. A global maximum switch ensures this. Figure 3.24 shows how the control signals from all of the rooms are sent to the global maximum switch. The highest value then controls the OAF.
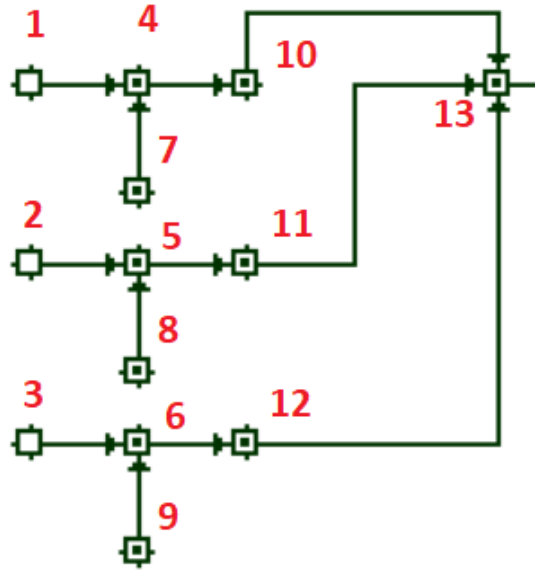
Figure 3.23: Recirculation control A - CONTAM control network.
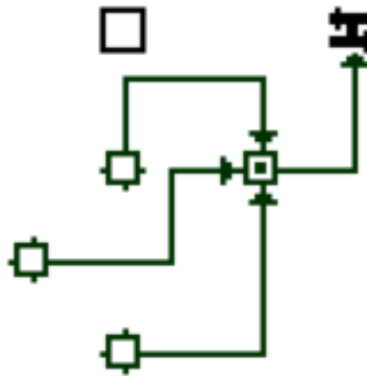
Figure 3.24: Recirculation control - AHU.

3.3.8   Recirculation control B - CO$_2$ and HCHO

The control strategy is based on CO$_2$ and HCHO measurements. Each parameter has an upper limit value that decides which parameter is decisive for the control. As for recirculation control A, the room with the highest concentration is decisive. The logic of the control is shown in Figure 3.25.
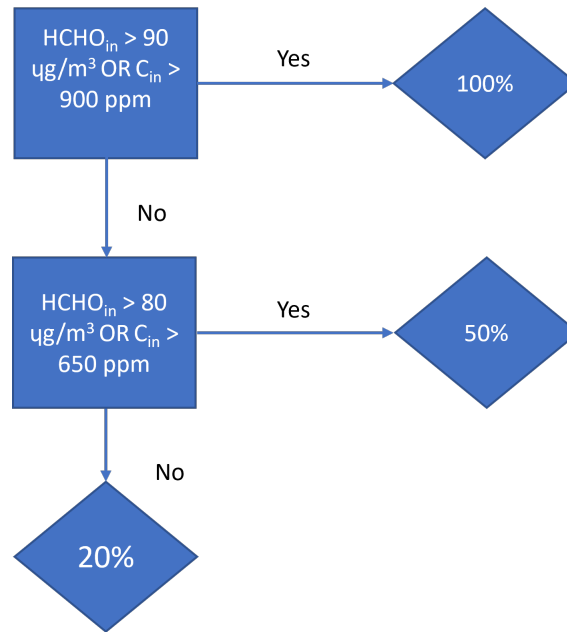
Figure 3.25: Recirculation control B - Control strategy based on CO_2 and HCHO measurements.

The control network was constructed with the same principles as for recirculation control A. The control network for CO_2 control was copied from case A, and an additional network based on HCHO measurements was constructed in the exact same way as shown in Figure 3.23. Figure 3.26 shows the control network for recirculation control B. The lower branch (A) is a copy of the CO_2 control from recirculation control A. The upper branch is an HCHO control constructed with two upper limit switches activated at 90 and 80 $\mu g/m^3$ and a lower limit switch ensuring a signal of 20% at all times. A maximum switch(1) transmits the highest signal based on the HCHO measurements to another maximum switch (2). The maximum switch (2) compares the CO_2 and HCHO control outputs and transmits the highest value to the AHU OAF control. The AHU control network is identical to the one used in control A, shown in Figure 3.24.
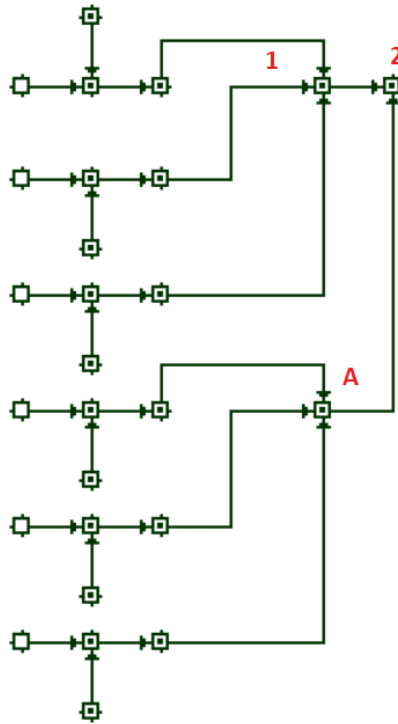
Figure 3.26: Recirculation control B - CONTAM control network.

3.3.9   Recirculation control C - PM$_{2.5}$

This recirculation control is based on indoor measurements of PM$_{2.5}$. The main reasoning for the control is that the indoor concentration of PM$_{2.5}$ depends on the outdoor air concentration of particulate matter. Lowering the OAF will lower the overall concentration of indoor particulate matter. Figure 3.27 shows the control algorithm implemented in the CONTAM simulations.
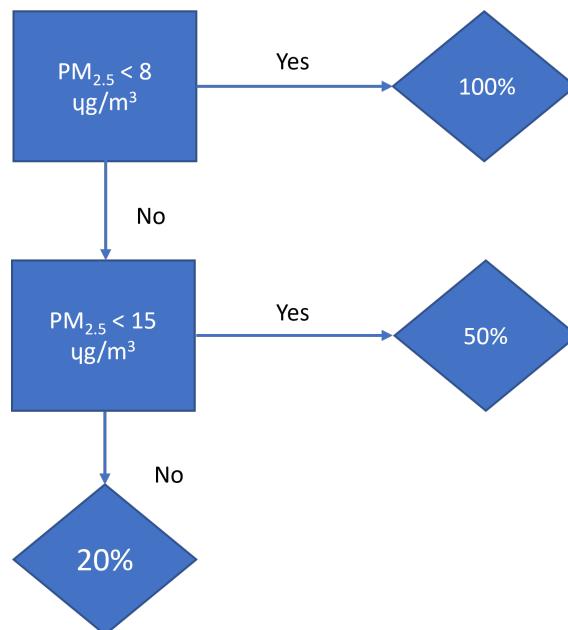
Figure 3.27: Recirculation control C - Control strategy based on PM$_{2.5}$ measurements.

As the algorithm shows, the base OAF is 100 %. If the indoor air concentration of $PM_{2.5}$ is between 8 $\mu g/m^3$ and 15 $\mu g/m^3$ the OAF is set to 50 %. If the measured indoor concentration is higher than 15 $\mu g/m^3$, the OAF is set to 20 %.

Figure 3.28 shows the control network in CONTAM. Elements 1-3 represent measurements of $PM_{2.5}$. Elements 4 and 5 are upper limit switches connected to upper limit constants (7 and 8). If the measured concentration is higher than 15 $\mu g/m^3$ the modifier (10) transmits a signal of 20 %. If the measured concentration is higher than 8 $\mu g/m^3$, the modifier (11) transmits a signal of 50 %. The lower branch consists of a lower limit switch (6) activated at all times because the lower limit constant (9) is set to 0.1. Therefore, the modifier (12) will always transmit a signal of 100 %. A minimum switch (13) ensures that the signal transmitted to the OAF control at the AHU is the lowest. The OAF control at the AHU is equal to the one used for recirculation control A and B, except that a global minimum switch replaces the global maximum switch. The minimum switch ensures that the room with the highest indoor concentration of $PM_{2.5}$ controls the OAF.
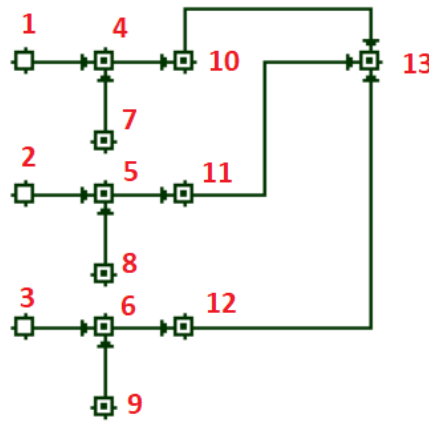
Figure 3.28: Recirculation control C - CONTAM control network.

3.3.10 Assessment of IAQ

As described in Section 2.1, the resulting IAQ can be assessed by investigating the concentration of indoor air pollutants and temperature. The assessment of IAQ was conducted by analyzing the number of hours exceeding the threshold limits presented. In addition, the resulting CO_2 concentration for each case was used to calculate the PPD according to Figure 2.1.

3.3.11 Calculation of energy use

The aim for DCV is to lower the energy use while maintaining or increasing the IAQ. A simplified calculation was used to compare the possible energy savings. The energy consumption was not given directly by the simulation output. Therefore, an approach to estimate the energy consumption for ventilation was found by calculating the supply air's annual heating and cooling demand. Equation 2.6 was used as a basis to calculate the energy demand for heating of the supply air after passing through the heat exchanger.

Some assumptions have to be made to calculate the energy use for heating. According to the manufacturer of the UNI 2 AHU, the efficiency of the heat exchanger η_T is 75 %. Therefore, η_T was set to 75 % in the calculation. To calculate the energy use, the constructed indoor air temperature described in Section 3.2.6 was used as extract air temperature. For simplicity, the temperature in room 1 was used as the general extract air temperature. The supply air temperature

after the air had passed to the heat exchanger was found by Equation 3.1 (Ingebrigtsen 2015).

$$T_{supply} = \eta_T \cdot (T_{extract} - T_{out}) + T_{out} \qquad (3.1)$$

Then the energy demand for heating the supply air to the desired set point temperature was found by Equation 3.2 (Ingebrigtsen 2015).

$$\Phi = \dot{V} \cdot \rho \cdot C_{pl} \cdot (T_{set} - T_{supply}) \qquad (3.2)$$

In the calculations C_{pl} was set to 1005 $[J/(kg \cdot K)]$ and ρ was set to 1.2 [kg/m^3]. An example of the calculation of heating demand for one time-step i shown in Appendix B.1.

Equation 2.7 was used to calculate and estimate the energy use for operating the supply and extract fan. The fan diagrams for the UNI 2 AHU were used to calculate the SFP during and outside the working hours. The fan diagrams are available in Appendix C.1. When calculating the SFP, the same work-line was used for all calculations. The work-line is marked with an X in Figure 3.29.
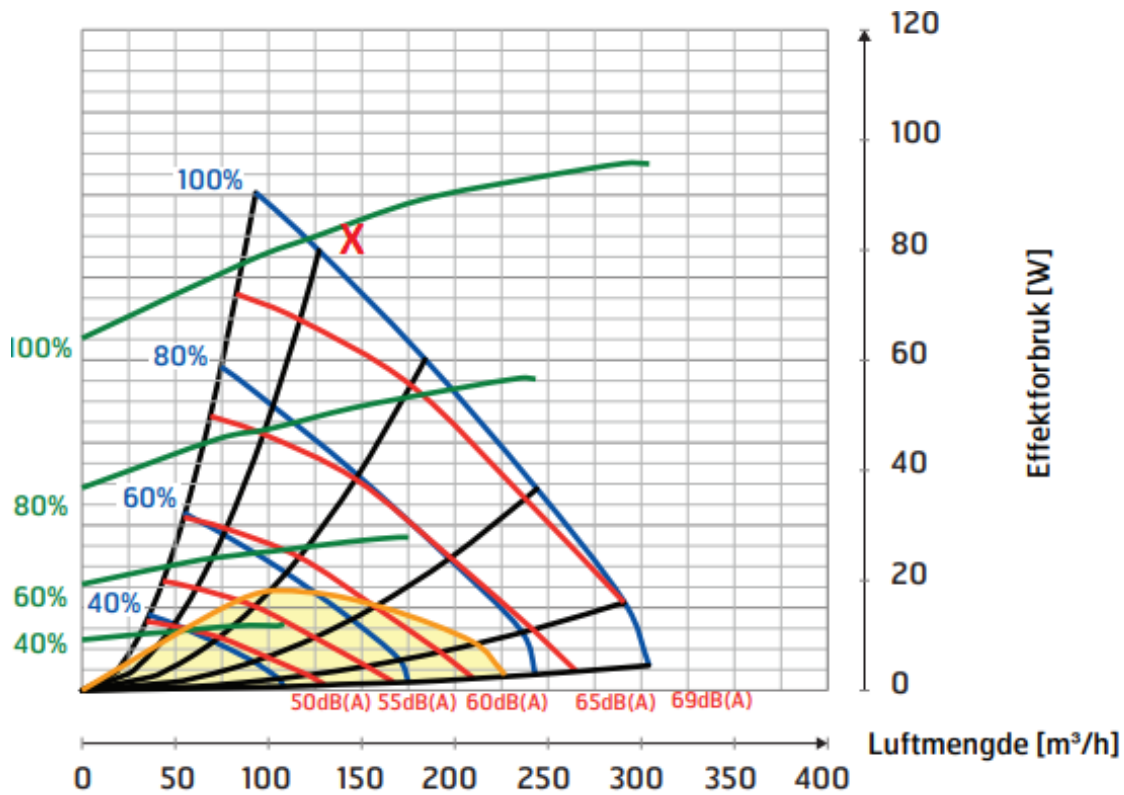
Figure 3.29: Fan diagram for supply fan.

Chapter 4

Results

This chapter presents the results from the simulations conducted in CONTAM. First, the simulations are presented as graphs displaying the supply airflow rate, the concentration of CO_2, HCHO and $PM_{2.5}$, and the performance for the recirculation control algorithms. Then the resulting energy use for heating of the supply air and power consumption of the fans is presented. For each of the simulated cases, a weekday is presented.

4.1 IAQ and ventilation

The following subsections presents the ventilation rates and IAQ for the 5 DCV control cases and the CAV case simulated in CONTAM. The results are presented as graphs displaying the indoor pollutants in each room (1,2,3). In addition, the airflow rates and resulting OAF for the recirculation cases (A, B, C) are presented.

4.1.1 Case - CAV

Figure 4.1 shows the indoor air concentration of CO_2 and HCHO when the ventilation is controlled with traditional CAV. Since the HCHO generation rate is calculated to be higher than for a low polluting building, the HCHO concentration exceeds 100 $\mu g/m^3$ outside working hours. Most of the time, the CO_2 concentration is kept below 1000 ppm, but for room 1, the extra person present from 11.30 - 12.30 increases the CO_2 level for a short period.
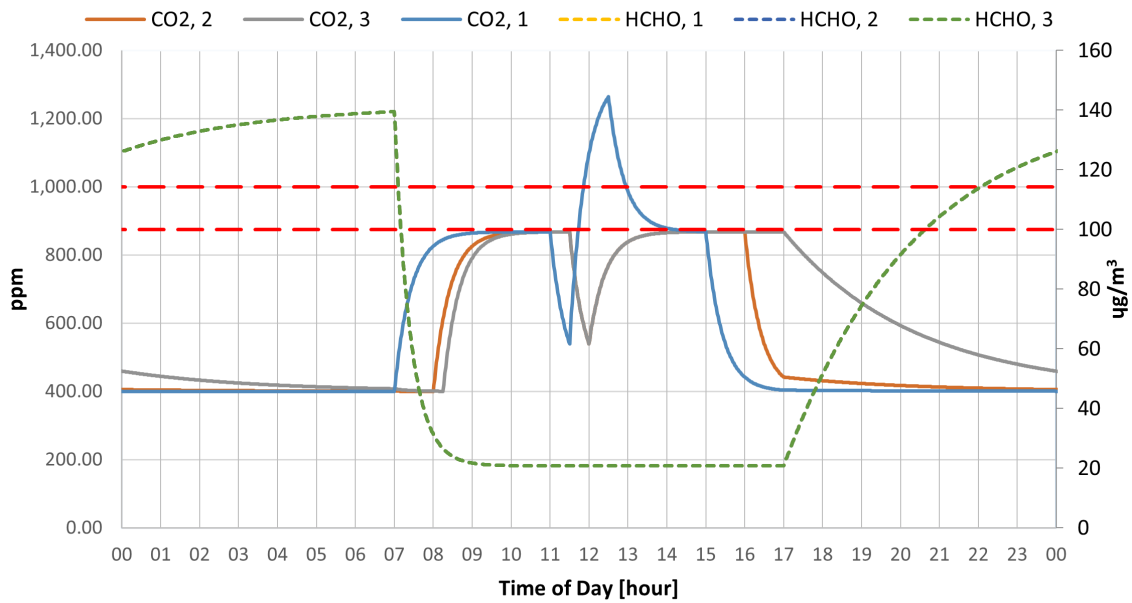
Figure 4.1: CAV - Concentration of CO_2 and HCHO on a weekday.

In addition to the supply airflow rates, Figure 4.2 shows the indoor air concentration of $PM_{2.5}$. The $PM_{2.5}$ is at all times kept within acceptable levels.
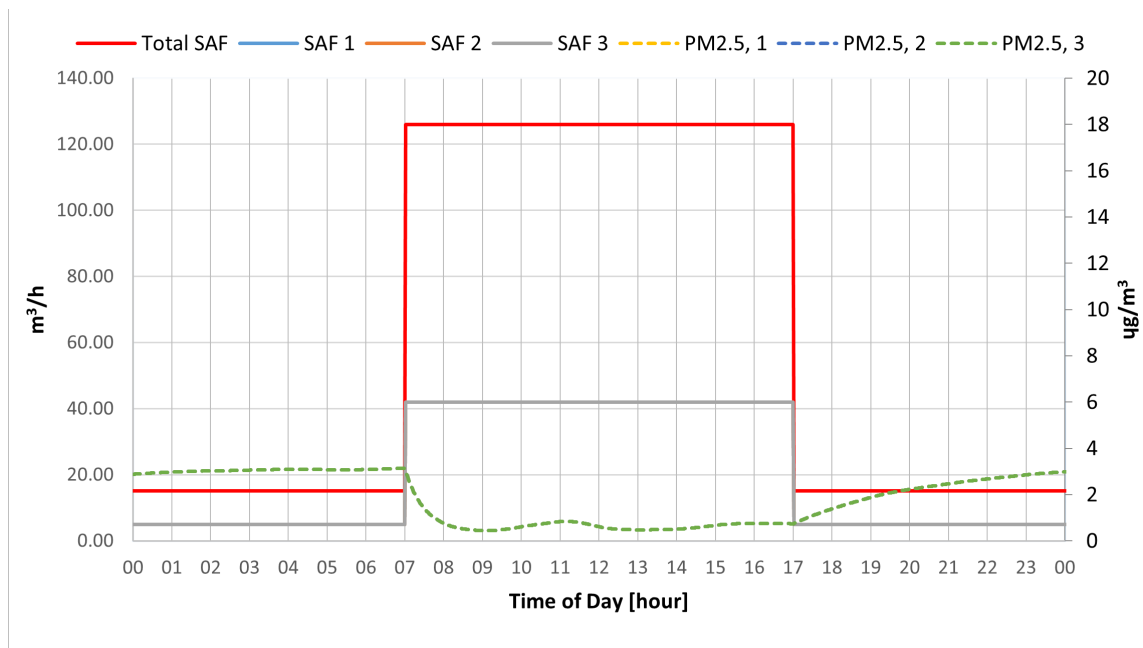
Figure 4.2: CAV - Concentration of $PM_{2.5}$ and supply airflow rates on a weekday.

Figure 4.3 shows that the indoor air temperature is kept around 21 °C for most of the time. As expected, the CAV ventilation control achieves good IAQ. Since the offices are designed for one person only, it can not be expected that the ventilation will keep the CO_2 concentration below 1000 ppm when the room is over-occupied.
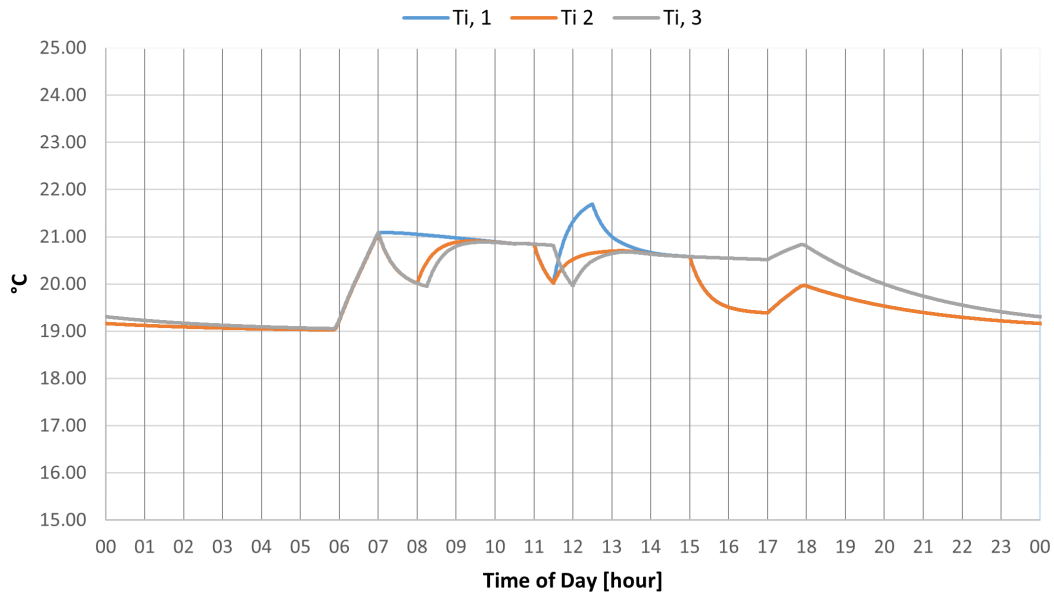
Figure 4.3: CAV - Resulting indoor air temperature on a weekday.

4.1.2   Case 1 - Upper limit CO_2

100 % OAF

Figure 4.4 and 4.5 shows the concentration of CO_2 , HCHO, $PM_{2.5}$ and the distribution of the supply airflow rates.
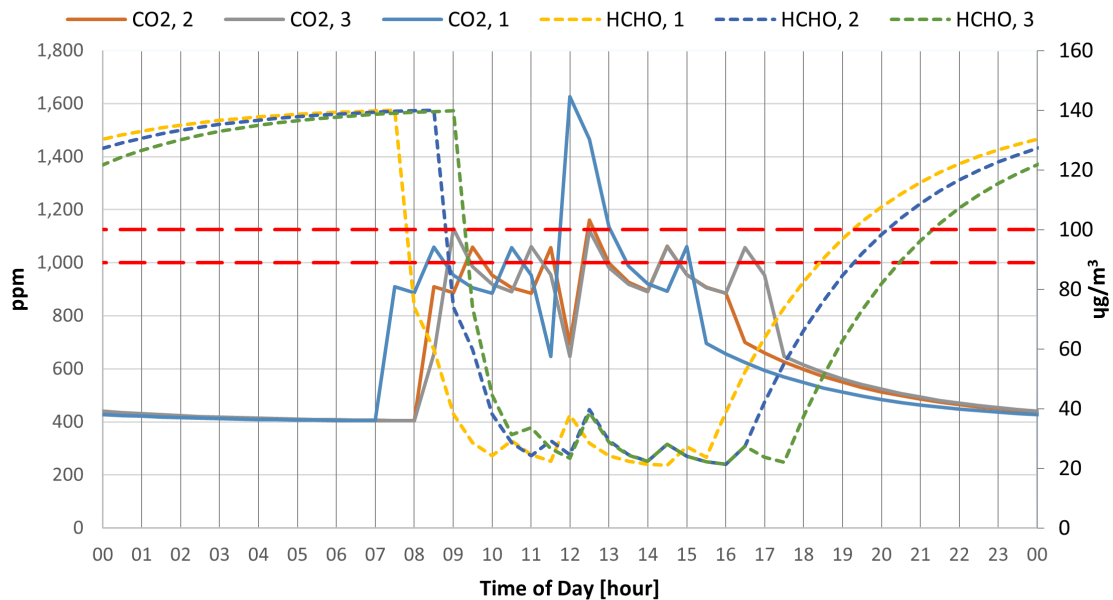
Figure 4.4: Case 1 - Concentration of CO_2 and HCHO with 100% OAF on a weekday.

The graph presenting CO_2 shows that the concentration is kept below 1000 ppm for most of the day. However, as expected, with increased occupancy in room one from 11:30 until 12:30, there

is a significant rise in the CO_2 concentration. The concentration of HCHO is below the threshold of 100 $\mu g/m^3$ during working hours. Outside working hours, the concentration of HCHO is above the threshold marker. This indicates that the minimum airflow rate is too low compared to the generation rate of HCHO. The minimum ventilation is set to be the "common" ventilation rate used for unoccupied rooms. This ventilation rate is calculated for buildings that can be classified as low polluting. As the figure shows, this ventilation rate is not enough when the generation rate for HCHO is set to 691 $\mu g/h$.
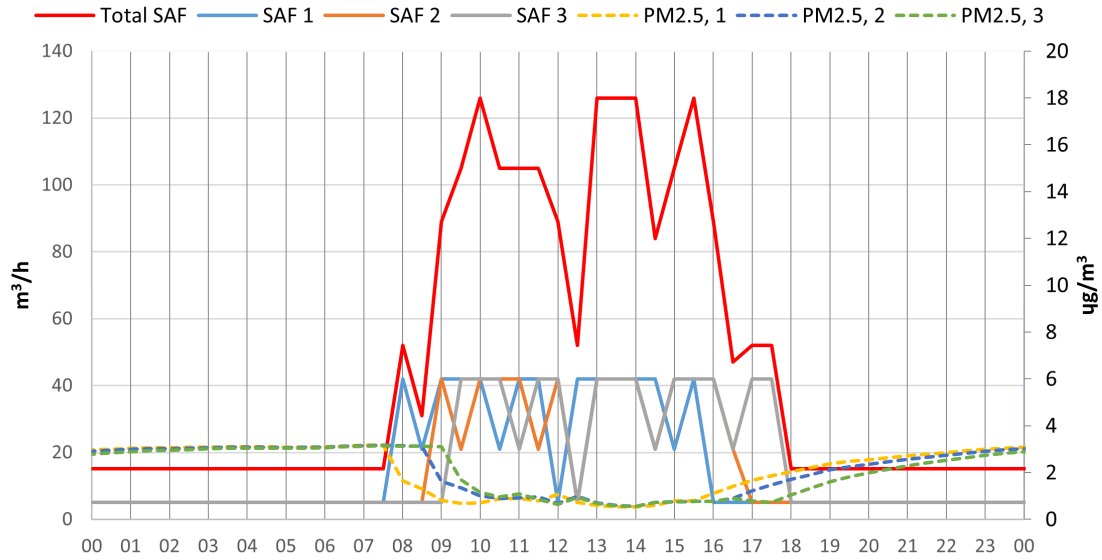
Figure 4.5: Case 1 - Concentration of PM$_{2.5}$ and supply airflow rates with 100% OAF on a weekday.

Since the highest amount of supply air in each room is set to 42 m^3/h in this case, the supply airflow rate is at max for most of the working hours with this control. However, the overall total supply airflow rate is lower than for the CAV case. Figure 4.6 shows that the indoor air temperature is slightly higher than for CAV but still acceptable.
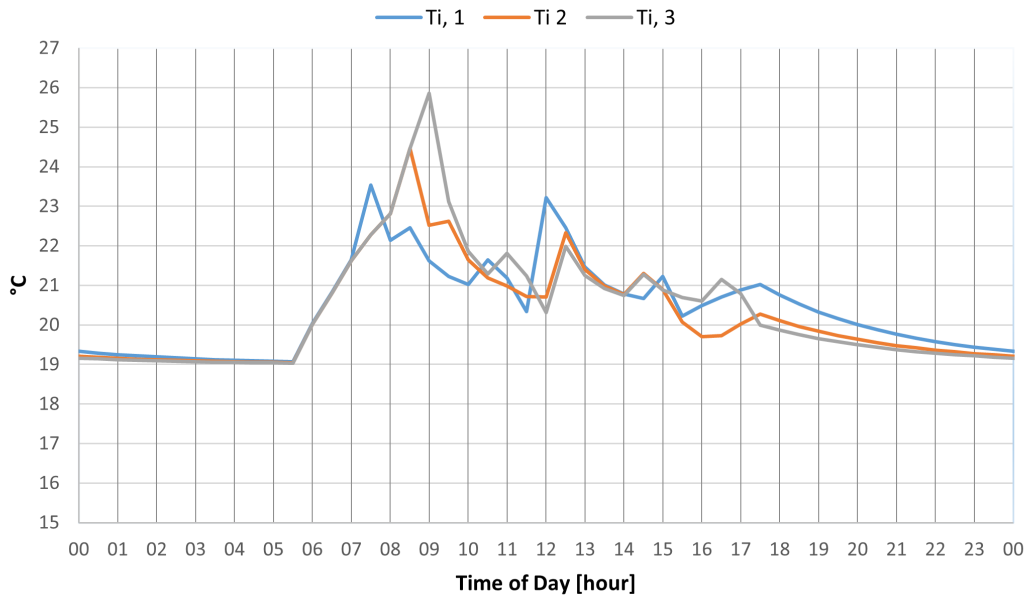
Figure 4.6: Case 1 - Resulting indoor air temperature on a weekday.

4.1.3 Case 2 - Upper limit HCHO

100 % OAF

Figure 4.7 and 4.8 shows the concentration of CO_2, HCHO, $PM_{2.5}$ and the supply airflow rates for room 1,2, and 3 in addition to the total supply airflow rate from the AHU for Case 2 with 100 % OAF.
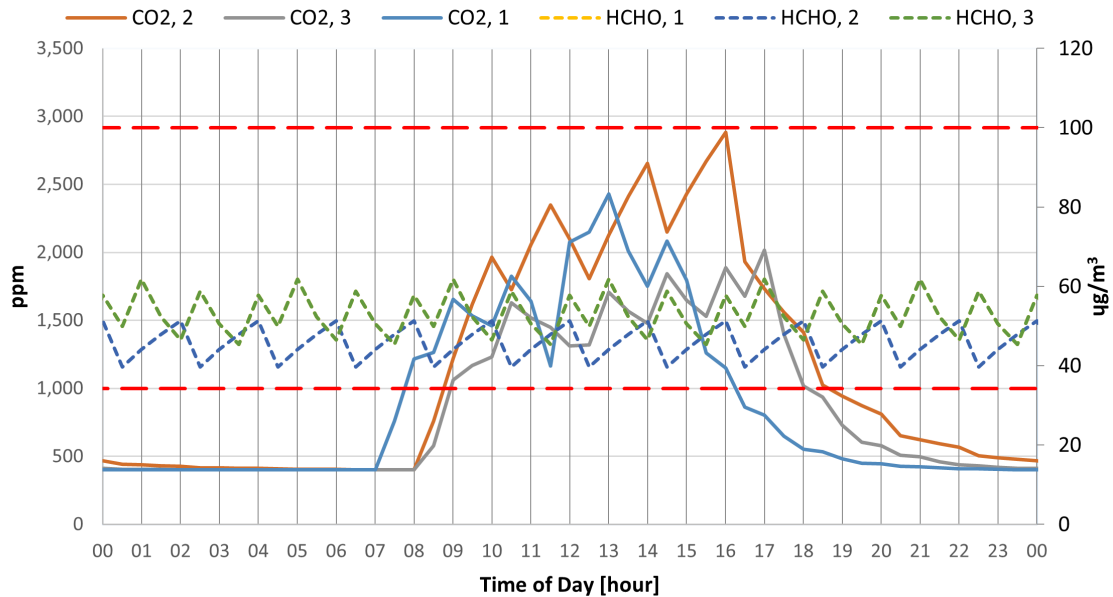
Figure 4.7: Case 2 - Concentration of CO_2 and HCHO with 100% OAF on a weekday.

Figure 4.7 shows that the concentration of CO_2 quickly rises above the threshold of 1000 ppm when

the rooms are occupied. The concentration of HCHO is kept way below the threshold marker of $100 \ \mu g/m^3$ at all times. The concentration of HCHO is kept fluctuating around $50 \ \mu g/m^3$. This shows a significant gap in the required airflow rates to ensure an acceptable CO_2 concentration compared to an acceptable HCHO concentration. The main reasoning for this specific control was to compare results from the simulation with measurements in the laboratory. However, the results show that DCV solely based on HCHO measurements will not achieve acceptable IAQ.
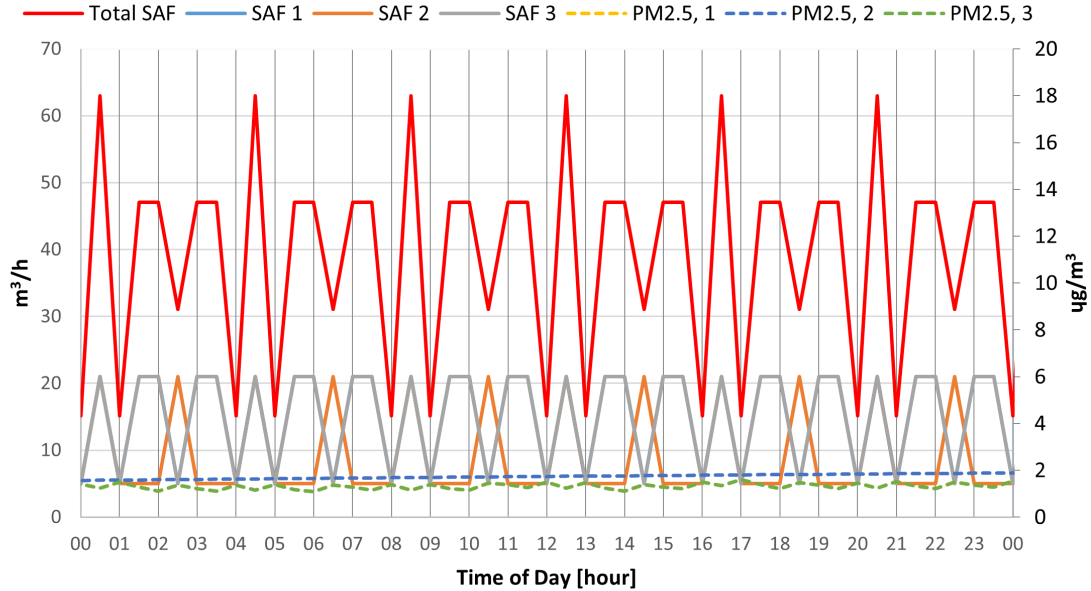
Figure 4.8: Case 2 - Concentration of $PM_{2.5}$ and supply airflow rates with 100% OAF on a weekday.

Figure 4.8 shows that the emission rate of HCHO used in the simulation is not strong enough to get the required fresh air demand higher than 50 % of the design airflow rate calculated by the standards set in TEK 17. The most obvious point to be taken from this control is that stand-alone HCHO control fails to ensure good IAQ within working hours.

4.1.4 Case 3 - Proportional CO_2 with upper limit HCHO

100 % OAF

Figure 4.9 and 4.10 shows the concentration of CO_2, HCHO, $PM_{2.5}$ and the supply airflow rates for room 1,2, and 3 in addition to the total supply airflow rate from the AHU for Case 3 with 100 % OAF.
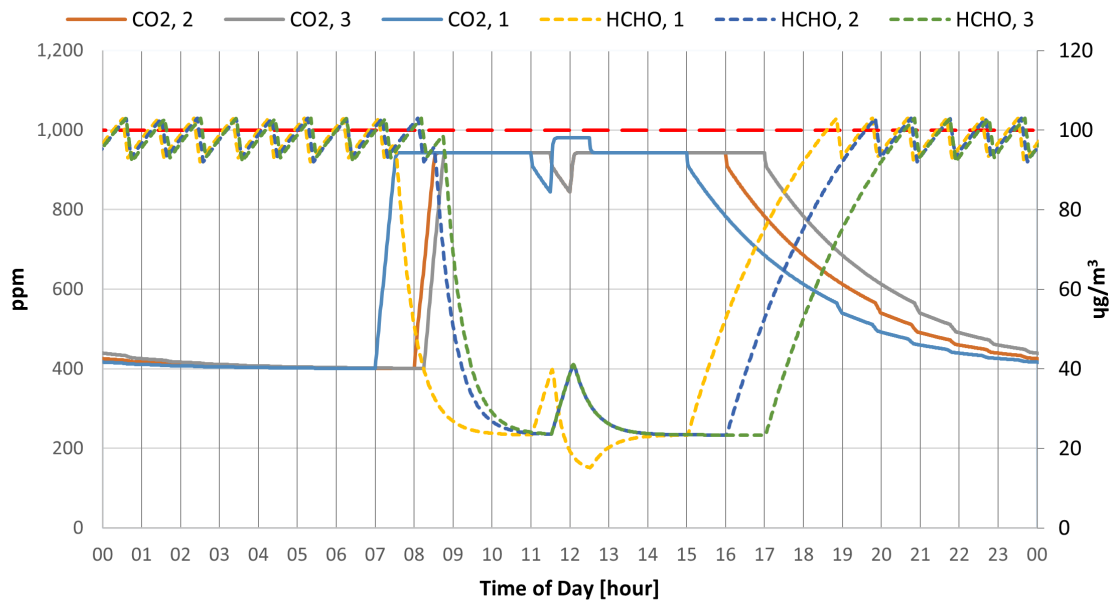
Figure 4.9: Case 3 - Concentration of CO_2 and HCHO with 100 % OAF on a weekday.

This control algorithm manages to keep the CO_2 concentration below 1000 ppm in all rooms. During working hours, the CO_2 measurements control the supply airflow, and the HCHO concentration is kept way below the threshold. Outside working hours, the HCHO concentration controls the supply airflow, and the concentration of HCHO is kept fluctuating around 100 $\mu g/m^3$.
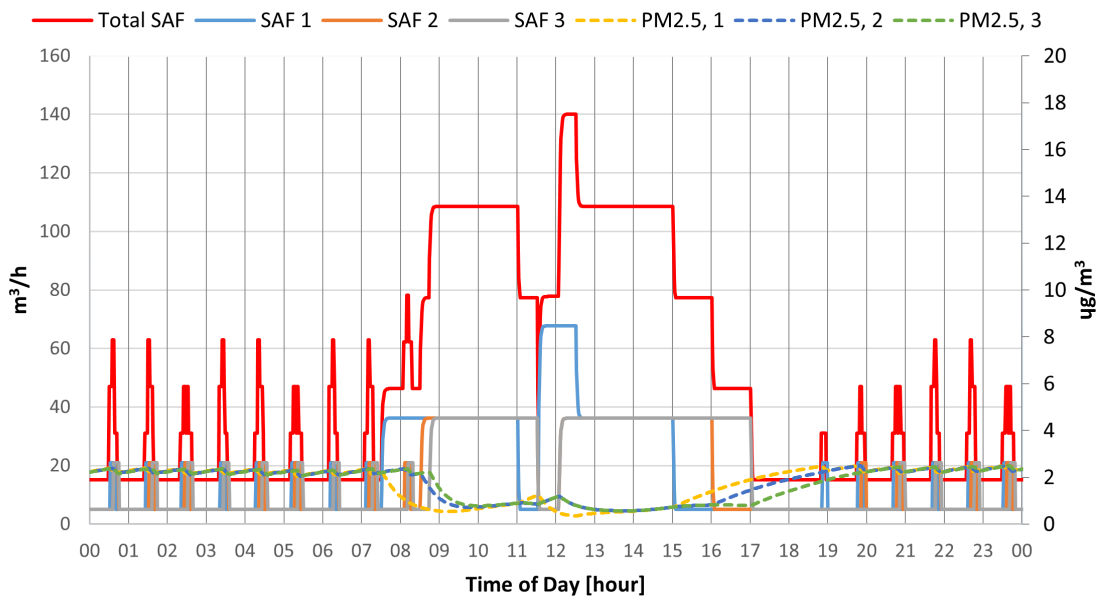
Figure 4.10: Case 3 - Concentration of $PM_{2.5}$ and supply airflow rates with 100 % OAF on a weekday.

As seen in Figure 4.10, the required total supply airflow rate is below 100% of the minimum airflow rate set by TEK 17 for most of the time. However, the supply airflow is higher than the standards set by TEK 17 for room 1 when there are two people present in the room. As shown by the graphs for HCHO in Figure 4.9 and the supply airflow graphs in Figure 4.10, the airflow is increased and

lowered between 21 m^3/h and $5m^3/h$ one time every hour, outside the working hours.

Figure 4.11 shows how the control manages to keep the indoor air temperature at acceptable levels at all times during a weekday. The peak in temperature is early in the day, between 08.00 and 09.00. When the ventilation rate is increased, the indoor air temperature is quickly reduced.
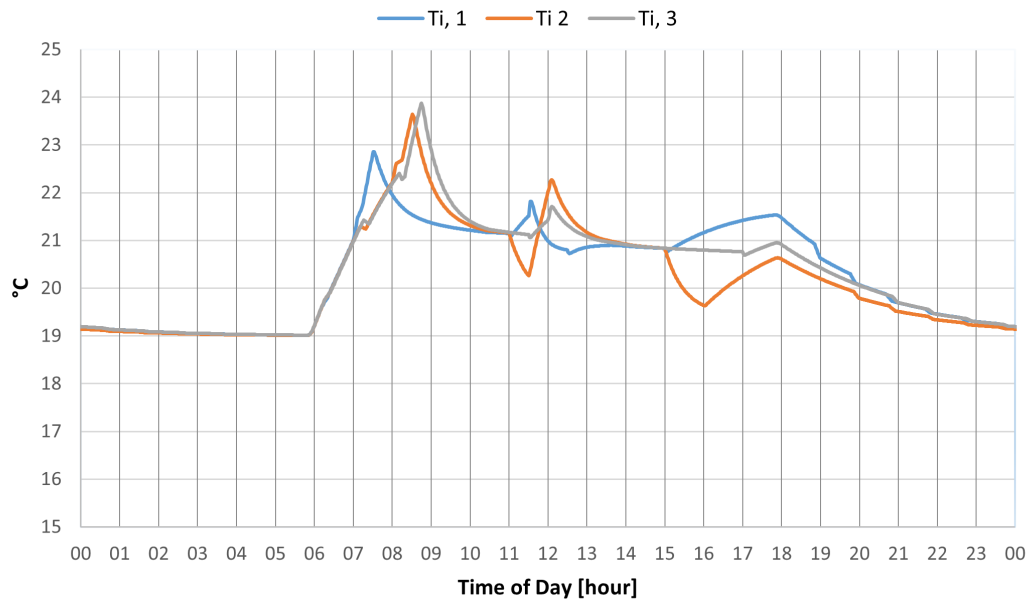
Figure 4.11: Case 3 - Indoor air temperature with 100 % OAF on a weekday.

Low polluting building - 100 % OAF

Figure 4.12 shows the concentration of CO_2 and HCHO if the generation rate in the rooms is set to be equal to a low polluting building (350 $\mu g/h$). The graph shows that the base ventilation outside working hours is enough to prevent the accumulation of HCHO outside working hours.
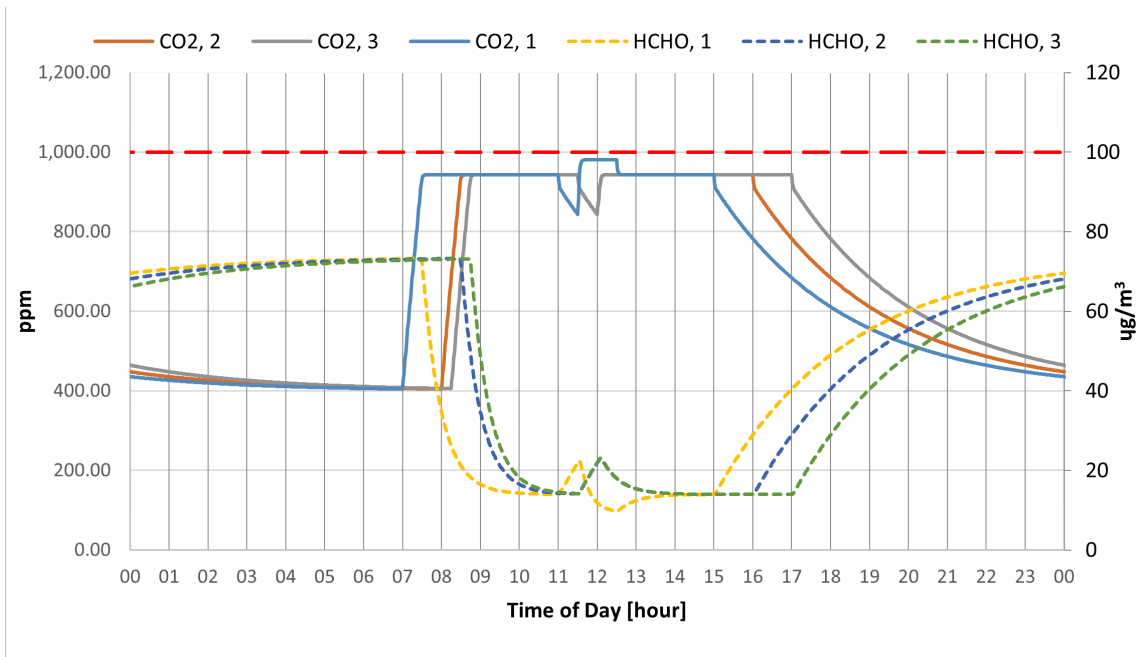
Figure 4.12: Case 3 - Concentration of CO_2 and HCHO with 100 % OAF and lower HCHO generation rate on a weekday.

As seen by Figure 4.12, the lower generation rate of HCHO lowers and stabilizes the ventilation outside the working hours. Since the level of HCHO never exceeds the threshold limit, the fluctuation is avoided as seen in Figure 4.13.
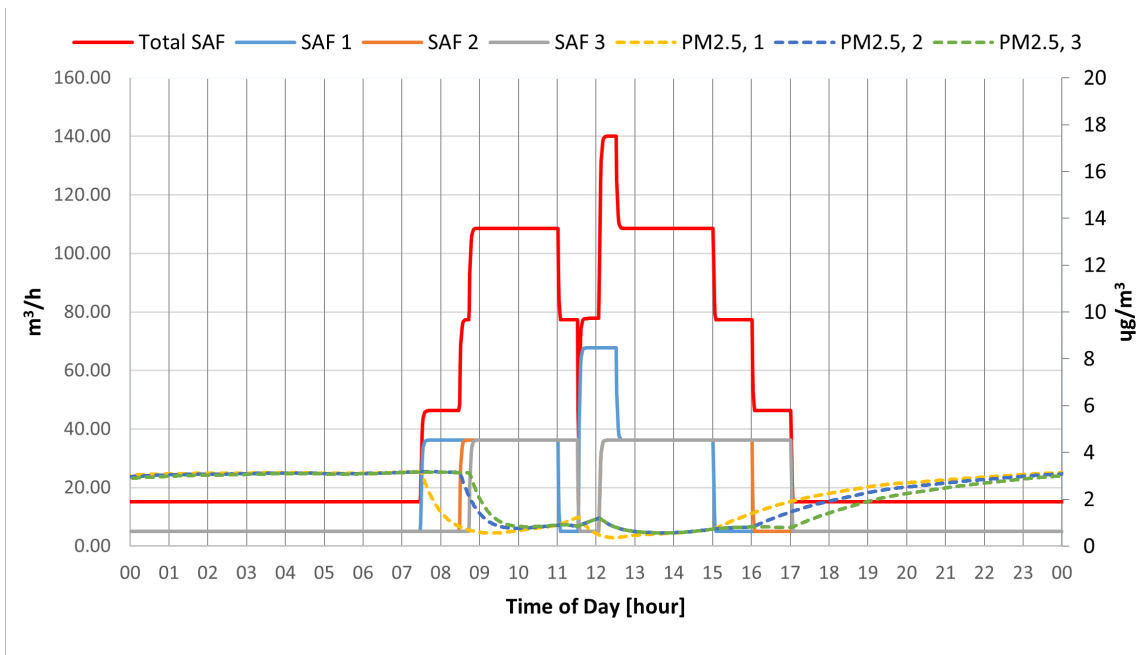
Figure 4.13: Case 3 - Ventilation rates and distribution of $PM_{2.5}$ with 100% OAF and lower HCHO generation rate on a weekday.

Recirculation control A - OAF controlled by indoor concentration of CO_2
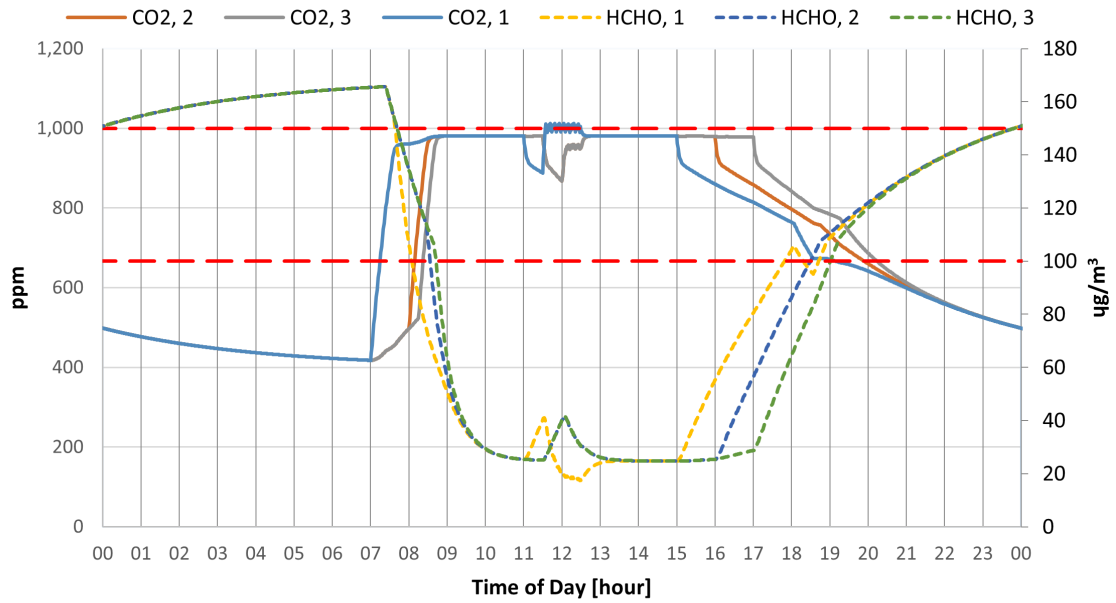
Figure 4.14: Case 3 - concentration of CO_2 and HCHO with OAF controlled by CO_2 measurements on a weekday.

Figure 4.14 shows the concentration of CO_2 and HCHO when the recirculation is controlled by indoor CO_2 measurements. For this case, the CO_2 is kept at an acceptable level, but HCHO exceeds the threshold limit outside the working hours. However, the recirculation control introduces fluctuations.

Figure 4.15 shows the distribution of supply airflows. Because the CO_2 is controlled by a proportional control, the supply airflow rate is increased to counteract the reduced OAF.
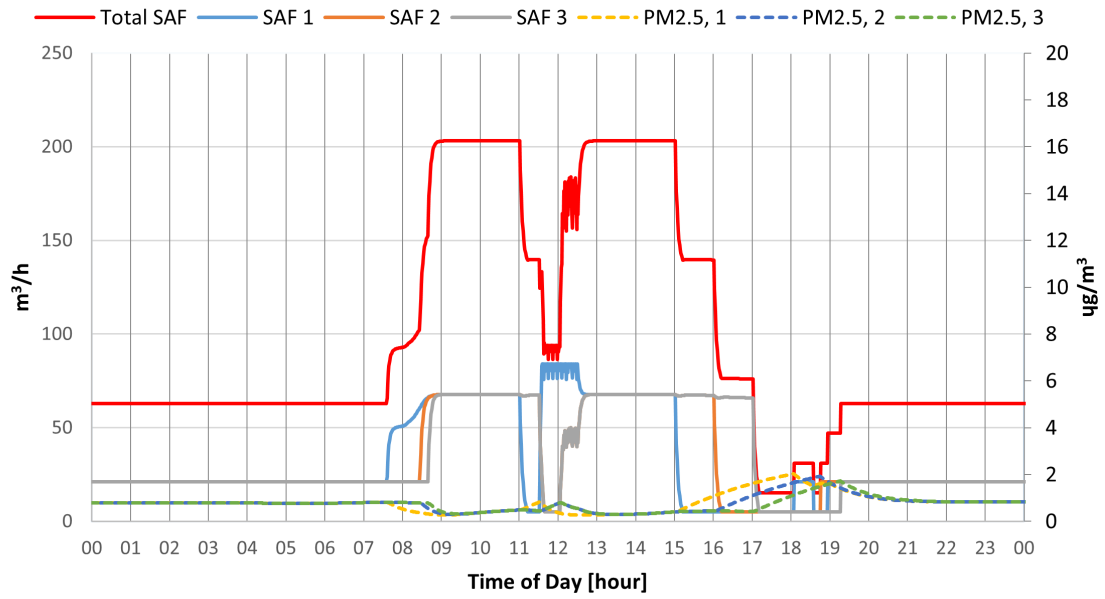
Figure 4.15: Case 3 - Concentration of $PM_{2.5}$ and supply airflow rates with OAF controlled by indoor air concentration of CO_2.
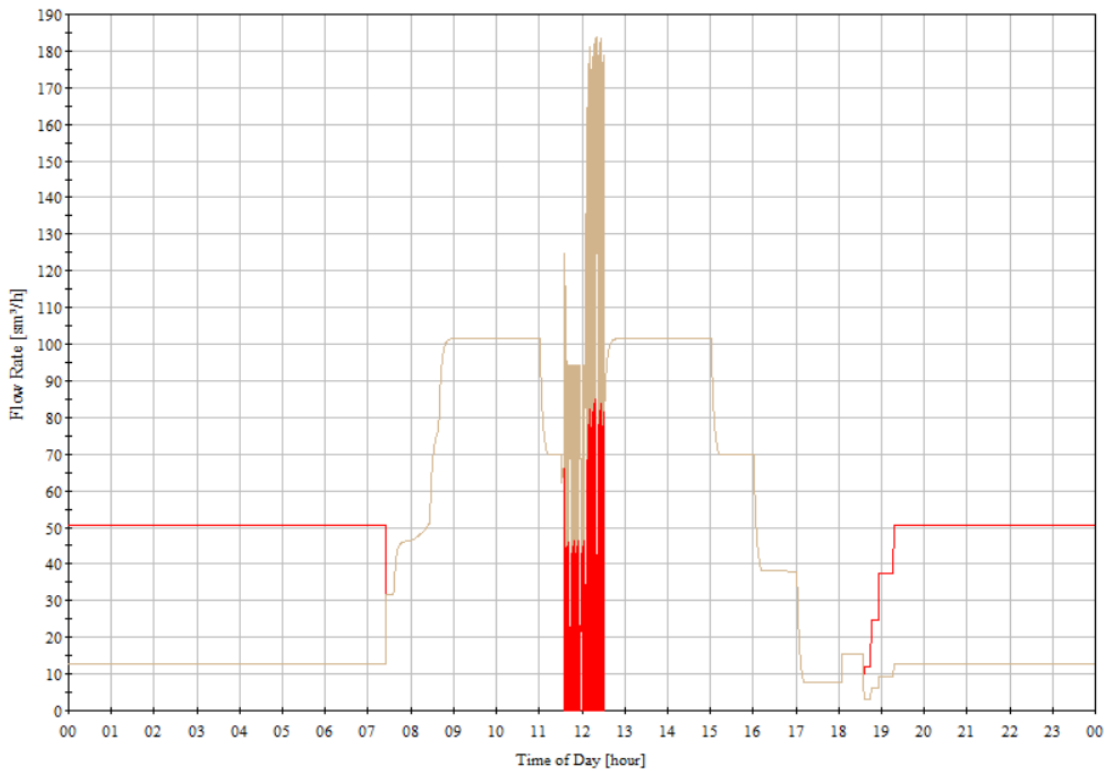
Figure 4.16: Case 3 - Recirculated air (Red) and outdoor air(brown) for recirculation control A.

Figure 4.16 shows the amount of recirculated air. The graph shows that the control of the recirculation damper is unstable. This graph shows that the combination of CO_2 measurements in the control of DCV and recirculation will not work.

Recirculation control B - OAF controlled by indoor concentration of CO_2 and HCHO

As seen in Figure 4.17, by introducing HCHO as part of the control algorithm for OAF, the concentration of both CO_2 and HCHO are kept below their threshold limits. The concentration of CO_2 follows the same trend as for the control with 100% OAF, but the HCHO is kept fluctuating around 100 $\mu g/m^3$.
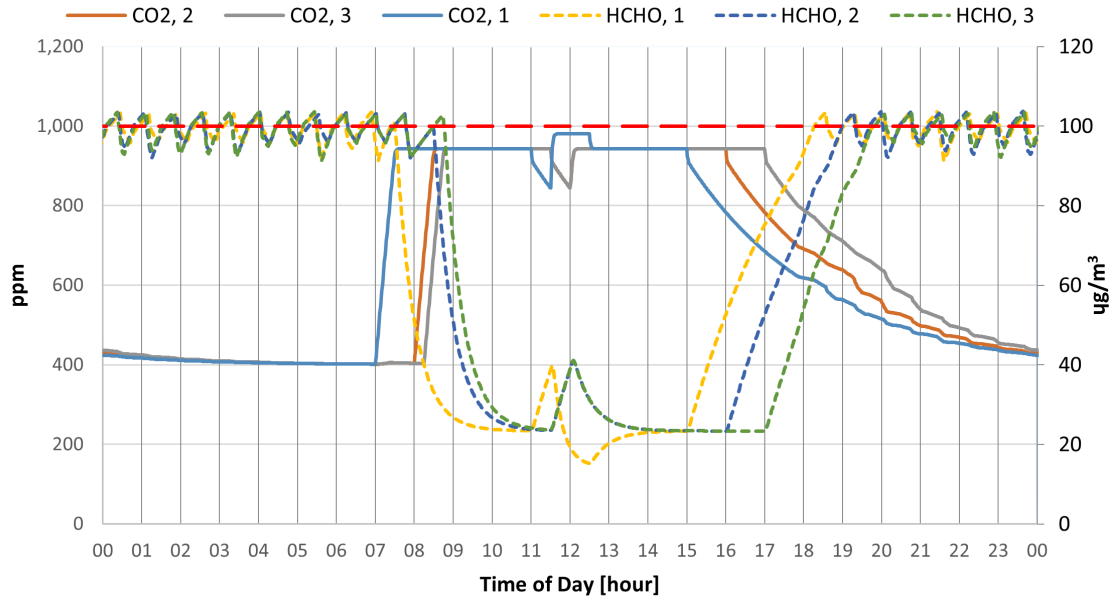
Figure 4.17: Case 3 - Concentration of CO_2 and HCHO with OAF controlled by CO_2 and HCHO

The fluctuations of HCHO concentration are due to the change in OAF. In Figure 4.18, it is clear that the OAF varies between 50 and 100 % outside the working hours.
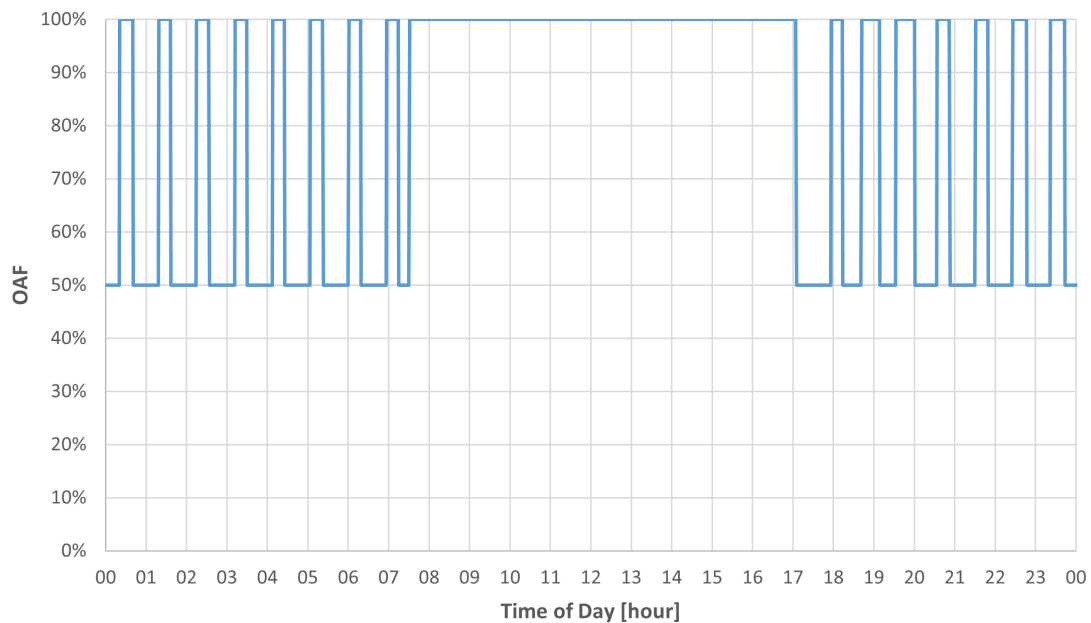
Figure 4.18: Case 3 - OAF air during weekdays with OAF control based on indoor CO_2 and HCHO measurements.
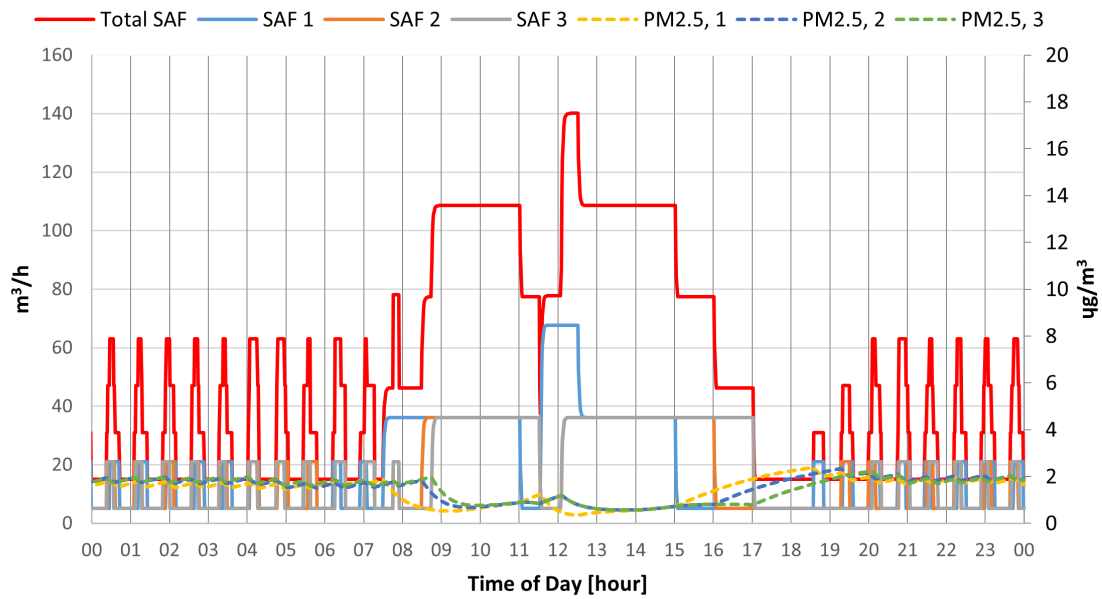
Figure 4.19: Case 3 - Concentration of $PM_{2.5}$ and supply airflow rates with OAF controlled by indoor concentration of CO_2 and HCHO.

The fluctuations outside working hours is visualized in Figure 4.19. The maximum required total supply airflow for this control is 140 m^3/h. However, the fresh air demand for room 1 with increased CO_2 generation is 68 m^3/h. The requirements for fresh air supply in TEK 17 (43.5 m^3/h) would be sufficient for the other rooms with a lower generation rate.

Recirculation control C - OAF controlled by indoor concentration of $PM_{2.5}$

When case 3 is simulated with OAF controlled by the indoor concentration of $PM_{2.5}$, the simulation ends up operating with 100 % OAF at all times. This is because the outdoor concentration of $PM_{2.5}$ is not high enough. Figure 4.20 shows the distribution of supply air and indoor concentration of $PM_{2.5}$. The concentration of $PM_{2.5}$ is kept at 2 $\mu g/m^3$ for most of the day and even lower during working hours.
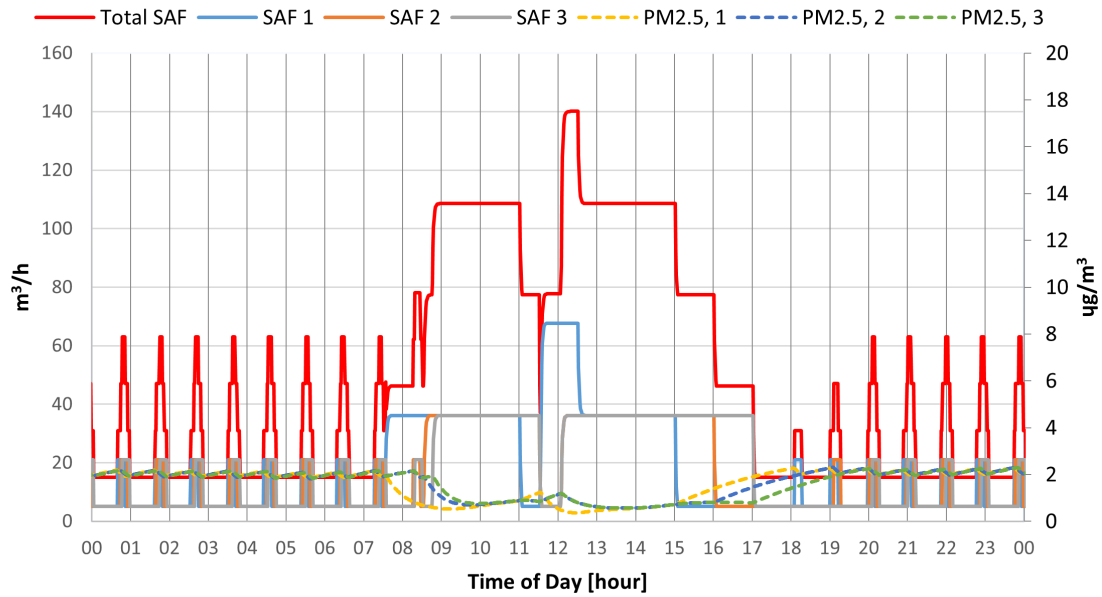
Figure 4.20: Case 3 - Concentration of $PM_{2.5}$ and supply airflow rates with OAF controlled by $PM_{2.5}$ measurements.

Since the OAF is kept at 100% at all times, this control ends up being identical to Case 3 without any recirculation control.

4.1.5 Case 4 - Proportional HCHO with upper limit CO_2

100 % OAF

Figure 4.21 shows the concentration of CO_2 and HCHO for case 4 with 100 % OAF. The control manages to keep the HCHO concentration below the threshold limit of 100 $\mu g/m^3$ at all times. During working hours, CO_2 becomes the dominant parameter and decisive for the supply air demand. The increase in ventilation quickly lowers the concentration of HCHO. The CO_2 concentration, on the other hand, quickly increases but is kept slightly below 1000 ppm for most of the working hours. For room 1, the extra person increases the CO_2 generation so that the pollution load exceeds 1000 ppm until the extra person leaves the room.
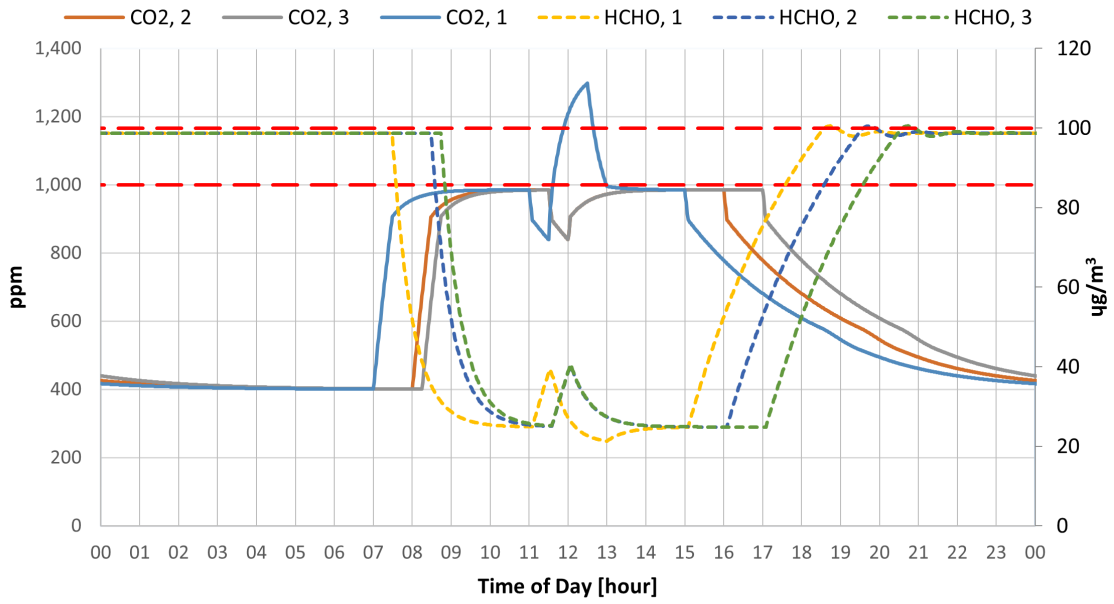
Figure 4.21: Case 4 - Concentration of CO_2 and HCHO with 100 % OAF.

The total supply airflow in Figure 4.22 shows that the ventilation rate is at maximum only for 1 hour during working hours. For most of the working hours, the ventilation rate is kept at 34 m^3/h in each room.
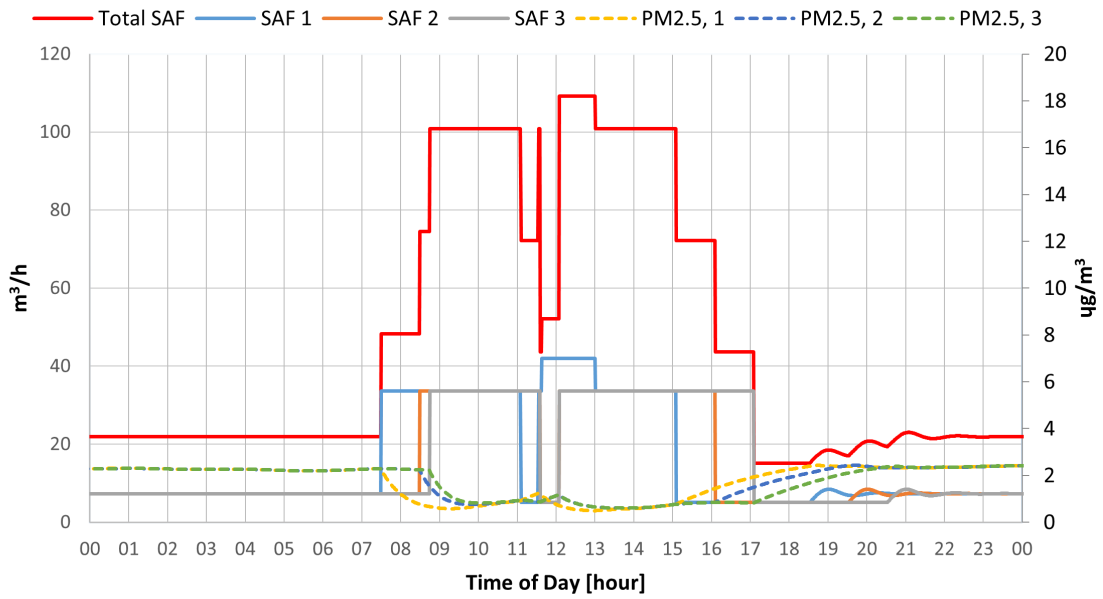
Figure 4.22: Case 4 - Concentration of $PM_{2.5}$ and supply airflow rates with 100 % OAF.

As seen by Figure 4.23, the temperature stays within recommended levels during a typical workday.
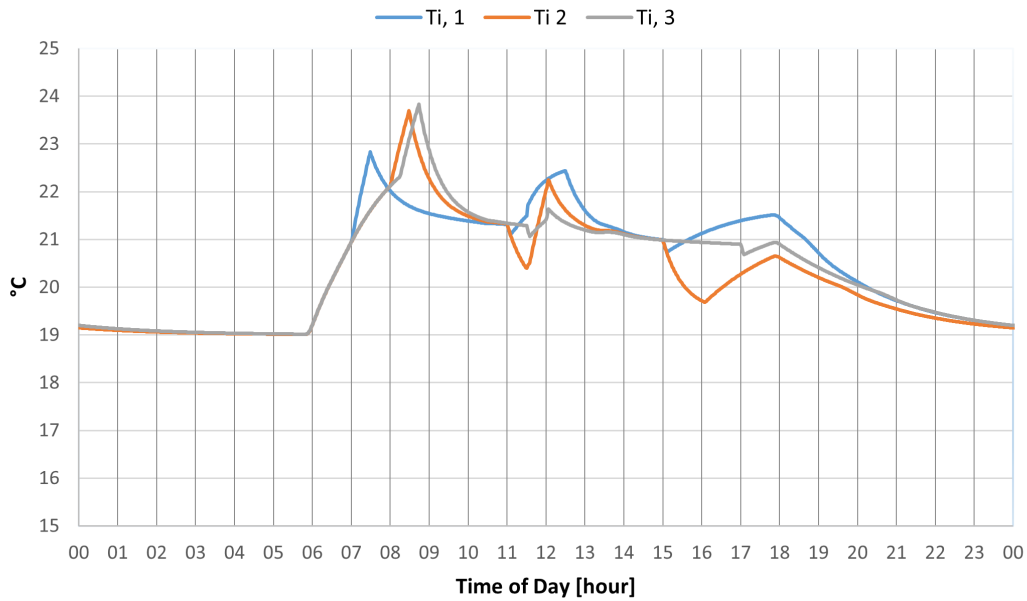
Figure 4.23: Case 4 - Indoor air temperature with 100 % OAF.

Recirculation control A - OAF controlled by indoor CO_2 concentration

When case 4 is combined with the OAF control strategy based on indoor air CO_2 concentration, the resulting indoor concentration of CO_2 is quite unchanged compared to case 4 with 100 % OAF. However, outside working hours, the low OAF allows for the accumulation of HCHO. Therefore, the concentration of HCHO quickly exceeds the 100 $\mu g/m^3$ threshold when the CO_2 concentration is low.
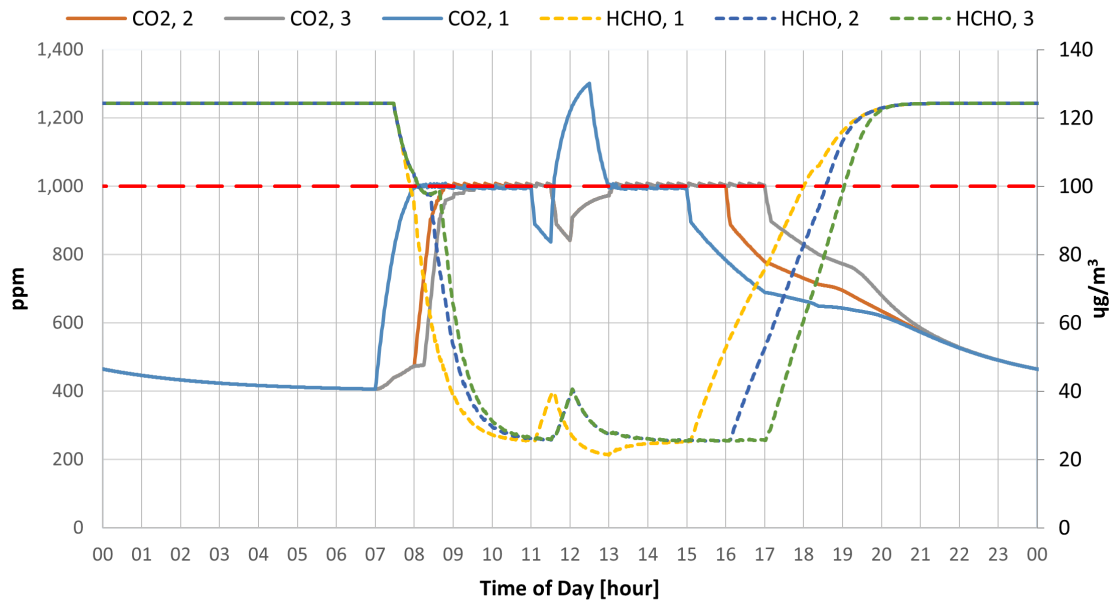
Figure 4.24: Case 4 - Concentration of CO_2 and HCHO with OAF controlled by CO_2 measurements.

As seen in Figure 4.25, the supply airflow rate is almost as high outside working hours. In addition, the implementation of OAF controlled by CO_2 creates fluctuations in the supply airflow control.
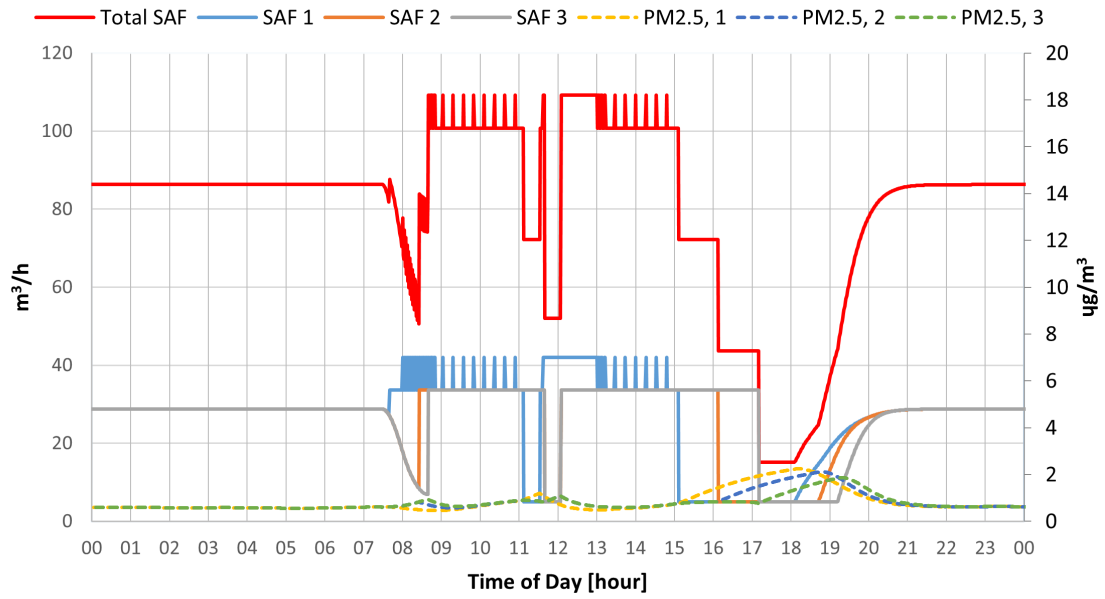
Figure 4.25: Case 4 - Concentration of $PM_{2.5}$ and supply airflow rates with OAF controlled by CO_2 measurements.

As seen in Figure 4.26, the control gets unstable during working hours. The control gets unstable because the control of the supply airflow and the recirculation control compete with each other. As soon as the CO_2 level is acceptable, the recirculation control will lower the OAF causing the need for a higher supply airflow rate.
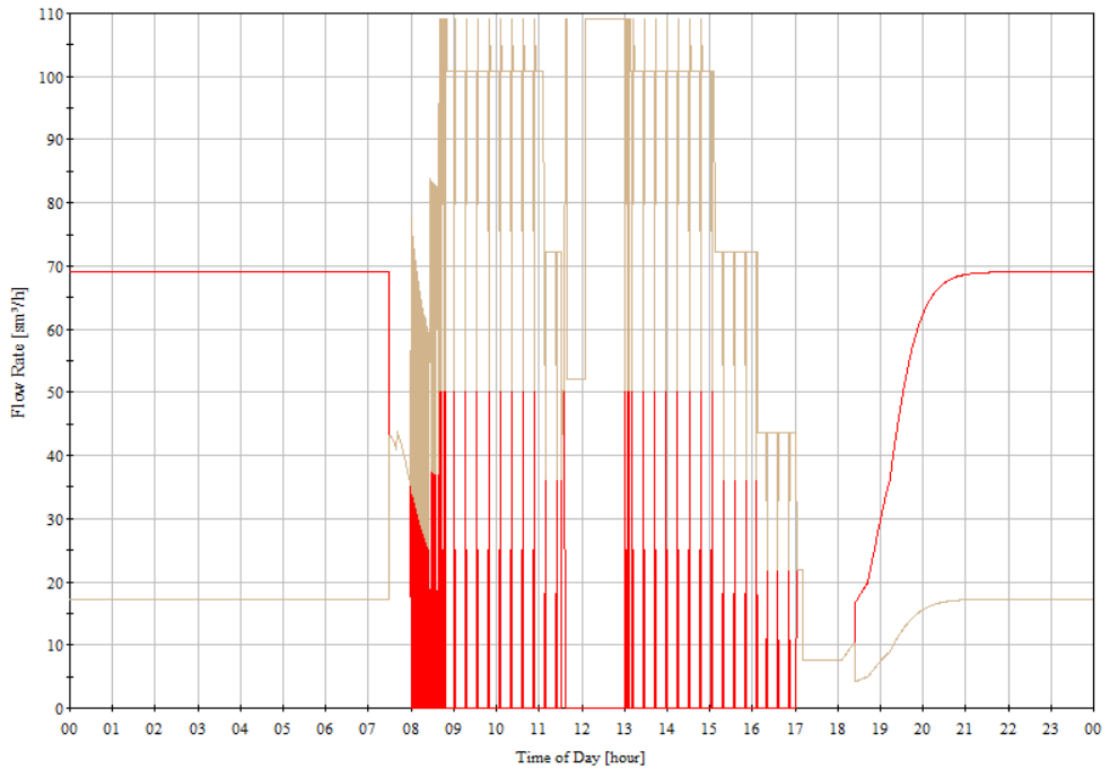
Figure 4.26: Case 4 - Recirculated air (red) and outdoor air (brown) when recirculation is controlled by indoor concentration of CO_2.

Recirculation control B - OAF controlled by indoor CO_2 and HCHO concentration

For case 4 with OAF control based on HCHO and CO_2 measurements, the CO_2 concentration is quite similar to the other recirculation control cases. However, the implementation of HCHO measurements in the recirculation control manages to keep the concentration of HCHO from exceeding the threshold limit.
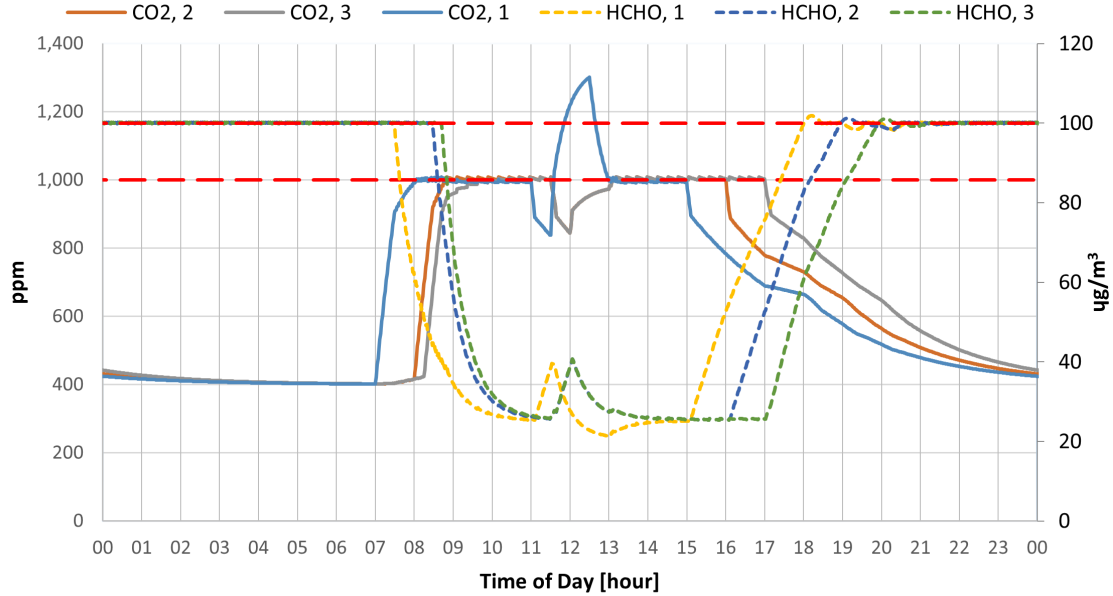
Figure 4.27: Case 4 - Concentration of CO_2 and HCHO with 100 % OAF.

As for the previous case with recirculation based solely on CO_2 measurements, the distribution of supply air is very similar for the case with 100 % OAF during the occupied hours. But as seen in Figure 4.28, the control gets really unstable.
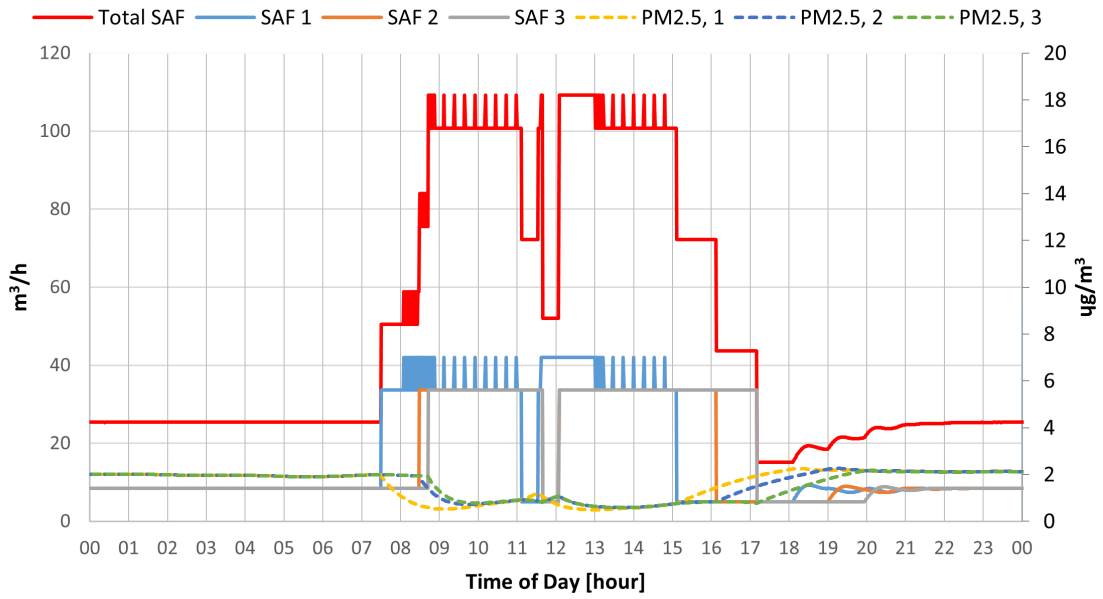
Figure 4.28: Case 4 - Concentration of $PM_{2.5}$ and supply airflow rates with OAF controlled by CO_2 and HCHO measurements.

The recirculation control causes fluctuations in the supply air control as seen in Figure 4.28. In Figure 4.29, the resulting fluctuations in the recirculation control is shown. As the figure shows, the fluctuations would cause the recirculation damper to work non-stop.
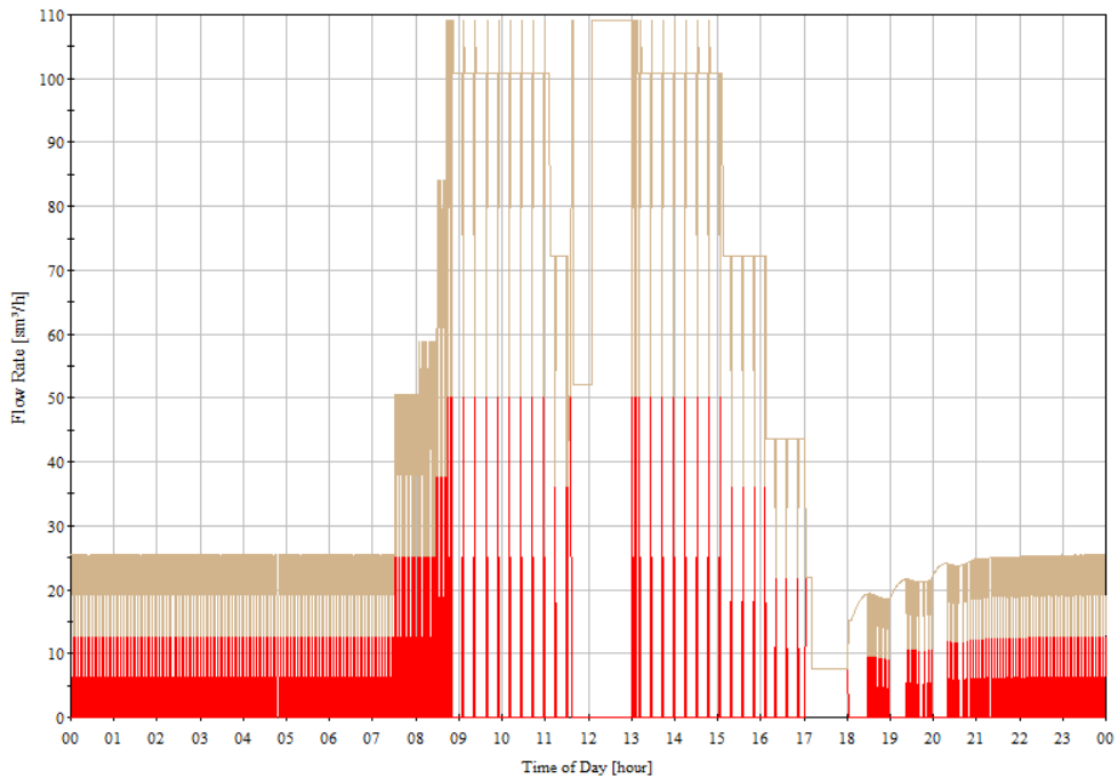
Figure 4.29: Case 4 - Recirculated air (Red) and outdoor air (brown) when recirculation is controlled by indoor concentration of CO_2 and HCHO.

Recirculation control C - OAF controlled by indoor PM$_{2.5}$ concentration

Similar to case 3 with recirculation controlled by the indoor concentration of PM$_{2.5}$. The concentration of PM$_{2.5}$ is kept low at all times. Therefore, the OAF is 100% at all times as seen by Figure 4.30. Therefore, the control becomes identical to Case 4 with 100 % OAF.
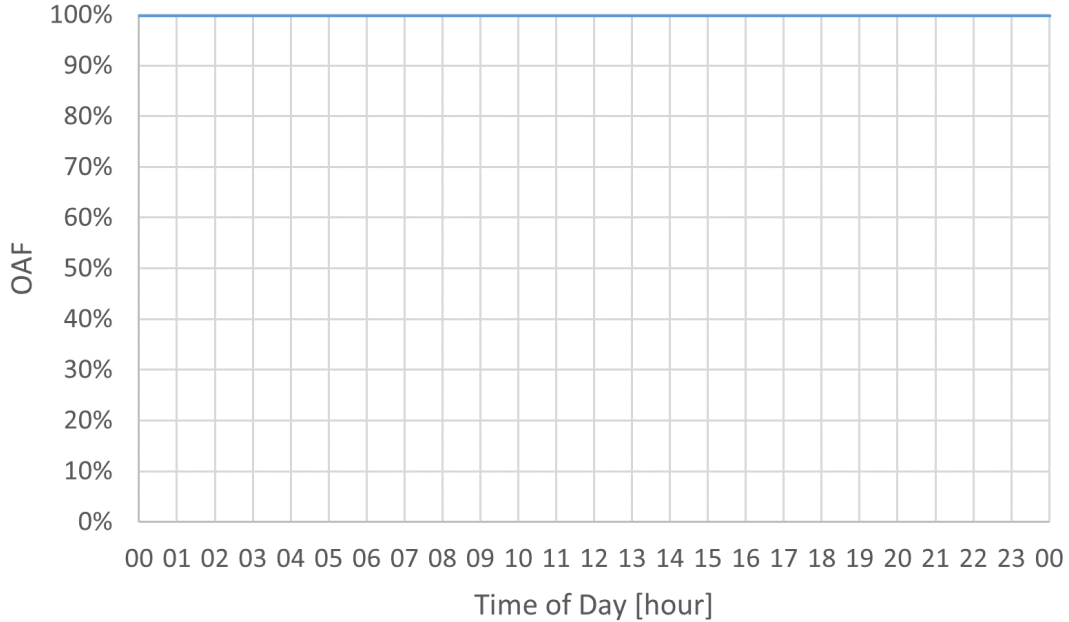
Figure 4.30: Case 4 - OAF when recirculation is controlled by indoor concentration of PM$_{2.5}$.

4.1.6   Case 5 - Proportional CO$_2$ with upper limit temperature

100 % OAF

Figure 4.31 shows that the concentration of CO$_2$ and HCHO for case 5 is quite similar as for case 3 with 100 % OAF. However, the CO$_2$ and temperature control will allow for HCHO to accumulate outside the working hours. This allows for HCHO to exceed the threshold value with the chosen generation rate for HCHO. However, if the HCHO generation is equal to the demand for a low polluting building, the base ventilation of 5 m^3/h will be enough to keep the HCHO from exceeding 100 $\mu g/m^3$.
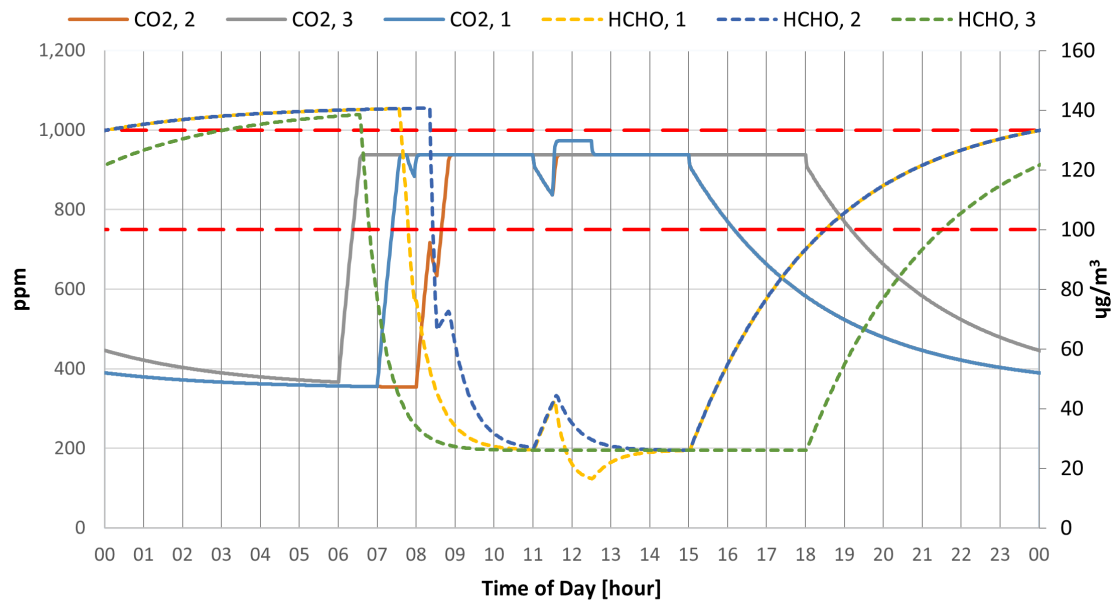
Figure 4.31: Case 5 - Concentration of CO_2 and HCHO with 100 % OAF on a weekday.

Figure 4.32 shows that the supply airflow rates are similar to case 3. The difference is a small increase in the supply airflow rate in room 2.
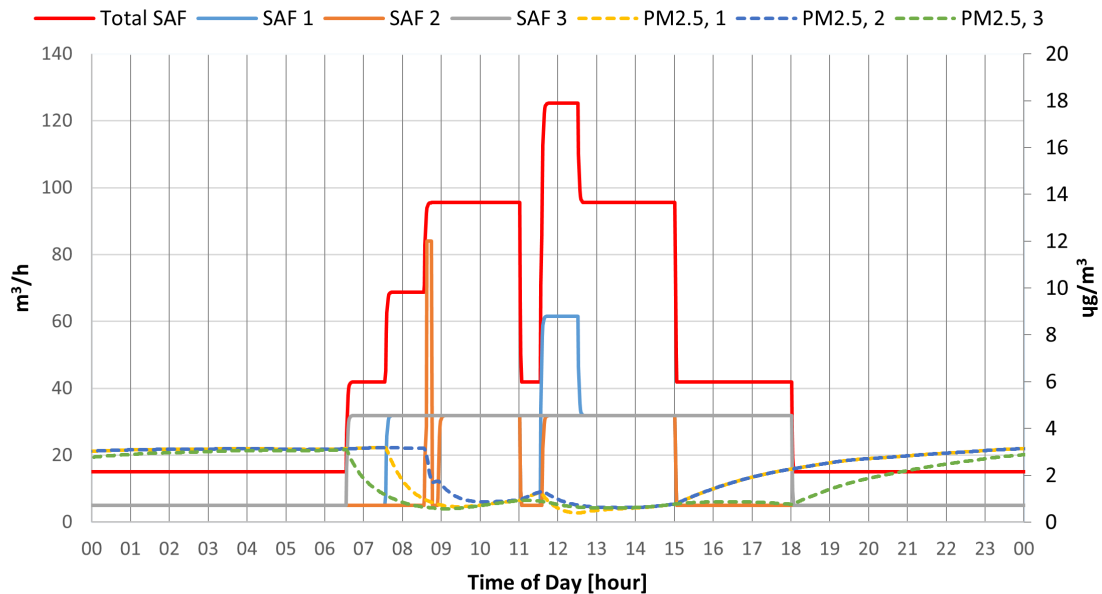
Figure 4.32: Case 5 - Concentration of $PM_{2.5}$ and supply airflow rates with 100% OAF on a weekday.

The reason for the increase in supply airflow rate in room two is shown in Figure 4.33. The upper limit for the temperature control is set to 23 °C. The sudden increase in heat load due to the extra person is enough to increase indoor air temperature. However, the ventilation control quickly copes and lowers the indoor air temperature by increasing the supply airflow rate. For the rest of the working hours, the ventilation rate due to indoor air concentration of CO_2 is enough to keep the indoor air temperature below 23 °C.
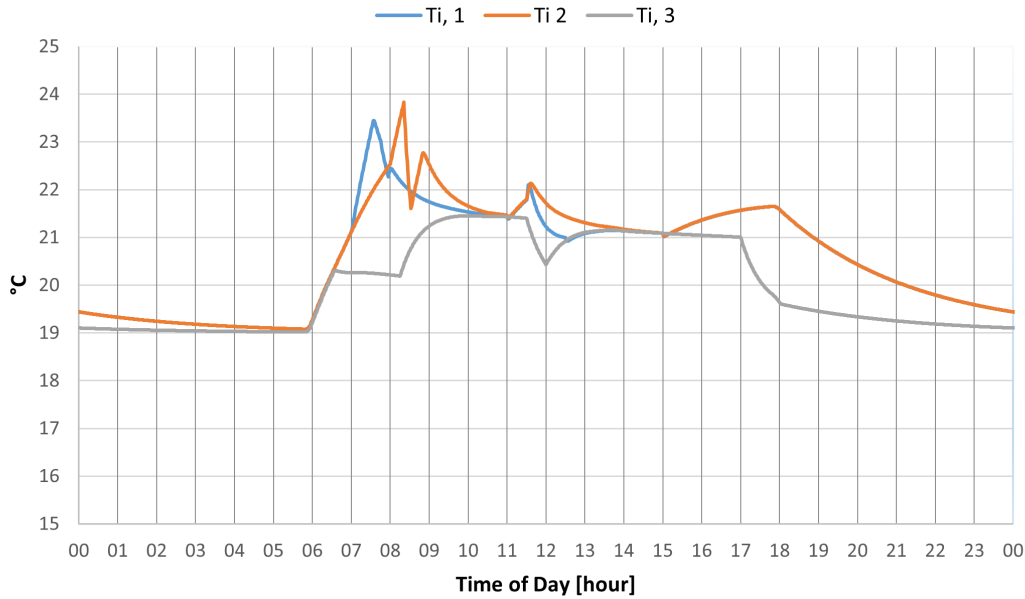
Figure 4.33: Case 5 - Indoor air temperature with 100% OAF.

4.1.7 IAQ summarized

Number of hours exceeding threshold limits

Table 4.1 shows the number of hours the DCV control strategies are unable to keep pollutants below specified threshold values. The exceeding hours are calculated for the simulated reference week. The recirculation controls are not included in the table.

Table 4.1: Number of hours exceeding threshold limit values.

Case	CO2			HCHO	PM$_{2.5}$
	Room 1	Room 2	Room 3		
CAV	5.5	0	0	126.2	0
Case 1	15	10	12.5	130.5	0
Case 2	42.5	50	47.5	0	0
Case 3 - 100 % OAF	0	0	0	< 1	0
Case 4 - 100 % OAF	13.3	0	0	1.8	0
Case 5	0	0	0	133.9	0

The concentration of PM$_{2.5}$ is kept below the threshold limit of 15 $\mu g/m^3$ at all times. The performance of cases 3 and 4 in terms of achieving the desired IAQ is quite similar. With 100% OAF both cases have negligible hours exceeding 100 $\mu g/m^3$ HCHO. Case 4 exceeds the threshold of CO$_2$ for 13 hours weekly and 2.5 hours during working hours. Case 5 performs well in keeping the level of CO$_2$ below 1000 ppm, but HCHO exceeds the threshold limit for almost 140 hours during the simulated week. This is even higher than the CAV case and the simple CO$_2$ upper limit control (case 1).

PPD

Figure 4.34 shows the daily average PPD based on CO$_2$ concentration during working hours. The graphs show the average PPD for all three rooms. The PPD is not calculated for the recirculation

control cases.
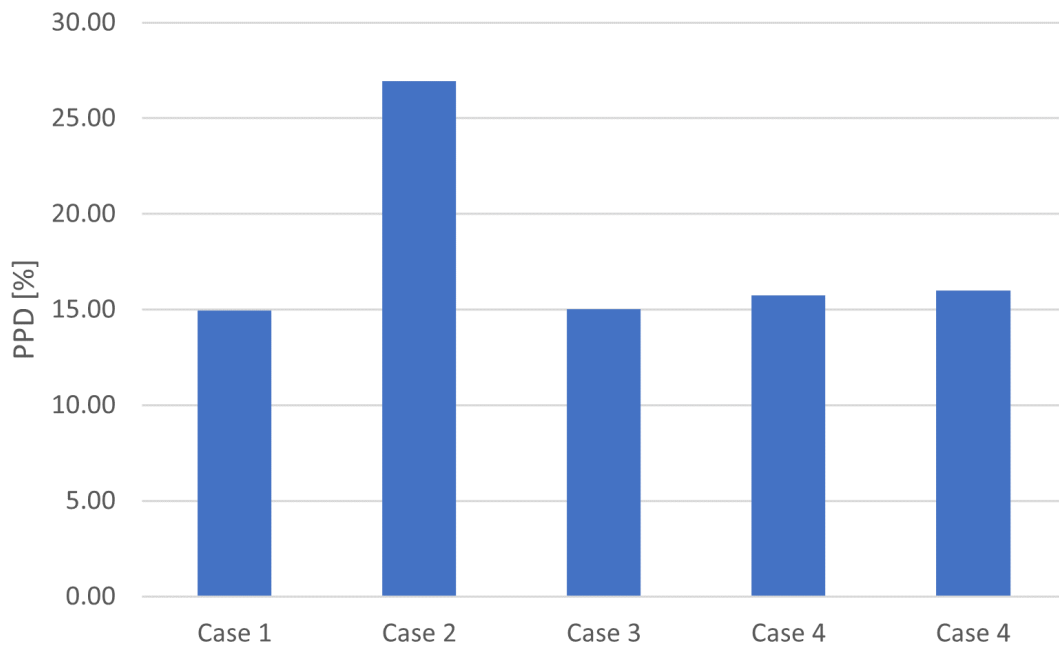
Figure 4.34: Daily average PPD based on concentration of CO_2.

The PPD for cases 3, 4, and 5 is 15, 16, and 16 %. This shows that the short amount of time with increased occupancy in room 1 does not significantly impact PPD.

4.2 Energy consumption compared to CAV

This section assesses the energy use and possible savings for cases 3, 4, and 5 compared to a traditional CAV. Figure 4.35 shows the estimated weekly energy use for heating of ventilation air in kWh. Since the recirculation controls simulated in this thesis proved to be very unstable, the energy consumption for cases combined with recirculation control is not calculated. The graphs show that the cold outdoor air temperature in the reference week results in relatively high energy demand for heating the supply air. Case 5 has the lowest ventilation rate outside the working hours. Therefore, Case 5 saves the most energy with up to 37 % compared to CAV.
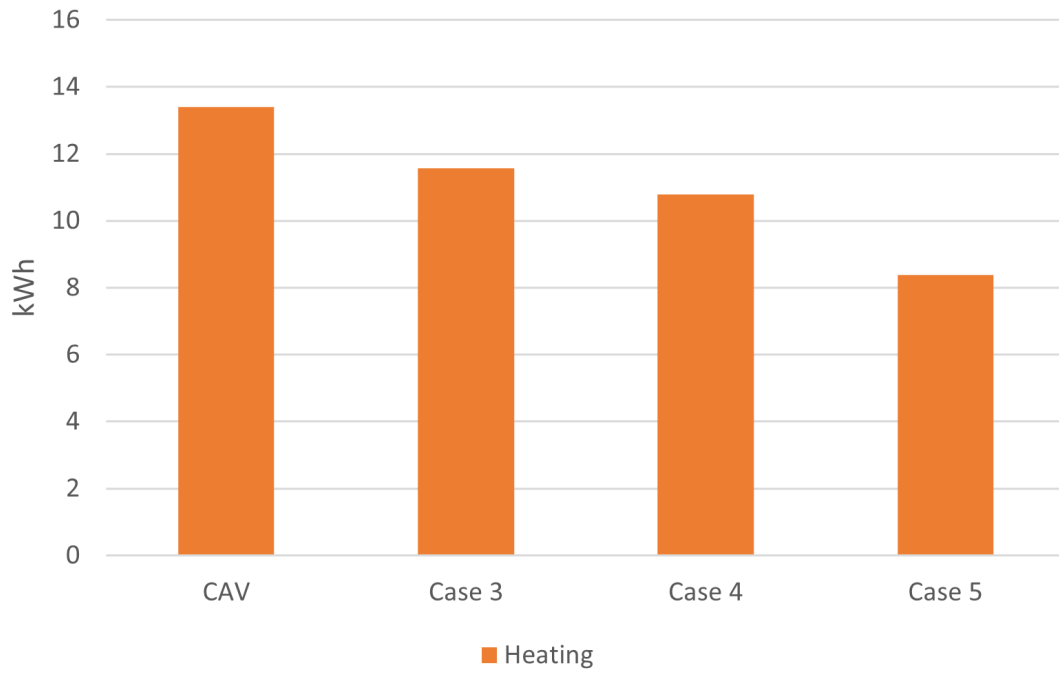
Figure 4.35: Weekly estimated energy use for heating of ventilation air.

In Figure 4.36, the estimated energy use for the operation of fans is shown. The graphs show that the DCV control strategies can save a great amount of energy compared to CAV. All the DCV control requires less than 50% of energy for operating the fans compared to CAV. Case 4 has the lowest average ventilation rate in the working hours. Therefore, Case 4 saves up to 64 % for the operation of fans compared to CAV.
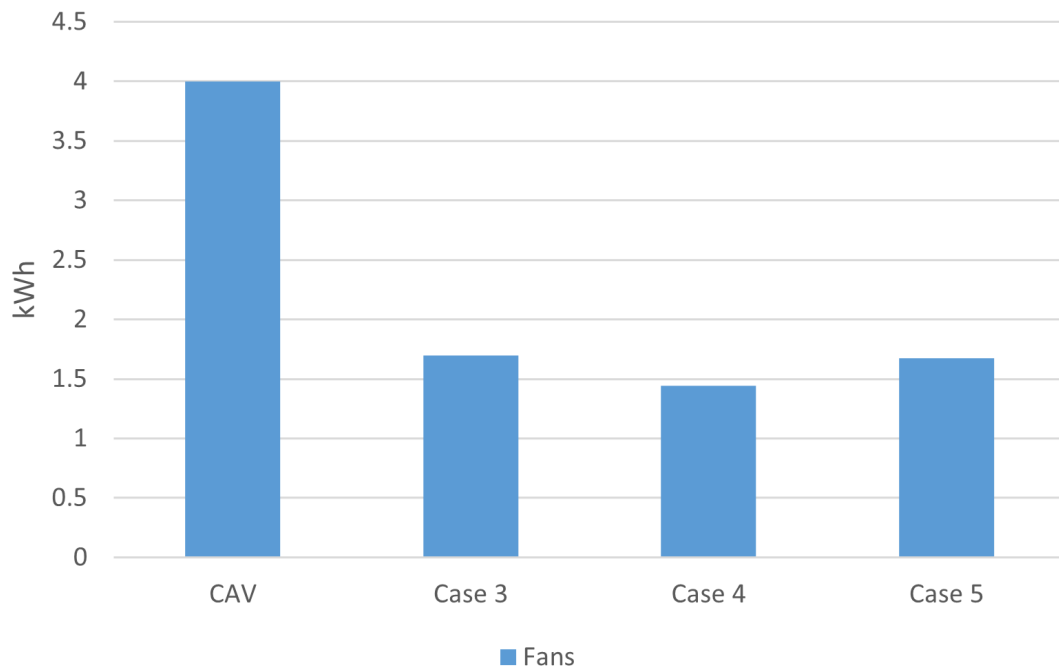
Figure 4.36: Weekly estimated energy use for operation of fans.

In total, Case 5 saves the most energy compared to the other DCV cases for the simulated reference week, with a total amount of 42%.

Chapter 5

Discussion

5.1 Methodology

5.1.1 Full-scale laboratory model

Unfortunately, coupling the AHU, dampers, and sensors was more comprehensive than expected. Therefore, measurements that could be compared with the CONTAM simulation could not be conducted. Since the measurements were to be conducted in the laboratory, the CONTAM simulation was delimited to represent the full-scale laboratory model. In hindsight, another method to create a reliable CONTAM model to test control strategies for DCV could have been to perform measurements in another building with a working DCV system. Measurements could have been completed before constructing a model to reflect the measurements in CONTAM. However, the ventilation floor plan with recirculation control from Figure 3.1 is not a standard method of constructing DCV. Therefore, this type of recirculation control would not be constructed and simulated in CONTAM without planning the DCV system in the laboratory.

5.1.2 CONTAM inputs

The simulation model set up in CONTAM is based on a set of presumptions. As mentioned in Section 3.2, CONTAM operates with the assumption of fully mixed zones. A zone with 100 % ventilation efficiency may not be representative in actual buildings. The placement of the IAQ sensor is not taken into account in the simulation model. As described in Section 2.4.1, the sensor placement could have a major impact on the controllability of a DCV system. Therefore, the ventilation efficiency would have an impact in a real building.

Temperature

The most evident flaw with the CONTAM simulations is the lack of calculated indoor air temperature. SIMIEN is validated by NS-EN 15265:2007 (*SIMIEN Wiki* n.d.). Therefore, the method described in Section 3.2.6 is deemed adequate to represent the indoor air temperature for the reference week. However, the calculation of temperature is only correct for the cases with 100 % OAF. Since the calculations are set up with constant supply indoor air temperature, a DCV control strategy including CO_2 control will achieve acceptable indoor air temperature for most of the time. Equation 2.6 can be used to conduct spot calculations of the required airflow rate to avoid the rooms from overheating. If the indoor air temperature is to be kept below 26 °C, the heat loads have to be reduced. This indicates that the heat loads used in the SIMIEN summer simulation conducted as part of engineering the ventilation plan for the full-scale model in the laboratory were too high. However, the simulation implies that it would be challenging to prevent too high indoor air temperatures on warm summer days without cooling. In addition to ventilation, other

measures can be implemented to reduce solar heat load. In a new building with the ambition to be classified as Zero Emission Building (ZEB), it would be expected to implement energy-saving measures to prevent overheating in the summer months.

Pollutants

The indoor generation rate of pollutants is assumed based on a literature review on the specific pollutants. The generation of HCHO is highly dependant on indoor temperature and RH (Wolkoff & Kjærgaard 2007). Therefore, the generation rate used in the simulations must be classified as rough estimates. In reality, the generation rate of HCHO will vary and not be constant as in the simulations. In addition to RH, the CONTAM simulation does not account for other VOCs other than HCHO. However, HCHO can be characterized as a representative VOC.

The outdoor concentration of PM used in the simulation is based on actual measurements from a contaminant file. A weakness of the CONTAM simulation is the fact that indoor generation of PM is not based on any occupant-related actions but constructed as a constant coefficient that makes up 50 % of the indoor concentration. However, the concentration is highly dependant on outdoor sources (Rackes & Waring 2013). Since outdoor concentration is most dominant, constructing the indoor generation rate of $PM_{2.5}$ as a constant coefficient is adequate to investigate the impact on the IAQ. Only the $PM_{2.5}$ fraction is assessed in this thesis. Other fractions are present indoors, but $PM_{2.5}$ is more relevant in assessing the IAQ than PM_{10}. In studies by Rackes and Waring, the indoor air concentration of PM_{10} is very similar to $PM_{2.5}$. Thus, $PM_{2.5}$ is a good indicator of the concentration of PM in a zone (Rackes & Waring 2013).

5.2 Comparison of control strategies

In terms of achieving the desired IAQ, the proportional CO_2 with HCHO upper limit control (Case 3), and proportional HCHO with CO_2 upper limit control (Case 4) manages to maintain sufficient IAQ. For all the simulated control strategies, the indoor concentration of $PM_{2.5}$ is always below the threshold marker set by WHO. However, the infiltration in the simulation may not represent the actual leakage in the office areas built in the laboratory. Therefore, more PM may well enter via leakage areas and other direct connection to the outdoors.

Solely based on achieving and maintaining the desired IAQ, Case 3 is the best alternative of the 5 simulated control algorithms. A proportional CO_2 control combined with an upper limit HCHO threshold manages to maintain good IAQ during and outside working hours. The generation rate of CO_2 in the room is more irregular than for HCHO. Therefore, a proportional controller based on CO_2 will quicker cope with the changes in pollution generation rate. With a sudden increase in CO_2 pollution, the control still manages to keep the level of CO_2 below 1000 ppm. However, this requires a higher ventilation rate than the typical design supply airflow rate.

Comparing the supply airflow rates, Case 3 utilizes higher ventilation rates than the normal maximum design airflow rate when a room is over-occupied. To deliver a ventilation rate of 72 m^3/h, the ventilation system must be designed accordingly. This would include increased diameter sizes in the ductwork and possibly an AHU with more capacity. For a small office area, these extra investments may not be immense. However, for large office buildings, over-dimensioning may be a significant investment cost. If the maximum ventilation rates are set according to TEK 17 standards, cases 3 and 4 will, in practice, operate with the same supply airflow rates during working hours.

Case 4 with upper limit CO_2 control and a proportional HCHO control must be said to perform better than case 3 with all aspects considered. The control keeps CO_2 and HCHO within acceptable levels at all times except if two persons occupy a room. A slight increase in CO_2 level when the room is occupied by more people than planned must be acceptable. The highest concentration of CO_2 is 1300 ppm. This correlates to a PPD of 31.6 % according to Figure 2.1. However, as the calculated PPD in Figure 4.34 shows, the short amount of time with higher occupancy will not

affect the overall PPD.

Case 5 ensures good IAQ in the working hours, but outside working hours, the level of HCHO is too high. By comparing the weekly energy consumption for Case 5 with case 4. Case 4 requires slightly more energy for heating but less for the operation of fans. This implies that throughout the year, the overall energy use may be pretty equal or lower than for the more common CO_2 and temperature DCV control (Case 5). All aspects considered, Case 4 with an upper limit setpoint control of CO_2 combined with a proportional HCHO control is the best alternative of the assessed DCV control strategies.

It is expected that the HCHO contaminant rate will decrease over time (Holøs et al. 2019). Therefore, the HCHO contaminant rate used in this thesis may be way too high to represent a building after the off-gassing phase. However, a control to prevent exceeding limits of HCHO may still be relevant, and if not, the DCV control can be altered to CO_2 combined with temperature. Since LCS has improved in recent years, implementing HCHO control will not necessarily be a costly investment. Therefore, there should be no significant drawbacks in implementing HCHO measurements as part of the DCV control to achieve a healthy indoor environment. The Arduino sensors related to this thesis measures both HCHO and temperature. Therefore, a possible control strategy could be to use DCV control based on CO_2 and HCHO in the first years of a building's lifetime. When the "off-gassing" phase as described by Holøes et al. (Holøs et al. 2019) has passed, a control strategy based on CO_2 and temperature measurements can be implemented as the new DCV control strategy.

5.3   Results compared to literature

Control of DCV

DCV controlled by CO_2 is a subject widely investigated. Therefore, a reasonable question to ask is, "Are the control strategies presented in this thesis realistic to be used in and actual systems". In the "Guide to demand control ventilation", the relevance for proportional or setpoint control of CO_2 controlled DCV is discussed (Bhatia n.d.). According to the guide, setpoint control is best in rooms with varying occupancy densities. The setpoint approach for control of DCV based on CO_2 measurements is adequate for the prerequisites for the cell offices in this control. However, if the intended use of the offices is to be altered, the occupancy densities may also be different. For instance, if the three cell offices were to be altered to an open office landscape. Thus, upper limit setpoint control is good enough for the specified cell offices but is not as adaptable as proportional control.

IAQ

The SIMIEN simulation conducted to verify the constructed indoor air temperature verifies the indoor concentration of CO_2 at the same time. Comparing the CO_2 output from SIMIEN with output from a reconstructed CONTAM simulation shows the same results. Therefore, the resulting CO_2 concentration from each simulated case in this thesis is trustworthy. As mentioned in Section 2.1.2, RH has major impact of the PAQ (Vellei et al. 2017). The RH is not calculated in the CONTAM simulation. Hence, an essential factor in assessing the IAQ is not included.

To indicate how accurate the emission rate is, the resulting HCHO level in the simulated cell offices can be compared to values provided by Salthammer (Salthammer 2019). According to Salthammer, the log-normal concentration of measured HCHO indoors at living conditions is 23.1 $\mu g/m^3$. Even though the full-scale laboratory model represents offices and not living conditions, this indicates that the HCHO levels found in the CONTAM simulation may be higher than the actual conditions in the full-scale laboratory model.

A study investigated the impact of DCV compared to CAV on selected offices in the U.S (Rackes & Waring 2013). The indoor concentration of $PM_{2.5}$ for a simulated office in Philadelphia was

approximately 2 - 3 times higher than the results found in this thesis. The outdoor pollution load was higher in the Philadelphia case, therefore, the conclusion of the study conducted by Rackes and Waring supports the results regarding PM in this thesis. DCV does not have a significant impact on the indoor concentration of $PM_{2.5}$ compared to CAV. Because of the relatively low levels of outdoor $PM_{2.5}$ used in the CONTAM simulations, recirculation control C became irrelevant. Essentially filtration of the outdoor air is enough to maintain good IAQ regarding PM. However, in other areas with higher pollution load, a recirculation control based on $PM_{2.5}$ measurements may still be relevant.

Rackes and Waring did not investigate the impact on HCHO, but they investigated the general impact on VOC. Their study concluded that DCV allowed for VOC to accumulate overnight (Rackes & Waring 2013). In their study, TVOC concentrations accumulate similar to the accumulation of HCHO shown by the CAV simulation in this thesis. As for HCHO in this thesis, the TVOC was reduced quickly when the ventilation rate was increased. Since the HCHO control algorithms in this thesis lower the concentration of HCHO outside working hours, it would lower TVOC concentration. Therefore, depending on the selected DCV control principle, DCV will be able to lower the concentration of HCHO and other VOCs compared to CAV. However, this will only apply to situations with high amounts of HCHO. If other VOCs are the most dominant pollutant, TVOC may still be allowed to accumulate outside working hours.

As mentioned in Section 2.3.1, studies show that a ventilation control to prevent accumulation of non-occupant related pollutants could be controlled by purging sequences (Chao & Hu 2004). The strategies investigated in this thesis will eliminate the need for purging sequences because it will be a constant control that prevents the accumulation of non-occupant related pollution. However, as Chao and Hu point out, measurements should be conducted to identify the most dominant non-occupant related pollution.

Energy saving potential

The calculation of energy use must be seen as rough estimates. The calculation is solely based on presumptions. The calculation does not consider differences in occupancy or annual differences in the generation rate of HCHO. Both parameters would have an impact on supply airflow rates for the controls. The energy-saving potential of different DCV fan control strategies such as static pressure reset DCV and pressure control is not assessed in this thesis. The calculation for the specific energy use for fans may be inaccurate in terms of specific energy use in kWh. It is hard to determine the actual SFP values in a simulation. The CONTAM model does not calculate the pressure loss in the ductwork. As described in Section 2.3.2, the pressure loss will have an impact on SFP and energy use. However, the pressure loss in the ductwork will be quite similar for all the cases. Therefore, the comparison in percentage between the DCV control strategies can be used as an indication of the energy consumption. A typical distribution of energy use due to ventilation is 55% for the operation of fans, 28 % for cooling, and 17 % for heating(SINTEF Byggforsk 2000). Since the appointed week for the CONTAM simulation was conducted during wintertime, the energy demand for heating of the supply air was much higher than for operating the fans. However, throughout the year, it is expected that the energy demand for fans will be higher. Therefore can the CO_2 set point control used in case 4 be a better option than the proportional controller used in Case 5 to save energy.

Even though the energy calculations are rough estimates, they can be compared to other studies investigating DCV. Some studies imply even higher energy-saving potential. Delwati et al. concluded that in fan energy consumption, measurements and simulations indicated an energy-saving potential of up to 84 % (Delwati et al. 2018). Other studies concluded that DCV controlled by CO_2 saved a total of 38% in energy use compared to CAV operating with full airflow from 07.00 - 17.00 (Mysen et al. 2005). The study by Mysen et al. was conducted in various classrooms in the Oslo area. Even though the study was conducted in another city and in a different type of building, the findings substantiate the potential to save energy found in this thesis.

5.4 Research questions

How are other pollutants affected when the DCV system is controlled based on CO2 concentration?

HCHO represents one VOC in the CONTAM simulation. The simulations show that during working hours, the ventilation rate controlled by indoor air concentration of CO_2 lowers the level of HCHO. Outside working hours, the level of CO_2 is quickly reduced. If the base ventilation rate is too low compared to the generation rate of HCHO, HCHO will accumulate until the level of CO_2 once again is increased. With a constant temperature on the supply airflow rate, case 5 indicates that the ventilation airflow will keep the room air temperature at acceptable levels most of the time. Control solely based on CO_2 will prevent an increase in other pollutants when the rooms are occupied. To thoroughly investigate how the different parameters are affected under different control strategies, actual measurements should be performed in the laboratory.

The concentration of $PM_{2.5}$ is kept below the threshold limit values set by FHI and WHO at all times. Therefore, the simulations indicate no need to include measurements of $PM_{2.5}$ as part of the DCV control.

How do formaldehyde perform compared to CO_2 in terms of controlling a DCV system?

Case 2 shows that ventilation control solely based on HCHO will struggle to achieve sufficient IAQ during working hours. In low polluting buildings, HCHO control will struggle even more. Case 3 and 4 show how a combination of CO_2 and HCHO keeps the IAQ sufficient throughout the day. However, the performance of non-occupant related pollution DCV control is dependent on the generation rate. Case 3, with a low generation rate for HCHO, shows that for low polluting buildings, base ventilation in compliance with the TEK 17 standards (Direktoratet for byggkvalitet n.d.) is enough to prevent the accumulation of HCHO. Implementing HCHO as part of the control strategy can be used as a safety measure to avoid high concentrations of HCHO and other VOCs. To sum up, the simulations show that compared to CO_2, DCV controlled solely based on measurements of HCHO is inadequate.

Will implementation of recirculation control save energy for heating the supply air while still achieving sufficient IAQ?

The CONTAM simulation shows that the proposed recirculation strategies should not be implemented as part of a DCV control strategy. The simulation shows that recirculation control based on the same pollutants that control the supply airflow rate will probably not work. The DCV control and the recirculation control will compete against each other and create an unstable control.

It must be noted that the simulations performed in this thesis are done with relatively stable pollutant conditions. Lower or higher emission rates would change the result from the simulations. For instance, would a lower emission rate of HCHO change the base ventilation rate needed to keep the concentration of HCHO below the threshold of 100 $\mu g/m^3$. The proposed control algorithms would perform differently with other prerequisites than those used in the specific CONTAM simulation file in this thesis. The contaminant file used in the CONTAM simulations contains low outdoor concentrations $PM_{2.5}$. In other areas with more pollution and worse filter efficiency, a recirculation strategy based on indoor or outdoor air concentration of PM may be more applicable.

Will the CONTAM simulations be adequate to investigate the impact of DCV?

The CONTAM simulations are adequate to investigate the impact of different control strategies for DCV. However, CONTAM is only adequate in terms of investigating the impact of the IAQ. Calculations of energy use are an essential part of investigating the impact of DCV. The energy calculations conducted in this thesis can not be used to state the actual energy use in kWh. Since the presumptions used to calculate energy use are the same for all the simulated cases. The controls can be compared to each other regarding how they would perform in terms of energy use. But,it is possible to couple the CONTAM simulations with other simulation programs that calculates indoor air temperature and energy consumption. However, it is possible to use the output to estimate

energy consumption. Therefore, the CONTAM simulations are adequate to investigate the impact of different DCV control strategies.

How does the proposed control strategies perform compared to CAV in terms of energy use?

The calculations show that there are possibilities in saving energy for heating, operation of fans. The simulation results show that the best energy-saving possibility is to reduce the energy demand for the operation of fans. All the DCV control strategies that include CO_2 measurements will lower energy use due to lower supply airflow rates throughout the day. Case 4 with DCV controlled by a CO_2 setpoint control and HCHO proportional controller achieves acceptable IAQ and lowers the energy use for the supply and extract fans compared to CAV by up to 64 %. More accurate energy calculations can be performed with a running test rig in the laboratory. When The actual energy use for fans may be different from the estimates in this thesis.

Chapter 6

Conclusion

This thesis aimed to facilitate the construction of a suitable full-scale model in the laboratory. The planning of the full-scale model in the laboratory set the framework for the CONTAM simulation model. CONTAM was used to simulate DCV control strategies that can be implemented in the actual DCV system under construction in the laboratory.

Simulations show that DCV solely based on HCHO measurements are inadequate, but a combination of CO_2 and HCHO measurements show potential. Based on the control strategies simulated in CONTAM, case 4 with DCV control based on indoor air concentration of HCHO combined with an upper limit control based on indoor air concentration of CO_2 would be the best option to maintain adequate IAQ for the proposed laboratory set up. The control keeps the indoor pollutants below the threshold limit values without requiring higher ventilation rates than a standard design airflow rate.

None of the recirculation control algorithms investigated in this thesis should be implemented as a strategy to save energy. Nor do they increase the general IAQ with the current framework conditions in this thesis. The recirculation control competes with the supply air control, causing unstable controls. Recirculation control based on measurements of $PM_{2.5}$ became irrelevant because of the low concentration of $PM_{2.5}$ in the outdoor air contaminant file. However, in areas with higher pollution load, recirculation based on measurements of PM may increase IAQ and is worth further investigation. Since none of the recirculation controls investigated in this thesis managed to increase IAQ or reduce energy consumption, the extra complexity introduced is deemed unnecessary. However, other recirculation control strategies may still be relevant in other scenarios and worth further investigation.

As expected, there is energy-saving potential with the use of DCV. The proposed control strategy based on indoor measurements of CO_2 and HCHO shows potential of saving up to 31 % of for control of the supply and extract fans compared to CAV. The most prominent potential in savings is due to the operation of the supply and extract fans. Compared to CAV, the energy saved in fan operation is estimated to be up to 64 %. Based on the findings in this thesis, DCV controlled by a proportional HCHO and an upper limit CO_2 control provides the best IAQ and should be investigated further in the full-scale model in the laboratory.

Chapter 7

Further work

The construction of the office areas in the laboratory was ongoing during the work on this thesis. When the construction is complete, further work can include investigation of the actual leakage areas of the rooms and perform measurements that would establish the generation rate of HCHO, TVOC, and PM in the office areas. Further work can include implementing the result from laboratory measurements to improve the CONTAM simulation model.

Further work should investigate how the control strategies perform in an actual system compared to the CONTAM simulations. The performance of the strategies should be tested under various conditions with various pollution loads. The CONTAM simulations did not include an investigation of how the proposed DCV control strategies would affect the concentration of TVOC and RH in the offices. When the DCV system in the laboratory is up and running, the impact on these parameters should be investigated.

In addition to performing measurements in the laboratory, the CONTAM simulations can be coupled with EnergyPlus to better analyze the resulting indoor air temperature for other weeks than the reference week used in this thesis. The resulting indoor air temperatures will give more detailed energy calculations for each of the DCV control algorithms.

Bibliography

2001 ASHRAE handbook : fundamentals (2001).
  URL: *https://sovathrothsama.files.wordpress.com/2016/03/ashrae-hvac-2001-fundamentals-handbook.pdf*

Alsmo, T. & Alsmo, C. (2014), 'Ventilation and relative humidity in swedish buildings', *Journal of Environmental Protection* **Vol.05No.11**, 15.
  URL: *//www.scirp.org/journal/paperinformation.aspx?paperid=49287*

Bhatia, A. (n.d.), 'Hvac - guide to demand control ventilation'. Available from: https://www.cedengineering.com/courses/hvac-guide-to-demand-control-ventilation.

Brook, R. D., Rajagopalan, S., Pope, 3rd, C. A., Brook, J. R., Bhatnagar, A., Diez-Roux, A. V., Holguin, F., Hong, Y., Luepker, R. V., Mittleman, M. A., Peters, A., Siscovick, D., Smith, Jr, S. C., Whitsel, L. & Kaufman, J. D. (2010), 'Particulate matter air pollution and cardiovascular disease: An update to the scientific statement from the american heart association', *Circulation (New York, N.Y.)* **121**(21), 2331–2378.

Buch, J. T. (2020), Control and optimization of ventilation in zero emission buildings using iot: A preliminary study on the use of low-cost iaq sensors.

Bulot, F. M. J., Johnston, S. J., Basford, P. J., Easton, N. H. C., Apetroaie-Cristea, M., Foster, G. L., Morris, A. K. R., Cox, S. J. & Loxham, M. (2019), 'Long-term field comparison of multiple low-cost particulate matter sensors in an outdoor urban environment', *Scientific reports* **9**(1), 7497–7497.

Chao, C. & Hu, J. (2004), 'Development of a dual-mode demand control ventilation strategy for indoor air quality control and energy saving', *Building and Environment* **39**(4), 385–397.
  URL: *https://www.sciencedirect.com/science/article/pii/S0360132303002579*

Chiesa, G., Cesari, S., Garcia, M., Issa, M. & Li, S. (2019), 'Multisensor iot platform for optimising iaq levels in buildings through a smart ventilation system', *Sustainability (Basel, Switzerland)* **11**(20), 5777.

Chojer, H., Branco, P., Martins, F., Alvim-Ferraz, M. & Sousa, S. (2020), 'Development of low-cost indoor air quality monitoring devices: Recent advancements', *Science of The Total Environment* **727**, 138385.
  URL: *https://www.sciencedirect.com/science/article/pii/S0048969720318982*

Delwati, M., Merema, B., Breesch, H., Helsen, L. & Sourbron, M. (2018), 'Impact of demand controlled ventilation on system performance and energy use', *Energy and buildings* **174**, 111–123.

Direktoratet for byggkvalitet (n.d.), 'Byggteknisk forskrift (tek17) med veiledning'.
  URL: *https://dibk.no/regelverk/byggteknisk-forskrift-tek17/*

Fisk, W., Destaillats, H. & Sidheswaran, M. (2011), 'Saving energy and improving iaq through application of advanced air cleaning technologies'.

Folkehelseinstituttet (2015), 'Anbefalte faglige normer for inneklima, rapport 2015:1'.
  URL: *https://www.fhi.no/globalassets/dokumenterfiler/rapporter/2015/anbefalte-faglige-normer-for-inneklima-pdf.pdf*

Fontanini, A. D., Vaidya, U. & Ganapathysubramanian, B. (2016), 'A methodology for optimal placement of sensors in enclosed environments: A dynamical systems approach', *Building and environment* **100**, 145–161.

Geng, Y., Ji, W., Lin, B. & Zhu, Y. (2017), 'The impact of thermal environment on occupant ieq perception and productivity', *Building and Environment* **121**, 158 – 167.
URL: *http://www.sciencedirect.com/science/article/pii/S0360132317302020*

Goletto, V., Mialon, G., Faivre, T., Wang, Y., Lesieur, I., Petigny, N. & Vijapurapu, S. (2020), 'Formaldehyde and total voc (tvoc) commercial low-cost monitoring devices: From an evaluation in controlled conditions to a use case application in a real building', *Chemosensors* **8**(1), 8.

Goyal, R. & Khare, M. (2010), 'Indoor air quality modeling for pm10, pm2.5, and pm1.0 in naturally ventilated classrooms of an urban indian school building', *Environmental monitoring and assessment* **176**(1-4), 501–516.

Gram, O. K. (2019), Use of low cost pollutant sensors for developing healthy demand controlled ventilation strategies - a case study in four primary school classrooms, Master's thesis.

Holøs, S. B., Yang, A., Lind, M., Thunshelle, K., Schild, P. & Mysen, M. (2019), 'Voc emission rates in newly built and renovated buildings, and the influence of ventilation – a review and meta-analysis', *International Journal of Ventilation* **18**(3), 153–166.
URL: *https://doi.org/10.1080/14733315.2018.1435026*

Ingebrigtsen, S. (2015), *Ventilasjonsteknikk : Del 1*, Vol. Del 1, Skarland Press, Oslo.

Ingebrigtsen, S. (2016), *Ventilasjonsteknikk : Del 2*, Vol. Del 2, Skarland Press, Oslo.

Jing, Gang;Cai, W. X. C. H. C., Jing, G., Cai, W., Zhang, X., Cui, C., Liu, H. & Wang, C. (2020), 'An energy-saving control strategy for multi-zone demand controlled ventilation system with data-driven model and air balancing control', *Energy : technologies, resources, reserves, demand, impact, conservation, management, policy : the international journal* **199**, 117328.

Jørgensen, T. (2020), Utilizing iot technology for healthy and energy efficient improvement of existing ventilation systems: Case study of indoor air quality in a primary school classroom using arduino sensors and contam simulations, Master's thesis.

Karagulian, F., Barbiere, M., Kotsev, A., Spinelle, L., Gerboles, M., Lagler, F., Redon, N., Crunaire, S. & Borowiak, A. (2019), 'Review of the performance of low-cost sensors for air quality monitoring', *Atmosphere* **10**(9), 506.

Krajčík, M., Kudiváni, L. & Mahdavi, A. (2016), Energy saving potential of personalized ventilation applied in an open space office under winter conditions, *in* 'Applied mechanics and materials', Vol. 861, pp. 417–424.

Kuula, J., Mäkelä, T., Aurela, M., Teinilä, K., Varjonen, S., González, & Timonen, H. (2020), 'Laboratory evaluation of particle-size selectivity of optical low-cost particulate matter sensors', *Atmospheric measurement techniques* **13**(5), 2413–2423.

Lan, L., Wargocki, P., Wyon, D. P. & Lian, Z. (2011), 'Effects of thermal discomfort in an office on perceived air quality, sbs symptoms, physiological responses, and human performance: The effects of thermal discomfort on health and human performance', *Indoor air* **21**(5), 376–390.

Lind, M., Holøs, S., Thunshelle, K., Yang, A. & Mysen, M. (2019), How does low relative humidity affect perceived air quality, thermal comfort and symptoms in modern office buildings in cold climates?, *in* D. Johansson, H. Bagge & Å. Wahlström, eds, 'Cold Climate HVAC 2018', Springer International Publishing, Cham, pp. 899–909.

Lowther, S. D., Jones, K. C., Wang, X., Whyatt, J. D., Wild, O. & Booker, D. (2019), 'Particulate matter measurement indoors: A review of metrics, sensors, needs, and applications', *Environmental science technology* **53**(20), 11644–11656.

Martin, C. R., Zeng, N., Karion, A., Dickerson, R. R., Ren, X., Turpie, B. N. & Weber, K. J. (2017), 'Evaluation and environmental correction of ambient co2 measurements from a low-cost ndir sensor', *Atmospheric measurement techniques* **10**(7), 2383–2395.

Martín-Garín, A., Millán-García, J., Baïri, A., Millán-Medel, J. & Sala-Lizarraga, J. (2018), 'Environmental monitoring system based on an open source platform and the internet of things for a building energy retrofit', *Automation in Construction* **87**, 201–214.
URL: *https://www.sciencedirect.com/science/article/pii/S0926580517300729*

Mendell, M. J. & Heath, G. A. (2005), 'Do indoor pollutants and thermal conditions in schools influence student performance? a critical review of the literature', *Indoor air* **15**(1), 27–52.

Miljødirektoratet (n.d.), 'Klimagassutslipp fra oppvarming av bygg'. Viewed: 26.02.2021.
URL: *https://miljostatus.miljodirektoratet.no/tema/klima/norske-utslipp-av-klimagasser/klimagassutslipp-fra-oppvarming-av-bygg/*

Morawska, L., Thai, P. K., Liu, X., Asumadu-Sakyi, A., Ayoko, G., Bartonova, A., Bedini, A., Chai, F., Christensen, B., Dunbabin, M., Gao, J., Hagler, G. S., Jayaratne, R., Kumar, P., Lau, A. K., Louie, P. K., Mazaheri, M., Ning, Z., Motta, N., Mullins, B., Rahman, M. M., Ristovski, Z., Shafiei, M., Tjondronegoro, D., Westerdahl, D. & Williams, R. (2018), 'Applications of low-cost sensing technologies for air quality monitoring and exposure assessment: How far have they gone?', *Environment International* **116**, 286–299.
URL: *https://www.sciencedirect.com/science/article/pii/S0160412018302460*

Mysen, M., Berntsen, S., Nafstad, P. & Schild, P. G. (2005), 'Occupancy density and benefits of demand-controlled ventilation in norwegian primary schools', *Energy and Buildings* **37**(12), 1234–1240.
URL: *https://www.sciencedirect.com/science/article/pii/S037877880500040X*

Mysen, M. & Schild, P. (2011), 'Requirements for well functioning demand controlled ventilation', *Rehva Journal* **48**(5), 14–18.
URL: *https://www.rehva.eu/fileadmin/hvac-dictio/05-2011/rj1105$_p$14$-$18$_r$equirements$-for-$well $-$ functioning $-$ demand $-$ controlled $-$ ventilation.pdf*

Mysen, M. & Schild, P. (2013), 'Behovsstyrt ventilasjon, dcv - krav og overlevering'.
URL: *https://www.sintef.no/contentassets/aab32f3b1f47475f91c7f61f46469b6d/behovsstyrt-ventilasjon-dcv-krav-og-overlevering.pdf*

Mysen, M. & Schild, P. (2014), 'Behovsstyrt ventilasjon, dcv–forutsetninger og utforming'.
URL: *https://www.sintef.no/globalassets/project/reduceventilation/behovsstyrt$_v$entilasjon$_d$cv$-$forutsetninger$_o$g$_u$tforming.pdf*

National Academies of Sciences, E., Medicine, Division, H., Medicine, Practice, B. o. P. H., Health, P., Alper, J., Madhavan, G. & Butler, D. A. (2016), *Health Risks of Indoor Exposure to Particulate Matter: Workshop Summary*, National Academies Press, Washington, D.C.

NIST (n.d.), 'Contam introduction'. Viewed: 03.03.2021.
URL: *https://www.nist.gov/el/energy-and-environment-division-73200/nist-multizone-modeling/software/contam*

OM ZEB (n.d.). Viewed: 01.06.2021.
URL: *https://www.zeb.no/index.php/no/om-zeb/about-the-zeb-centre*

Optivent Ultra VAV (n.d.). Viewed: 03.02.2021.
URL: *https://www.ventistal.no/produkter/item/692-optivent-ultra-vav*

Persily, A. & Jonge, L. (2017), 'Carbon dioxide generation rates for building occupants', *Indoor air* **27**(5), 868–879.

Rackes, A. & Waring, M. S. (2013), 'Modeling impacts of dynamic ventilation strategies on indoor air quality of offices in six us cities', *Building and environment* **60**, 243–253.

Rai, A. C., Kumar, P., Pilla, F., Skouloudis, A. N., Di Sabatino, S., Ratti, C., Yasar, A. & Rickerby, D. (2017), 'End-user perspective of low-cost sensors for outdoor air pollution monitoring', *Science of The Total Environment* **607-608**, 691–705.
URL: *https://www.sciencedirect.com/science/article/pii/S0048969717316935*

Ram, D. N. (2019), 'Indoor air quality (iaq) and energy efficiency', *ASHRAE transactions* **125**(1), 231.

Salthammer, T. (2019), 'Formaldehyde sources, formaldehyde concentrations and air exchange rates in european housings', *Building and Environment* **150**, 219–232.
URL: *https://www.sciencedirect.com/science/article/pii/S0360132318307960*

Salthammer, T., Mentese, S. & Marutzky, R. (2010), 'Formaldehyde in the indoor environment', *Chemical reviews* **110**(4), 2536–2572.

Seem, J. E., House, J. M., Kelly, G. E. & Klaassen, C. J. (2000), 'A damper control system for preventing reverse airflow through the exhaust air damper of variable-air-volume air-handling units', *HVACR research* **6**(2), 135–148.

Siemens (2013), 'Demand control ventilation application guide for consulting engineers'.
URL: *https://www.downloads.siemens.com/download-center/Download.aspx?pos=downloadfct =getassetid1=A6V10592576*

SIMIEN Wiki (n.d.). Viewed: 25.05.2021.
URL: *https://www.programbyggerne.no/SIMIEN/validering*

SINTEF Byggforsk, (1990), 'Byggforskserien 552.103 oppvarming av boliger. energiforbruk og kostnader'.
URL: *https://www.byggforsk.no/dokument/519/oppvarming_av_boliger_energiforbruk_og_*

SINTEF Byggforsk (2000), 'Byggforskserien 552.335 prosjektering av energieffektive ventilasjonsanlegg'.
URL: *https://www.byggforsk.no/dokument/2960/prosjektering_av_energieffektive _ventilasjonsanlegg*

SINTEF Byggforsk (2005*a*), 'Byggforskserien 421.505 godt inneklima i yrkesbygninger'.
URL: *https://www.byggforsk.no/dokument/195/godt_inneklima_i_yrkesbygninger*

SINTEF Byggforsk (2005*b*), 'Byggforskserien 552.331 filtrering av luft i ventilasjonsanlegg'.
URL: *https://www.byggforsk.no/dokument/536/filtrering_av_luft_i_ventilasjonsanlegg*

SINTEF Byggforsk (2016*a*), 'Byggforskserien 552.323 behovsstyrt ventilasjon (dcv). prinsipper'.
URL: *https://www.byggforsk.no/dokument/535/behovsstyrt_ventilasjon_dcv_prinsipper*

SINTEF Byggforsk (2016*b*), 'Byggforskserien 552.325 behovsstyrt ventilasjon (dcv). systemløsninger og regulering'.
URL: *https://www.byggforsk.no/dokument/5160/behovsstyrt_ventilasjon _dcv_systemloesninger_og_regulering*

Spinelle, L., Gerboles, M., Kok, G., Persijn, S. & Sauerwald, T. (2017), 'Review of portable and low-cost sensors for the ambient air monitoring of benzene and other volatile organic compounds', *Sensors* **17**(7).
URL: *https://www.mdpi.com/1424-8220/17/7/1520*

Standard Norge (2005), *NS-EN ISO 7730:2005 Ergonomi i termisk miljø - Analytisk bestemmelse og tolkning av termisk velbefinnende ved kalkulering av PMV- og PPD-indeks og lokal termisk komfort (ISO 7730:2005)*, Standard Norge.

Standard Norge (2007), *NS-EN 15251:2007+NA:2014 Inneklimaparametere for dimensjonering og vurdering av bygningers energiytelse inkludert inneluftkvalitet, termisk miljø, belysning og akustikk*, Standard Norge.

Standard Norge (2012), *NS-EN 779:2012 Partikkelfiltre for vanlig ventilasjon - Bestemmelse av filtreringsevnen*, Standard Norge.

Standard Norge (2014), *NS 3031:2014 Beregning av bygningers energiytelse - Metode og data*, Standard Norge.

Standard Norge (2019), *NS-EN 16798-1:2019 Bygningers energiytelse - Ventilasjon i bygninger - Del 1: Inneklimaparametere for dimensjonering og vurdering av bygningers energiytelse inkludert inneluftkvalitet, termisk miljø, belysning og akustikk (Modul M1-6)*, Standard Norge.

Stefano Paolo Corgnati, Manuel Gameiro da Silva, R. A. E. A. J. J. C. M. F. J. K. A. K. M. B. W. O. Z. P. P. W. (2011), *Indoor climate quality assessment*, Vol. no. 14 of *REHVA guidebook*, Rehva, Brussels.

Sterud, T. (2009), 'Working time in the european union: Norway'.
URL: *https://www.eurofound.europa.eu/publications/report/2009/working-time-in-the-european-union-norway*

Taal, A. & Itard, L. (2020), 'Fault detection and diagnosis for indoor air quality in dcv systems: Application of 4s3f method and effects of dbn probabilities', *Building and environment* **174**, 106632.

Veiledning, best.nr. 444: Klima og luftkvalitet på arbeidsplassen (2016). Viewed: 28.02.2021.
URL: *https://www.arbeidstilsynet.no/contentassets/3f86f6d2038348d18540404144f76a22 /luftkvalitet-pa-arbeidsplassen.pdf*

Vellei, M., Herrera, M., Fosas, D. & Natarajan, S. (2017), 'The influence of relative humidity on adaptive thermal comfort', *Building and Environment* **124**, 171 – 185.
URL: *http://www.sciencedirect.com/science/article/pii/S0360132317303505*

Wargocki, P., Knudsen, H. & Frontczak, M. (2007), 'The effect of using low-polluting building materials on ventilation requirements and energy use in buildings'.

Wargocki, P., Porras-Salazar, J. A., Contreras-Espinoza, S. & Bahnfleth, W. (2020), 'The relationships between classroom air quality and children's performance in school', *Building and environment* **173**(C), 106749.

Wargocki, P., Saputa, D. A., Kuehn, T. H., Fisk, W. J., Barney Burroughs, H. E., Siegel, J. A., Muller, C. O., Jackson, M. C., Conrad, E. A. & Veeck, A. (2015), 'Ashrae position document on filtration and air cleaning'.
URL: *https://www.ashrae.org/file library/about/position documents/filtration-and-air-cleaning-pd.pdf*

Wei, W., Wargocki, P., Zirngibl, J., Bendžalová, J. & Mandin, C. (2020), 'Review of parameters used to assess the quality of the indoor environment in green building certification schemes for offices and hotels', *Energy and Buildings* **209**, 109683.
URL: *https://www.sciencedirect.com/science/article/pii/S0378778819328579*

WHO (2010), 'Who guidelines for indoor air quality: selected pollutants'.
URL: *https://www.euro.who.int/$_{data/assets/pdf_file}$/0009/128169/e94535.pdf*

Wolkoff, P. (2013), 'Indoor air pollutants in office environments: Assessment of comfort, health, and performance', *International Journal of Hygiene and Environmental Health* **216**(4), 371–394.
URL: *https://www.sciencedirect.com/science/article/pii/S1438463912001046*

Wolkoff, P. & Kjærgaard, S. K. (2007), 'The dichotomy of relative humidity on indoor air quality', *Environment International* **33**(6), 850–857.
URL: *https://www.sciencedirect.com/science/article/pii/S0160412007000773*

Yasuda, T., Yonemura, S. & Tani, A. (2012), 'Comparison of the characteristics of small commercial ndir co2 sensor models and development of a portable co2 measurement device', *Sensors* **12**(3), 3641–3655.
URL: *https://www.mdpi.com/1424-8220/12/3/3641*

Yurko, G., Roostaei, J., Dittrich, T., Xu, L., Ewing, M., Zhang, Y. & Shreve, G. (2019), 'Real-time sensor response characteristics of 3 commercial metal oxide sensors for detection of btex and chlorinated aliphatic hydrocarbon organic vapors', *Chemosensors* **7**(3), 40.

Zhang, J., Li, X., Zhao, T., Yu, H., Chen, T., Liu, C. & Yang, X. (2015), 'A review of static pressure reset control in variable air volume air condition system', *Procedia Engineering* **121**, 1844 – 1850. The 9th International Symposium on Heating, Ventilation and Air Conditioning (ISHVAC) joint with the 3rd International Conference on Building Energy and Environment (COBEE), 12-15 July 2015, Tianjin, China.
URL: *http://www.sciencedirect.com/science/article/pii/S1877705815029938*

Zhang, T., Li, X., Rao, Y., Liu, Y. & Zhao, Q. (2020), 'Removal of formaldehyde in urban office building by the integration of ventilation and photocatalyst-coated window', *Sustainable Cities and Society* **55**, 102050.
URL: *http://www.sciencedirect.com/science/article/pii/S2210670720300378*

Zhang, X., Wargocki, P. & Lian, Z. (2016), 'Human responses to carbon dioxide, a follow-up study at recommended exposure limits in non-industrial environments', *Building and environment* **100**, 162–171.

Zhang, X., Wargocki, P., Lian, Z. & Thyregod, C. (2017), 'Effects of exposure to carbon dioxide and bioeffluents on perceived air quality, self-assessed acute health symptoms, and cognitive performance', *Indoor air* **27**(1), 47–64.

Appendix A

SIMIEN

A.1   SIMIEN summer simulation

Following is the output from a summer simulation conducted in SIMIEN. This simulation were used to determine the required airflow rates related to planning the office areas as described in Section 3.1.

Simuleringsnavn: Sommersimulering
Tid/dato simulering: 15:02 31/5-2021
Programversjon: 6.015
Simuleringsansvarlig: Jørgen
Firma: Undervisningslisens
Inndatafil: M:\...\Simulering av kontorarealer_3_like_for_CONTAM.smi
Prosjekt: Kontorbygg
Sone: Alle soner

Dimensjonerende verdier		
Beskrivelse	Verdi	Tidspunkt
Maksimal romlufttemperatur (Cellekontor_2):	27,8 °C	17:00
Maksimal operativ temperatur (Cellekontor_2)	27,3 °C	18:15
Maksimal CO2 konsentrasjon (Cellekontor_1)	1001 PPM	06:45

Sammendrag av nøkkelverdier for Cellekontor_1		
Beskrivelse	Verdi	Tidspunkt
Maks. innelufttemperatur	27,6 °C	15:00
Maks. operativ temperatur	27,0 °C	15:30
Maks. CO2 konsentrasjon	1001 PPM	06:45

Sammendrag av nøkkelverdier for Cellekontor_2		
Beskrivelse	Verdi	Tidspunkt
Maks. innelufttemperatur	27,8 °C	17:00
Maks. operativ temperatur	27,3 °C	18:15
Maks. CO2 konsentrasjon	960 PPM	07:15

Sammendrag av nøkkelverdier for Cellekontor_3		
Beskrivelse	Verdi	Tidspunkt
Maks. innelufttemperatur	27,8 °C	17:00
Maks. operativ temperatur	27,3 °C	18:15
Maks. CO2 konsentrasjon	960 PPM	07:15

Simuleringsnavn: Sommersimulering
Tid/dato simulering: 15:02 31/5-2021
Programversjon: 6.015
Simuleringsansvarlig: Jørgen
Firma: Undervisningslisens
Inndatafil: M:\...\Simulering av kontorarealer_3_like_for_CONTAM.smi
Prosjekt: Kontorbygg
Sone: Alle soner

Tilluft

[m³/h]

1 Summert tilluft alle soner

Simuleringsnavn: Sommersimulering
Tid/dato simulering: 15:02 31/5-2021
Programversjon: 6.015
Simuleringsansvarlig: Jørgen
Firma: Undervisningslisens
Inndatafil: M:\...\Simulering av kontorarealer_3_like_for_CONTAM.smi
Prosjekt: Kontorbygg
Sone: Alle soner

Varmetilskudd/kjøling

1 Internlaster
2 Oppvarming
3 Varmebatteri
4 Kjøling
5 Kjølebatteri
6 Solstråling

Simuleringsnavn: Sommersimulering
Tid/dato simulering: 15:02 31/5-2021
Programversjon: 6.015
Simuleringsansvarlig: Jørgen
Firma: Undervisningslisens
Inndatafil: M:\...\Simulering av kontorarealer_3_like_for_CONTAM.smi
Prosjekt: Kontorbygg
Sone: Alle soner

Dokumentasjon av sentrale inndata (1)		
Beskrivelse	Verdi	Dokumentasjon
Areal yttervegger [m²]:	13	
Areal tak [m²]:	0	
Areal gulv [m²]:	0	
Areal vinduer og ytterdører [m²]:	5	
Oppvarmet bruksareal (BRA) [m²]:	21	
Oppvarmet luftvolum [m³]:	50	
U-verdi yttervegger [W/m²K]	0,21	
U-verdi tak [W/m²K]	0,00	
U-verdi gulv [W/m²K]	0,00	
U-verdi vinduer og ytterdører [W/m²K]	1,19	
Areal vinduer og dører delt på bruksareal [%]	24,0	
Normalisert kuldebroverdi [W/m²K]:	0,06	
Normalisert varmekapasitet [Wh/m²K]	360	
Lekkasjetall (n50) [1/h]:	1,50	
Temperaturvirkningsgr. varmegjenvinner [%]:	85	

Dokumentasjon av sentrale inndata (2)		
Beskrivelse	Verdi	Dokumentasjon
Estimert virkningsgrad gjenvinner justert for frostsikring [%]:	85,0	
Spesifikk vifteeffekt (SFP) [kW/m³/s]:	2,50	
Luftmengde i driftstiden [m³/hm²]	12,00	
Luftmengde utenfor driftstiden [m³/hm²]	0,70	
Systemvirkningsgrad oppvarmingsanlegg:	0,89	
Installert effekt romoppv. og varmebatt. [W/m²]:	80	
Settpunkttemperatur for romoppvarming [°C]	20,0	
Systemeffektfaktor kjøling:	2,50	
Settpunkttemperatur for romkjøling [°C]	0,0	
Installert effekt romkjøling og kjølebatt. [W/m²]:	0	
Spesifikk pumpeeffekt romoppvarming [kW/(l/s)]:	0,00	
Spesifikk pumpeeffekt romkjøling [kW/(l/s)]:	0,00	
Spesifikk pumpeeffekt varmebatteri [kW/(l/s)]:	0,50	
Spesifikk pumpeeffekt kjølebatteri [kW/(l/s)]:	0,00	
Driftstid oppvarming (timer)	12,0	

Simuleringsnavn: Sommersimulering
Tid/dato simulering: 15:02 31/5-2021
Programversjon: 6.015
Simuleringsansvarlig: Jørgen
Firma: Undervisningslisens
Inndatafil: M:\...\Simulering av kontorarealer_3_like_for_CONTAM.smi
Prosjekt: Kontorbygg
Sone: Alle soner

Dokumentasjon av sentrale inndata (3)		
Beskrivelse	Verdi	Dokumentasjon
Driftstid kjøling (timer)	0,0	
Driftstid ventilasjon (timer)	24,0	
Driftstid belysning (timer)	12,0	
Driftstid utstyr (timer)	12,0	
Oppholdstid personer (timer)	12,0	
Effektbehov belysning i driftstiden [W/m²]	8,00	
Varmetilskudd belysning i driftstiden [W/m²]	8,00	
Effektbehov utstyr i driftstiden [W/m²]	11,00	
Varmetilskudd utstyr i driftstiden [W/m²]	11,00	
Effektbehov varmtvann på driftsdager [W/m²]	0,80	
Varmetilskudd varmtvann i driftstiden [W/m²]	0,00	
Varmetilskudd personer i oppholdstiden [W/m²]	15,00	
Total solfaktor for vindu og solskjerming:	0,16	
Gjennomsnittlig karmfaktor vinduer:	0,20	
Solskjermingsfaktor horisont/utspring (N/Ø/S/V):	1,00/1,00/1,00/1,00	

Inndata sommersimulering	
Beskrivelse	Verdi
Simuleringsdato	20/07
Simulerte døgn	5
Dagtype	Normal driftsdag
Bekledning [clo]	1,0
Aktivitetsnivå personer [met]	1,0
Bruker dim. klimadata fra database (N50)	-

Inndata bygning	
Beskrivelse	Verdi
Bygningskategori	Kontorbygg
Simuleringsansvarlig	Jørgen
Kommentar	

SIMIEN
Resultater sommersimulering

Simuleringsnavn: Sommersimulering
Tid/dato simulering: 15:02 31/5-2021
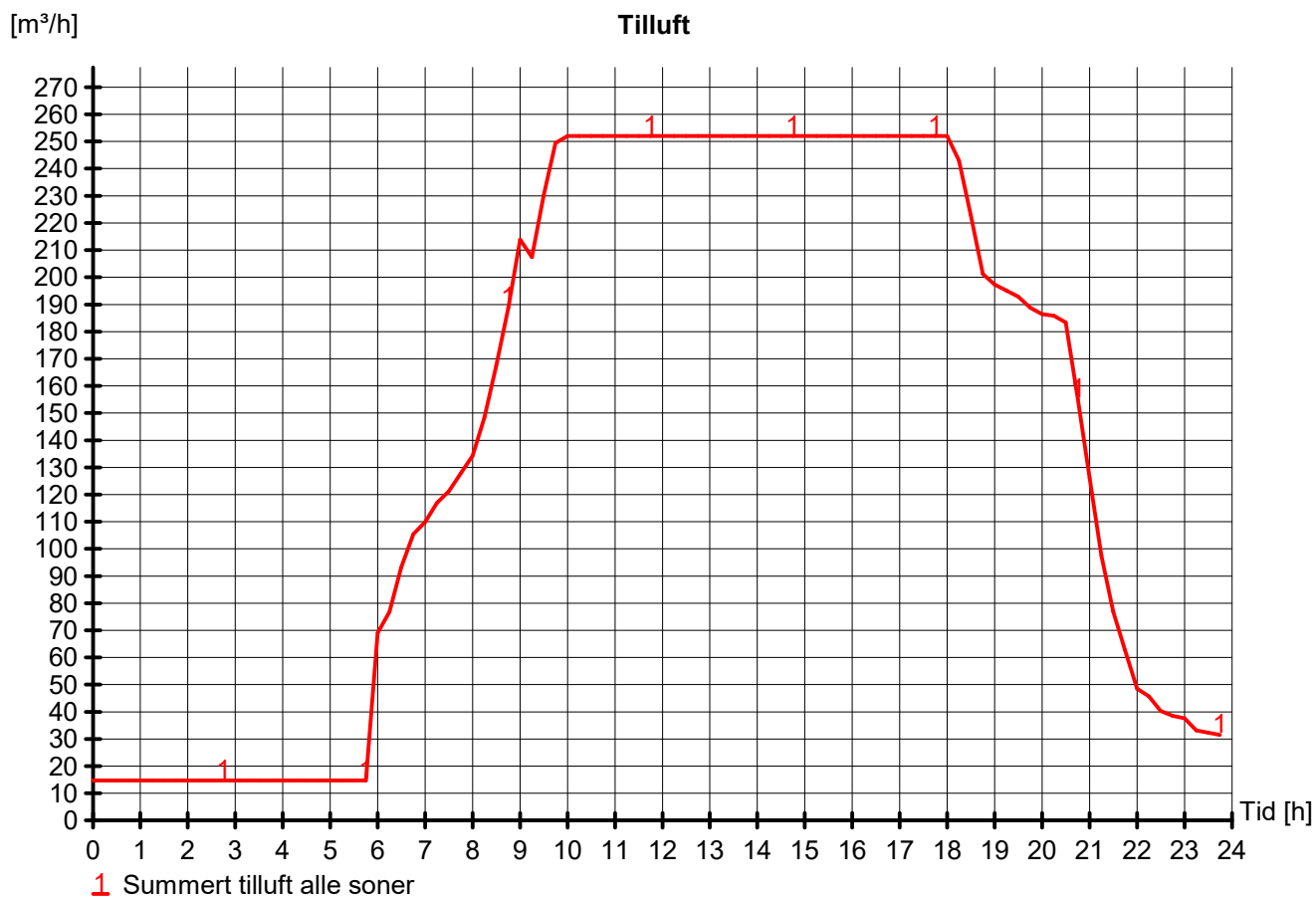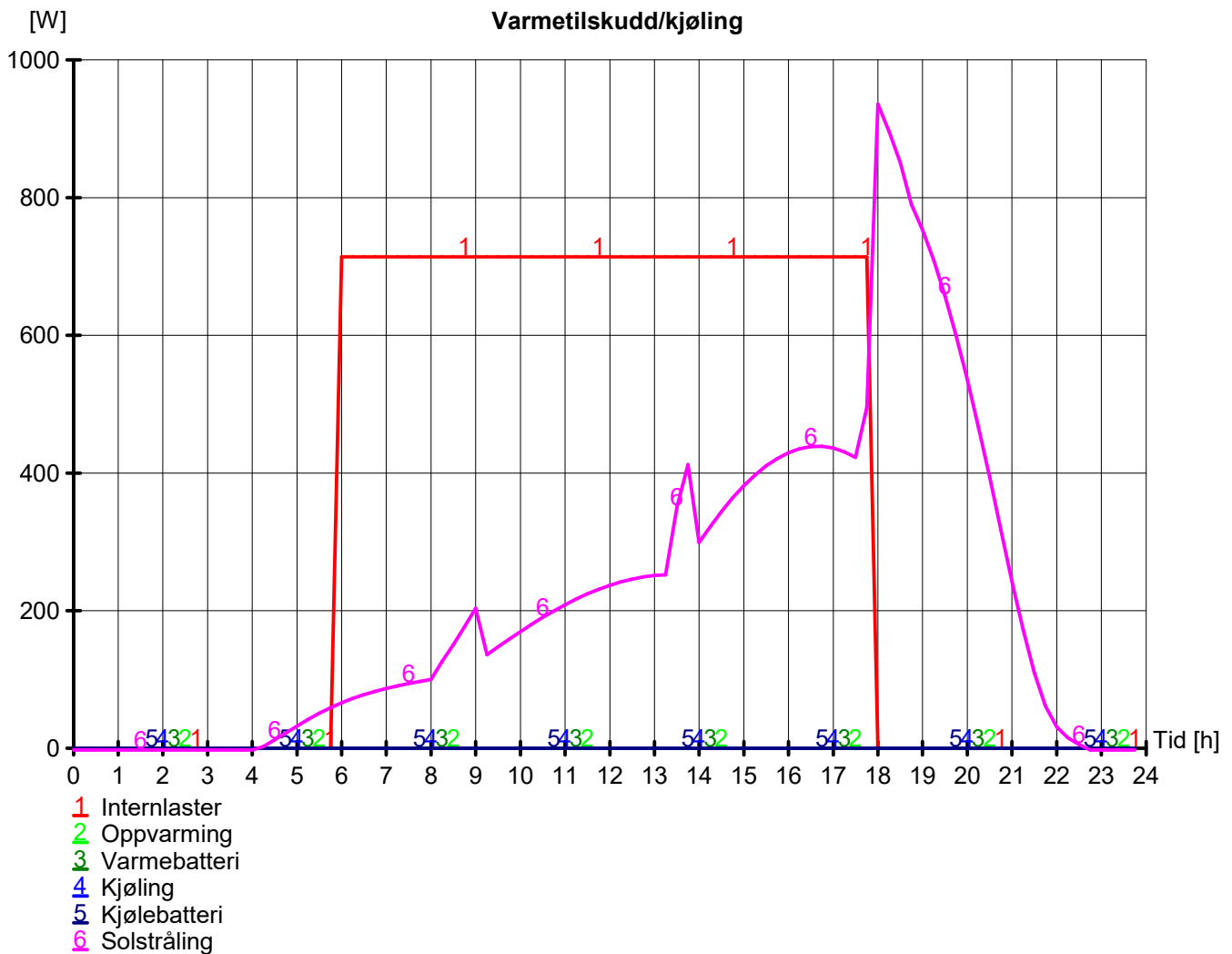Programversjon: 6.015
Simuleringsansvarlig: Jørgen
Firma: Undervisningslisens
Inndatafil: M:\...\Simulering av kontorarealer_3_like_for_CONTAM.smi
Prosjekt: Kontorbygg
Sone: Alle soner

Inndata klima	
Beskrivelse	Verdi
Klimasted	Trondheim
Breddegrad	63° 30'
Lengdegrad	10° 22'
Tidssone	GMT + 1
Klimadata	Fra database
Transmissivitet atmosfære	0,74
Absolutt luftfuktighet	9 g/kg
Markrefleksjonskoeffisient	0,20
Minimum utetemperatur	15,2 °C
Maksimum utetemperatur	24,4 °C
Vindhastighet	2,5 m/s

Inndata ekspertverdier	
Beskrivelse	Verdi
Konvektiv andel varmetilskudd belysning	0,30
Konvektiv andel varmetilsk. teknisk utstyr	0,50
Konvektiv andel varmetilsikudd personer	0,50
Konvektiv andel varmetilsikudd sol	0,50
Konvektiv varmoverføringskoeff. vegger	2,50
Konvektiv varmoverføringskoeff. himling	2,00
Konvektiv varmoverføringskoeff. gulv	3,00
Bypassfaktor kjølebatteri	0,25
Innv. varmemotstand på vinduruter	0,13
Midlere lufthastighet romluft	0,15
Turbulensintensitet romluft	25,00
Avstand fra vindu	0,60
Termisk konduktivitet akk. sjikt [W/m²K]:	20,00

A.2   SIMIEN winter simulation

Following is the output from a winter simulation conducted in SIMIEN. This simulation is the foundation for the constructed indoor air temperature used in the CONTAM simulations described in Section 3.2.6.

SIMIEN
Resultater vintersimulering

Simuleringsnavn: Vintersimulering
Tid/dato simulering: 15:15 31/5-2021
Programversjon: 6.015
Simuleringsansvarlig: Jørgen
Firma: Undervisningslisens
Inndatafil: M:\...\Simulering av kontorarealer_3_like_for_CONTAM.smi
Prosjekt: Kontorbygg
Sone: Alle soner

Dimensjonerende verdier		
Beskrivelse	Verdi	Tidspunkt
Maks. samtidig effekt forvarmebatteri gjenvinner (alle soner)	116 W / 5,5 W/m²	06:30
Maks. samtidig effekt varmebatterier:	91 W / 4,3 W/m²	07:45
Totalt installert effekt varmebatterier	630 W / 30,0 W/m²	07:45
Maks. samtidig effekt romoppvarming:	433 W / 20,6 W/m²	06:30
Totalt installert effekt romoppvarming	1050 W / 50,0 W/m²	06:30
Min. romlufttemperatur:	19,0 °C	06:30
Min. operativ temperatur:	19,4 °C	06:00
Maksimal CO2 konsentrasjon (Cellekontor_1)	1001 PPM	10:30

Sammendrag av nøkkelverdier for Cellekontor_1		
Beskrivelse	Verdi	Tidspunkt
Min. innelufttemperatur	19,0 °C	06:00
Min. operativ temperatur	19,4 °C	06:00
Maks. CO2 konsentrasjon	1001 PPM	10:30
Maks. effekt forvarmebatteri varmegjenvinner	39 W / 5,5 W/m²	06:45
Maksimal effekt varmebatterier:	30 W / 4,3 W/m²	08:00
Installert effekt varmebatterier	210 W / 30,0 W/m²	08:00
Maksimal effekt oppvarmingsanlegg:	144 W / 20,6 W/m²	06:30
Installert effekt romoppvarming	350 W / 50,0 W/m²	06:30

Sammendrag av nøkkelverdier for Cellekontor_2		
Beskrivelse	Verdi	Tidspunkt
Min. innelufttemperatur	19,0 °C	06:00
Min. operativ temperatur	19,4 °C	06:00
Maks. CO2 konsentrasjon	1001 PPM	10:30
Maks. effekt forvarmebatteri varmegjenvinner	39 W / 5,5 W/m²	06:45
Maksimal effekt varmebatterier:	30 W / 4,3 W/m²	08:00
Installert effekt varmebatterier	210 W / 30,0 W/m²	08:00
Maksimal effekt oppvarmingsanlegg:	144 W / 20,6 W/m²	06:30
Installert effekt romoppvarming	350 W / 50,0 W/m²	06:30

SIMIEN

Resultater vintersimulering

Simuleringsnavn: Vintersimulering
Tid/dato simulering: 15:15 31/5-2021
Programversjon: 6.015
Simuleringsansvarlig: Jørgen
Firma: Undervisningslisens
Inndatafil: M:\...\Simulering av kontorarealer_3_like_for_CONTAM.smi
Prosjekt: Kontorbygg
Sone: Alle soner

Sammendrag av nøkkelverdier for Cellekontor_3		
Beskrivelse	Verdi	Tidspunkt
Min. innelufttemperatur	19,0 °C	06:00
Min. operativ temperatur	19,4 °C	06:00
Maks. CO2 konsentrasjon	1001 PPM	10:30
Maks. effekt forvarmebatteri varmegjenvinner	39 W / 5,5 W/m²	06:45
Maksimal effekt varmebatterier:	30 W / 4,3 W/m²	08:00
Installert effekt varmebatterier	210 W / 30,0 W/m²	08:00
Maksimal effekt oppvarmingsanlegg:	144 W / 20,6 W/m²	06:30
Installert effekt romoppvarming	350 W / 50,0 W/m²	06:30

Tilluft

1 Summert tilluft alle soner

SIMIEN

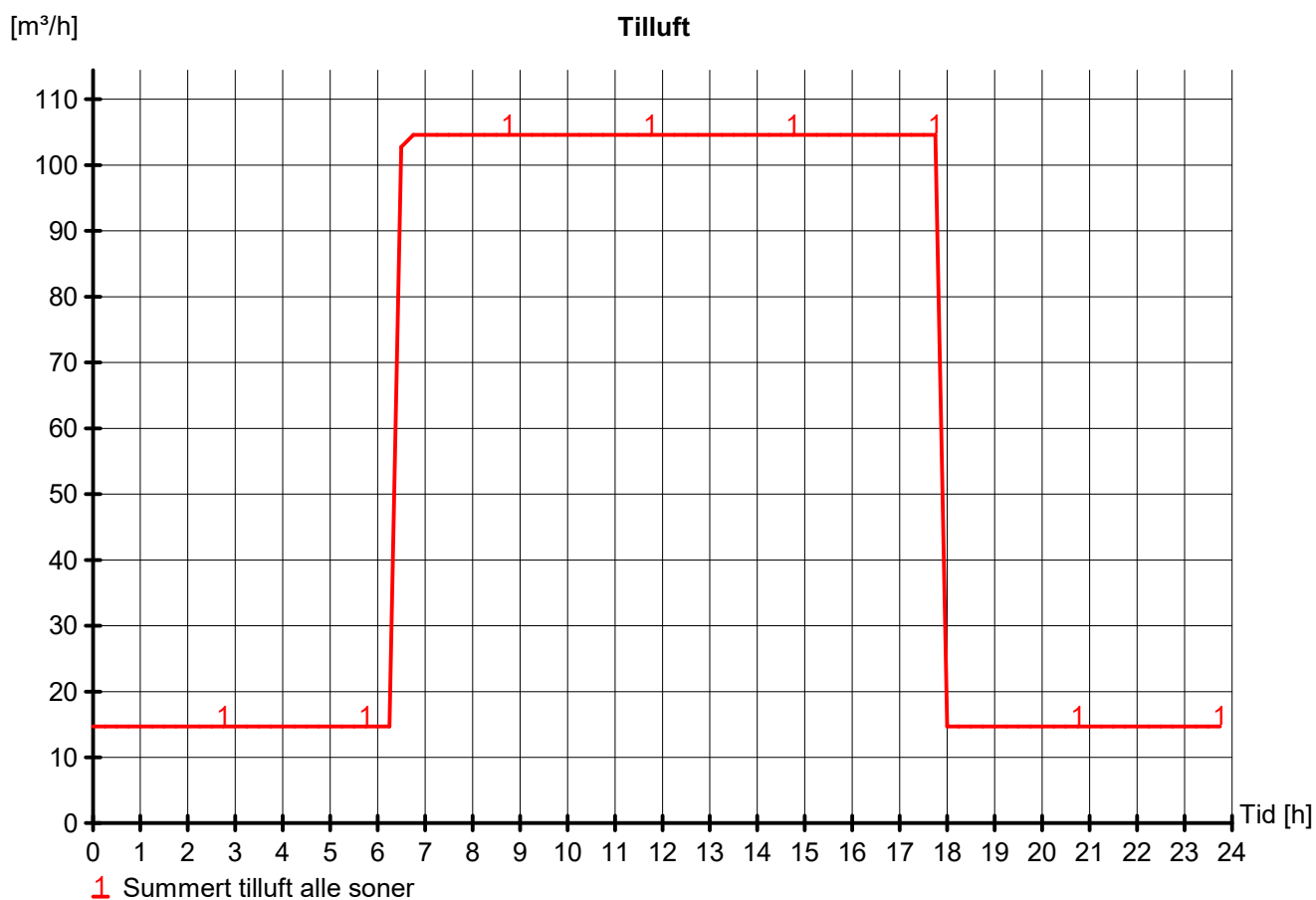**Resultater vintersimulering**

Simuleringsnavn: Vintersimulering
Tid/dato simulering: 15:15 31/5-2021
Programversjon: 6.015
Simuleringsansvarlig: Jørgen
Firma: Undervisningslisens
Inndatafil: M:\...\Simulering av kontorarealer_3_like_for_CONTAM.smi
Prosjekt: Kontorbygg
Sone: Alle soner

Varmetilskudd/kjøling

1 Internlaster
2 Oppvarming
3 Varmebatteri
4 Kjøling
5 Kjølebatteri
6 Solstråling

Simuleringsnavn: Vintersimulering
Tid/dato simulering: 15:15 31/5-2021
Programversjon: 6.015
Simuleringsansvarlig: Jørgen
Firma: Undervisningslisens
Inndatafil: M:\...\Simulering av kontorarealer_3_like_for_CONTAM.smi
Prosjekt: Kontorbygg
Sone: Alle soner

Dokumentasjon av sentrale inndata (1)		
Beskrivelse	Verdi	Dokumentasjon
Areal yttervegger [m²]:	13	
Areal tak [m²]:	0	
Areal gulv [m²]:	0	
Areal vinduer og ytterdører [m²]:	5	
Oppvarmet bruksareal (BRA) [m²]:	21	
Oppvarmet luftvolum [m³]:	50	
U-verdi yttervegger [W/m²K]	0,21	
U-verdi tak [W/m²K]	0,00	
U-verdi gulv [W/m²K]	0,00	
U-verdi vinduer og ytterdører [W/m²K]	1,19	
Areal vinduer og dører delt på bruksareal [%]	24,0	
Normalisert kuldebroverdi [W/m²K]:	0,06	
Normalisert varmekapasitet [Wh/m²K]	360	
Lekkasjetall (n50) [1/h]:	1,50	
Temperaturvirkningsgr. varmegjenvinner [%]:	85	

Dokumentasjon av sentrale inndata (2)		
Beskrivelse	Verdi	Dokumentasjon
Estimert virkningsgrad gjenvinner justert for frostsikring [%]:	85,0	
Spesifikk vifteeffekt (SFP) [kW/m³/s]:	2,50	
Luftmengde i driftstiden [m³/hm²]	12,00	
Luftmengde utenfor driftstiden [m³/hm²]	0,70	
Systemvirkningsgrad oppvarmingsanlegg:	0,89	
Installert effekt romoppv. og varmebatt. [W/m²]:	80	
Settpunkttemperatur for romoppvarming [°C]	20,0	
Systemeffektfaktor kjøling:	2,50	
Settpunkttemperatur for romkjøling [°C]	0,0	
Installert effekt romkjøling og kjølebatt. [W/m²]:	0	
Spesifikk pumpeeffekt romoppvarming [kW/(l/s)]:	0,00	
Spesifikk pumpeeffekt romkjøling [kW/(l/s)]:	0,00	
Spesifikk pumpeeffekt varmebatteri [kW/(l/s)]:	0,50	
Spesifikk pumpeeffekt kjølebatteri [kW/(l/s)]:	0,00	
Driftstid oppvarming (timer)	12,0	

Simuleringsnavn: Vintersimulering
Tid/dato simulering: 15:15 31/5-2021
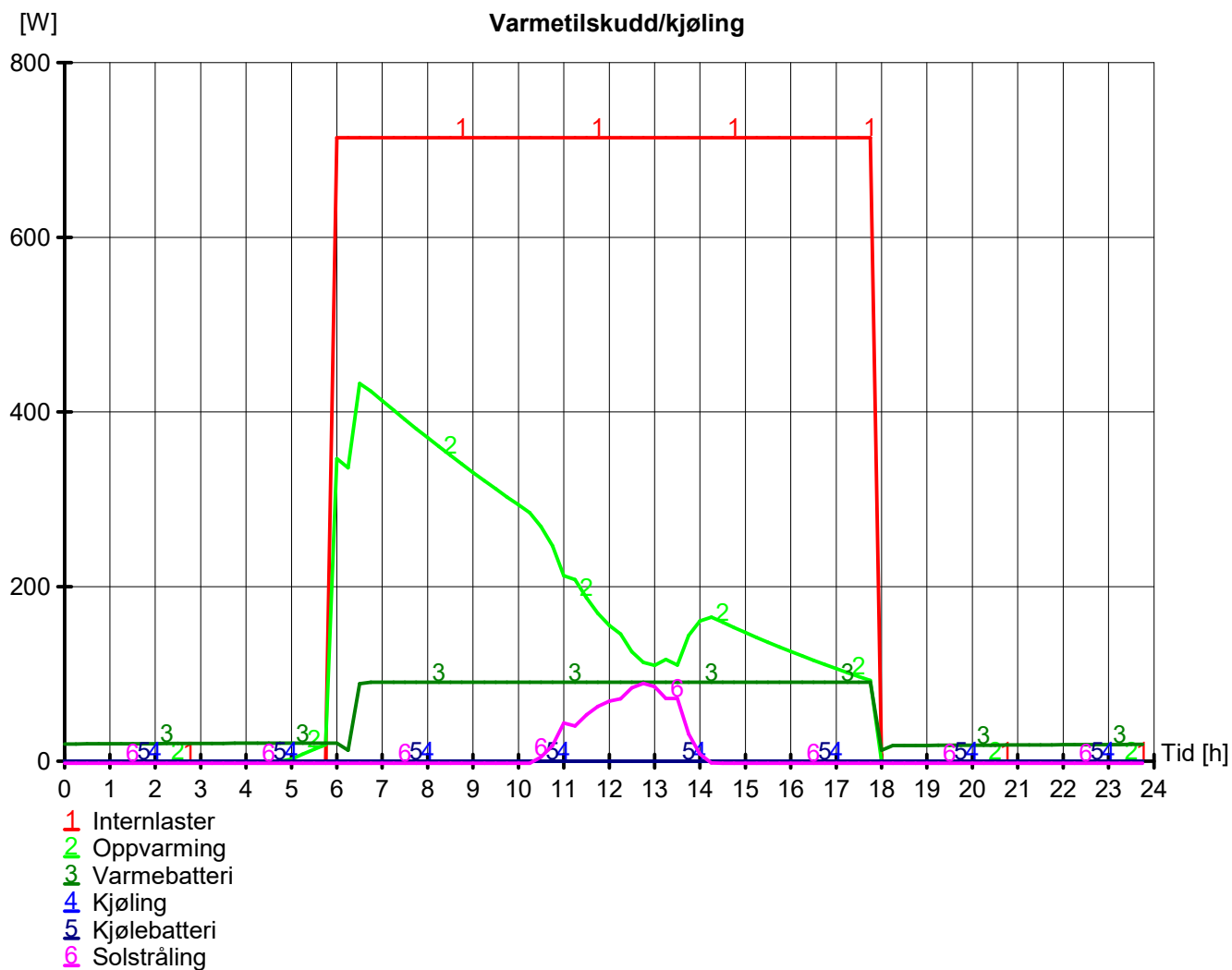Programversjon: 6.015
Simuleringsansvarlig: Jørgen
Firma: Undervisningslisens
Inndatafil: M:\...\Simulering av kontorarealer_3_like_for_CONTAM.smi
Prosjekt: Kontorbygg
Sone: Alle soner

Dokumentasjon av sentrale inndata (3)		
Beskrivelse	Verdi	Dokumentasjon
Driftstid kjøling (timer)	0,0	
Driftstid ventilasjon (timer)	24,0	
Driftstid belysning (timer)	12,0	
Driftstid utstyr (timer)	12,0	
Oppholdstid personer (timer)	12,0	
Effektbehov belysning i driftstiden [W/m²]	8,00	
Varmetilskudd belysning i driftstiden [W/m²]	8,00	
Effektbehov utstyr i driftstiden [W/m²]	11,00	
Varmetilskudd utstyr i driftstiden [W/m²]	11,00	
Effektbehov varmtvann på driftsdager [W/m²]	0,80	
Varmetilskudd varmtvann i driftstiden [W/m²]	0,00	
Varmetilskudd personer i oppholdstiden [W/m²]	15,00	
Total solfaktor for vindu og solskjerming:	0,16	
Gjennomsnittlig karmfaktor vinduer:	0,20	
Solskjermingsfaktor horisont/utspring (N/Ø/S/V):	1,00/1,00/1,00/1,00	

Inndata simulering av dimensjonerende vinterforhold	
Beskrivelse	Verdi
Simuleringsdato	24/12
Simulerte døgn	3
Dagtype	Normal driftsdag
Bekledning [clo]	1,0
Aktivitetsnivå personer [met]	1,0
Bruker dim. klimadata fra database	-

Inndata bygning	
Beskrivelse	Verdi
Bygningskategori	Kontorbygg
Simuleringsansvarlig	Jørgen
Kommentar	

SIMIEN

Resultater vintersimulering

Simuleringsnavn: Vintersimulering
Tid/dato simulering: 15:15 31/5-2021
Programversjon: 6.015
Simuleringsansvarlig: Jørgen
Firma: Undervisningslisens
Inndatafil: M:\...\Simulering av kontorarealer_3_like_for_CONTAM.smi
Prosjekt: Kontorbygg
Sone: Alle soner

Inndata klima	
Beskrivelse	Verdi
Klimasted	Trondheim
Breddegrad	63° 30'
Lengdegrad	10° 22'
Tidssone	GMT + 1
Klimadata	Fra database
Transmissivitet atmosfære	0,90
Absolutt luftfuktighet	1 g/kg
Markrefleksjonskoeffisient	0,60
Minimum utetemperatur	-19,6 °C
Maksimum utetemperatur	-17,4 °C
Vindhastighet	3,1 m/s

Inndata ekspertverdier	
Beskrivelse	Verdi
Konvektiv andel varmetilskudd belysning	0,30
Konvektiv andel varmetilsk. teknisk utstyr	0,50
Konvektiv andel varmetilsikudd personer	0,50
Konvektiv andel varmetilsikudd sol	0,50
Konvektiv varmoverføringskoeff. vegger	2,50
Konvektiv varmoverføringskoeff. himling	2,00
Konvektiv varmoverføringskoeff. gulv	3,00
Bypassfaktor kjølebatteri	0,25
Innv. varmemotstand på vinduruter	0,13
Midlere lufthastighet romluft	0,15
Turbulensintensitet romluft	25,00
Avstand fra vindu	0,60
Termisk konduktivitet akk. sjikt [W/m²K]:	20,00

Appendix B

Calculations

B.1 Example calculation of energy used for heating

Following is and example of energy for heating of air. The values in the calculation below is gathered from the simulation of the CAV system in CONTAM.

$$T_{supply} = \eta_T \cdot (T_{extract} - T_{out}) + T_{out} \qquad \text{(A.1)}$$

Where:

η_T = 0.75, $T_{extract}$ = 19°C, and T_{out} =1°C,

T_{supply} = 14.5 °C

Desired T_{supply} = 19 °C

The heating coil need to heat rise the temperature with Δ_T 4.5 °C

$$Q = \dot{m} \cdot C_p \cdot \Delta_T \text{ [kW]} \qquad \text{(A.2)}$$

Where:

$\dot{V} = 15.12[\frac{m^3}{h}] \rightarrow \dot{m} = 0.005040[\frac{kg}{s}]$

$C_p = 1005[\frac{J}{kg} \cdot K]$

Q = 0.0183613427138 [kW] for that specific time-step. In this case one minute.

Appendix C

Datasheets

Appendices C.1, C.2, C.3 and C.4 contains technical information on the components in the full-scale model in the laboratory, described in Section 3.1.

C.1   UNI 2

UNI 2 Luftbehandlingsaggregat

Ventilasjonsaggregat for leiligheter, småhus og eneboliger.

A

700084, 700085, 700086,
700087, 700088, 700089

- Temperaturvirkningsgrad i varmegjenvinner opp til 85 %.
  Spesifikk vifteeffekt i ventilasjonsanlegg (SFP) lavere enn 1,5.
- Ekstra stillegående.
- Enkel betjening, enkelt filterbytte og vedlikehold.
- Gir balansert ventilasjon med et svært godt inneklima.
- Mulighet for kommunikasjon via modbus.
- Moderne design.
- Effektiv og driftssikker - også i kulde.

	NOBB	GTIN	Modell
700084	44748393	7023677000848	UNI 2 RER Høyremodell, EC-vifter, med el.batteri
700085	44748404	7023677000855	UNI 2 REL Venstremodell, EC-vifter, med el.batteri
700086	44748412	7023677000862	UNI 2 R R Høyremodell, EC-vifter, uten el.batteri
700087	44748461	7023677000879	UNI 2 R L Venstremodell, EC-vifter, uten el.batteri

Tekniske data

	UNI 2 RE EC	UNI 2 R EC
Merkespenning	230 V 50 Hz	230 V 50 Hz
Sikringsstørrelse	10 A	10 A
Merkestrøm total	4,4 A	1,3 A
Merkeeffekt total	1015 W	215 W
Merkeeffekt elbatteri	800 W	-
Samlet merkeeffekt vifter	212 W	212 W
Merkeefffekt forvarme	-	-
Viftetype	B-hjul	B-hjul
Viftemotorstyring	0-10V	0-10V
Viftehastighet – max. turtall	3390 rpm	3390 rpm
Automatikk standard	CU60	CU60
Filtertype (TIL/FRA)	ePM1 55% (F7)	ePM1 55% (F7)
Filtermål (BxHxD)	335x130x113 mm	335x130x113 mm
Vekt	45 kg	45 kg
Kanaltilkobling	Ø125 mm	Ø125 mm
Høyde	780 mm	780 mm
Bredde	632 mm	632 mm
Dybde	408 mm	408 mm

Energiklasse: **A**

CTRL 0,65

LOKAL BEHOVSTYRING

Styring med sensor for ulike soner
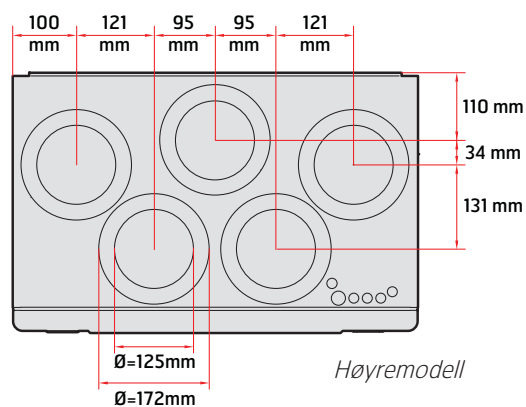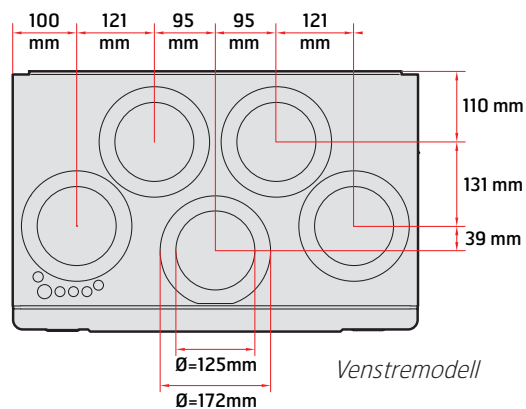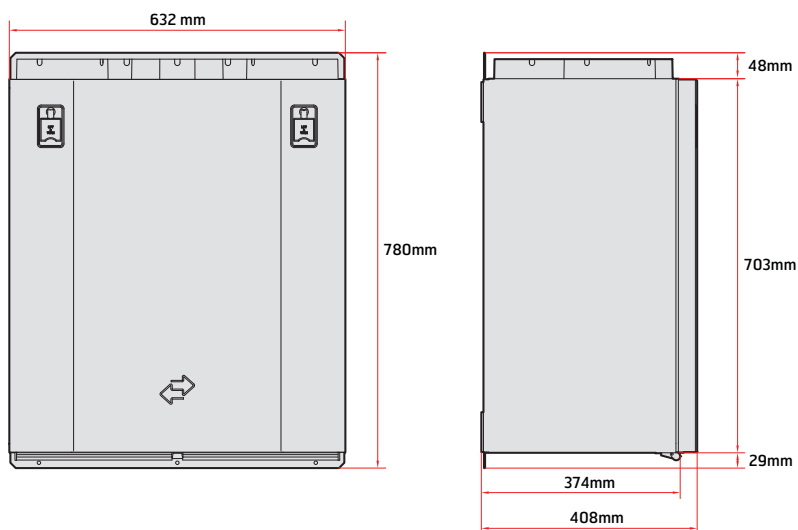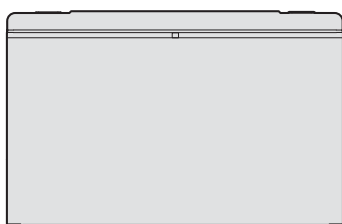**Tilbehør:** Avansert panel +
CO_2-føler/ bevegelsesvakt + spjeld
Resultat: Økt luftmengde i soner
som har behov

www.flexit.no

Målskisse

632 mm
780mm
48mm
703mm
29mm
374mm
408mm

100 mm | 121 mm | 95 mm | 95 mm | 121 mm
110 mm
131 mm
39 mm
Ø=125mm
Ø=172mm

Venstremodell

100 mm | 121 mm | 95 mm | 95 mm | 121 mm
110 mm
34 mm
131 mm
Ø=125mm
Ø=172mm

Høyremodell

Kapasitetsdiagram/Lyddata

Tilluftside
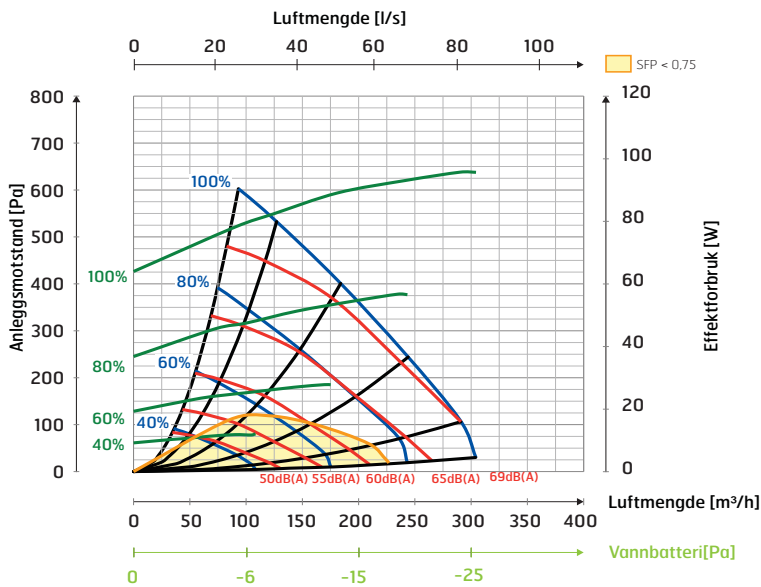
Avtrekkside
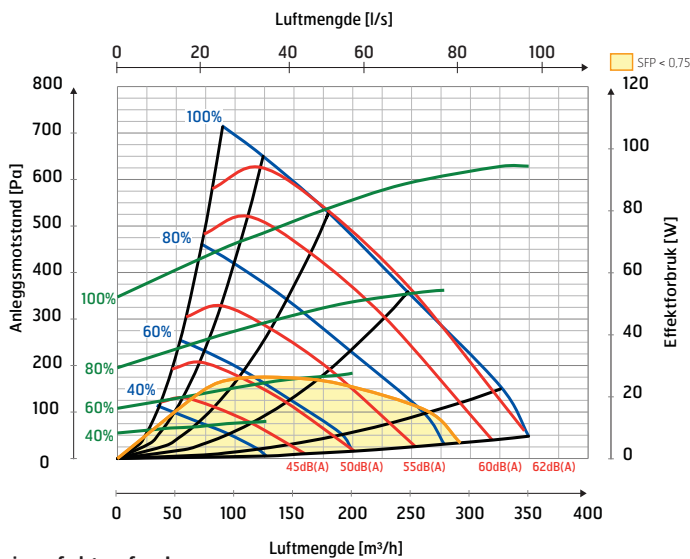
Korreksjonsfaktor for Lw

Hz	63 Lw(dB)	125 Lw(dB)	250 Lw(dB)	500 Lw(dB)	1000 Lw(dB)	2000 Lw(dB)	4000 Lw(dB)	8000 Lw(dB)	LwA (dBA)
Tilluft	6	6	3	-1	-8	-13	-22	-30	
Avtrekk	9	9	6	-5	-18	-21	-33	-33	
Avstrålt	-12	-12	-12	-19	-31	-35	-40	-41	-18

Forklaring til diagram

Lyddata er angitt som lydeffektnivå LwA i kapasitetsdiagrammene (dette er lyd til kanal).
Disse verdiene kan korrigeres ved hjelp av tabellen for de ulike oktavbåndene om man ønsker å se på Lw (uten tilpasning til A-bånd).

Korreksjonstabellen for respektive oktaver er angitt i Lw, noe som innebærer at man etter omregning pr. oktav for tilluft og avtrekk, får disse verdiene i Lw.

Avstrålt lyd fra aggregatet skal beregnes ut fra tilluftsdiagrammet.

Plassering

Aggregatet kan monteres på følgende vis:

1. Horisontalt på vegg. Her benyttes vedlagte veggbrakett ved montering.
   Kanaldeksel fås som tilbehør.
   Eneste monteringsvariant som er IP21-klassifisert.
2. På gulv (liggende på rygg). Her anbefales dempeføtter (fås som tilbehør).
3. I himling. Montering gjøres direkte i himling, uten veggbrakett.

Aggregatet leveres i både venstre og høyreutførelse, avhengig av hva som er gunstigst med tanke på kanalplassering.

De kan plasseres i kald sone, for eksempel på loft.
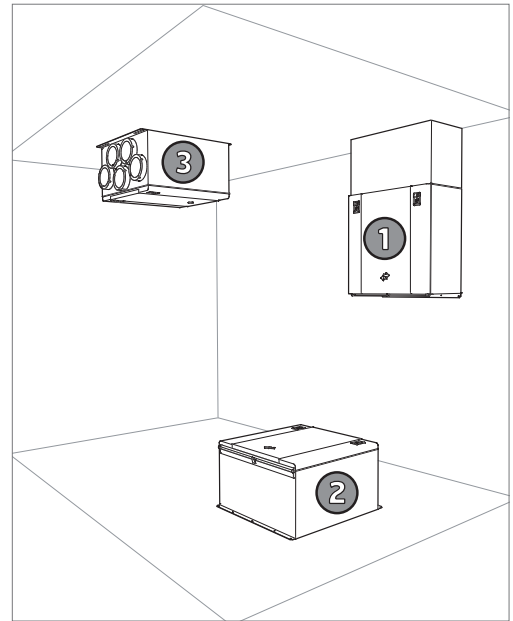
Nippelplassering

Venstremodell
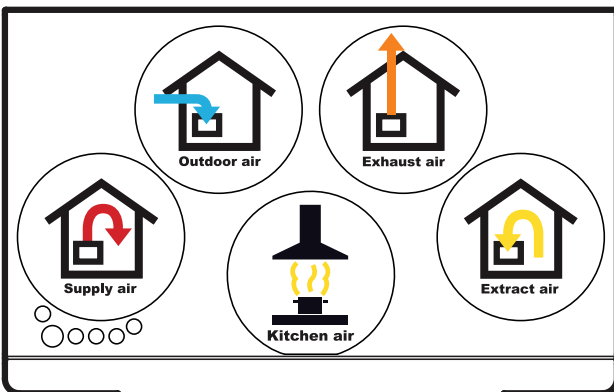
Høyremodell
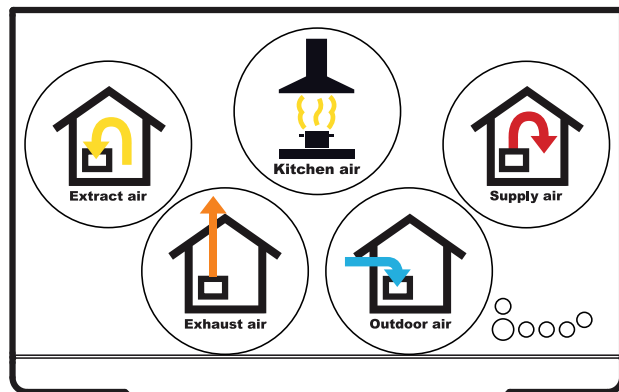
For mer informasjon om f.eks. montering, koblingsskjema og tilbehør, se www.flexit.no

C.2 Orion LØV med Sirius supply diffuser

Orion-LØV med Sirius

VAV-kammer for tilluft
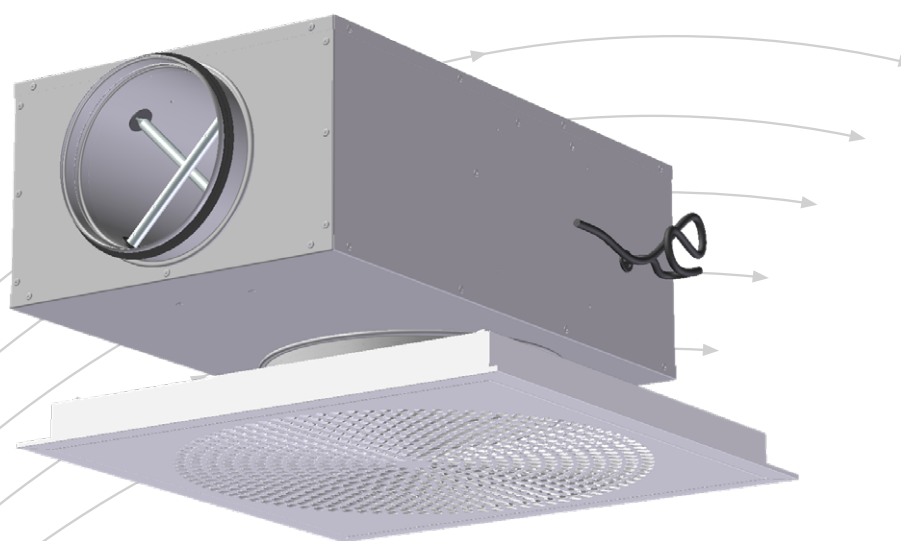
- Unik spjeldfunksjon
- Stort arbeidsområde
- Belimo MP-Bus
- MOD/BACnet
- LONWORKS
- Belimo KNX

TROX® TECHNIK

Auranor

Orion-LØV med Sirius

⊠ ANVENDELSE

Orion-LØV med Sirius er en tilluftsenhet med VAV-funksjon.
Den anvendes som volumregulator og tilluftsenhet i behovsstyrte ventilasjonssystemer. Orion-LØV har meget god induksjon, noe som gjør den velegnet for variable luftmengder.

⊠ FUNKSJON

Orion-LØV med Sirius har innebygget VAV-regulator for behovsstyring av luftmengde. Spjeldløsningen kan strupe høye trykk ved stor luftmengde og opprettholde lavt lydnivå, og kan redusere behovet for spjeld og lyddemper i områder inn mot ventilplasseringen i et kanalanlegg.
Orion-LØV med Sirius leveres med Belimo MP-Bus, LON, MOD/BACnet eller Belimo KNX for direkte bus-kommunikasjon mot SD-anlegg.
Måleavvik for området 10 - 20% av nominell: ±25%
                       20 - 40% av nominell: <±10%
                       40 - 100% av nominell: <±4%
Ved T-rør situasjon anbefales en avstand på minst 5 x ØD for å opprettholde samme målenøyaktighet.

Ventilfronten kan leveres med integrert bevegelsesføler eller bevegelse/temperaturføler. Bevegelse/temperaturføler skal kun brukes sammen med X-AIRCONTROL.
Produktblad for bevegelsesføler og bevegelse/temperaturføler finner du ved å følge denne linken:
www.trox.no/downloads/9434cbb5430242a0/Orion-X-Sense.
pdf?type=product_info

✷ UTFØRELSE

Orion-LØV med Sirius er utført som en komplett måle- og regulerings-enhet for behovsstyring av luftmengder i ventilasjonsanlegget. Måle-stasjonen måler differansetrykk via målestaver integrert i enheten.
Sirius er utstyrt med LHV-D3 VAV-regulator fra Belimo. Regulatorens spesifikasjoner finnes i tabellen nedenfor.
Komplett teknisk dokumentasjon kan lastes ned fra www.belimo.eu.
Orion-LØV med Sirius har demonterbar frontplate med LØV-perforering og kan leveres tilpasset forskjellige typer himlingssystemer.

Motor	LHV-D3-MP / MOD/BACnet / LON
Driftsspenning	AC 24 V 50/60 Hz, DC 24 V
Effektforbruk	2,5W
Dim effekt	4.5VA (max.8 A @5 ms)

Tabell 1, Teknisk-spesifikasjon, Belimo VAV-regulator

⬇ MATERIALE OG OVERFLATEBEHANDLING

Sirius er utført i galvanisert stål. Målekrysset er i aluminium, slanger og nipler er i plast. Spjeldet har påmontert polyester duk.
Anslutning har EPDM-gummipakning.

🛒 BESTILLINGSKODE, ventil-Orion-LØV Sirius

```
Orion-LØV-Sirius  –  TA  –  B  –  200  /  0
```

Produkt:

SL=Spesiallakk

Systemhimling:
TA=A-Kant
DC=Dampa Clip-In
DG=Dg-kant
DS=Ds-kant
EK 24=E-kant-T24
EK 15=E-kant-T15
X=X-kant

Dim:
Ø200
Ø250
Ø315
Ø400

Sensorvalg:
B=Bevegelse
BT1=Bevegelse og
     temperatur
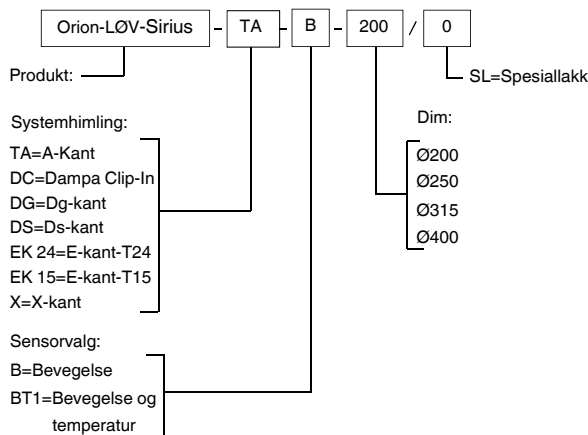
Eksempel:
Orion-LØV-Sirius-TA-B-200/0
Forklaring:
Orion-LØV-Sirius tilluftsventil med knekkekant A for T-profilhimling,
bevegelsessensor i ventilfront, anslutning ventil Ø200

🛒 BESTILLINGSKODE, Sirius

```
Sirius - 125-200 - 0 - 1- 0
```

Produkt:

MS = Merkeskjema

Dim:
125 - 200
160 - 250
200 - 315
250 - 400

Plugg:
0 = Uten plugg
1 = Wago 4 pol. Midi, Grå*
2 = Wago 4 pol. Midi, Grønn**

* = Kun for motorvalg 0
** = Kun for motorvalg 3,4,7

Tilkobling:
0 = Belimo MP-Bus
2 = Belimo LON-Bus
3 = Belimo MOD-Bus
4 = Belimo BACnet
7 = Belimo KNX
8 = MOD-Bus for XAC
9 = XAC-ZM MOD-Bus
9.1 = XAC-ZM MOD-Bus
     m/lysrele
9.2 = XAC-ZM MOD-Bus
     m/varme-kjølerele
9.3 = XAC-ZM MOD-Bus
     m/lys, varme-kjølerele
9.4 = XAC-ZM MP-Bus

Eksempel:
Sirius-125-200-0-1-0
Forklaring:
Sirius med innløp Ø125 og utløp Ø200, med Belimo MP-Bus, Wago-plugg påmontert,
uten merkeskjema.

Orion-LØV med Sirius
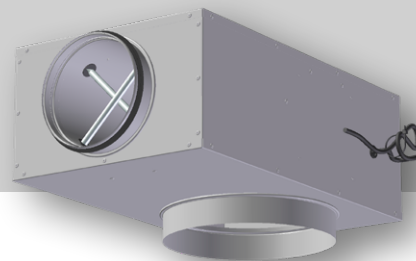
HURTIGVALG, Orion-LØV med Sirius

Sirius dim	[åpen] m³/h		
	25dB(A)	30dB(A)	35dB(A)
125	155	184	220
160	256	310	374
200	374	446	529
250	526	626	749

Sirius dim	(75Pa) m³/h		
	25dB(A)	30dB(A)	35dB(A)
125	144	184	220
160	234	295	374
200	367	443	529
250	342	569	734

Tabell 2, Hurtigvalgtabell Orion-LØV med Sirius

Sirius ØD.	(m³/h)	
	Minimum	Maksimum
125	26	265
160	43	434
200	70	700
250	106	1060

Tabell 3, Reguleringsområde for vav-regulator, luftmengde i m³/h. Se dimensjoneringsdiagram for lydeffekt og trykktap.

MÅL OG VEKT, Orion-LØV med Sirius

| Dim.	D	DA	B	H	L	L1	Vekt Sirius [kg]	Vekt Sirius med ventil [kg]
125-200	124	202	325	175	645	386	8	12
160-250	159	252	360	210	645	402	9	13
200-315	199	317	400	240	645	435	10,5	14,5
250-400	249	402	450	290	645	392	12	16

Tabell 4
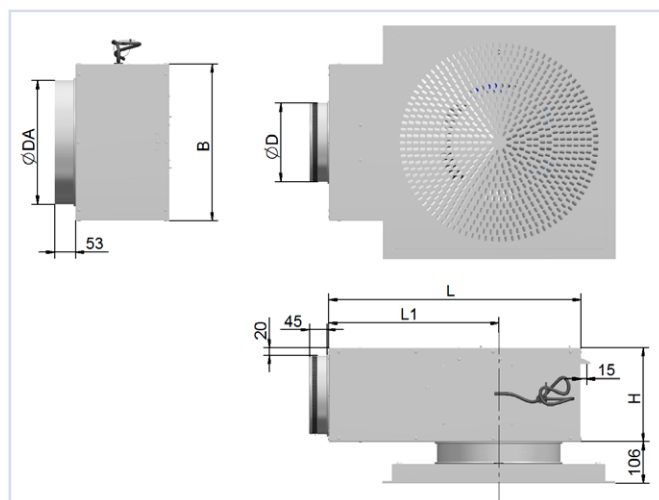
Figur 1, Målskisse Orion-LØV med Sirius

Orion-LØV med Sirius
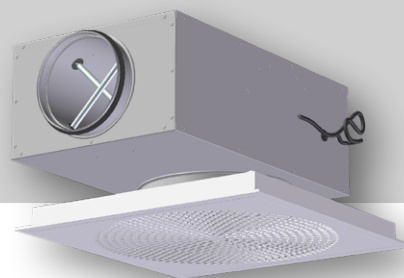
AKUSTISK DOKUMENTASJON

I diagrammene er det oppgitt summert A-veid lydeffektnivå fra ventil, L_{WA}. Korreksjonsfaktorene i tabell 5 på side 5 benyttes for å beregne avgitt frekvensfordelt lydeffektnivå, $L_W = L_{WA} + KO$. Lydtrykknivå i et rom med absorpsjon tilsvarende 10m² Sabine vil være 4 dB lavere enn avgitt lydeffektnivå.

Eksempel:
Sirius 125 med Orion-LØV tilluftventil, ønsket luftmengde 50 l/s.
Av diagram 1 finner vi at L_{WA} = 29dB(A) ved åpent spjeld og 45 Pa totaltrykktap. Vi ønsker å finne følgende data:

a) Avgitt lydeffektnivå i 250 Hz.

b) A-veid, samlet lydtrykknivå fra ventilen i et kontor med 4dB romdempning.

c) A -veid lydtrykknivå i et kontor ved 75 Pa totaltrykktap, dvs. 30 Pa struping over enhetens spjeld.

a) Korreksjonsfaktoren for 250 Hz er -2 dB. Avgitt lydeffekt i 250 Hz blir da: $L_W = L_{WA} + KO = 29 + (-2) = 27$ dB

b) Med 4dB romdempning blir A-veid lydtrykknivå:
29 - 4 = 25 dB(A)

c) Ved driftspunkt 50l/s og 75Pa totaltrykktap i diagrammet avleses 29dB(A). Med 4dB romdempning får vi lydtrykknivået: 29-4=25dB(A)

DIMENSJONERINGSDIAGRAM.

Diagram 1, Orion-LØV m/Sirius Ø125

Diagram 2, Orion-LØV m/Sirius Ø160

Diagram 3, Orion-LØV m/Sirius Ø200

Diagram 4, Orion-LØV m/Sirius Ø250
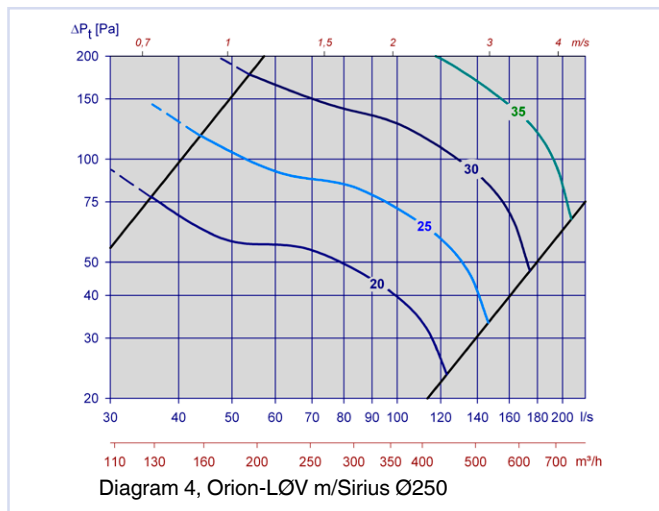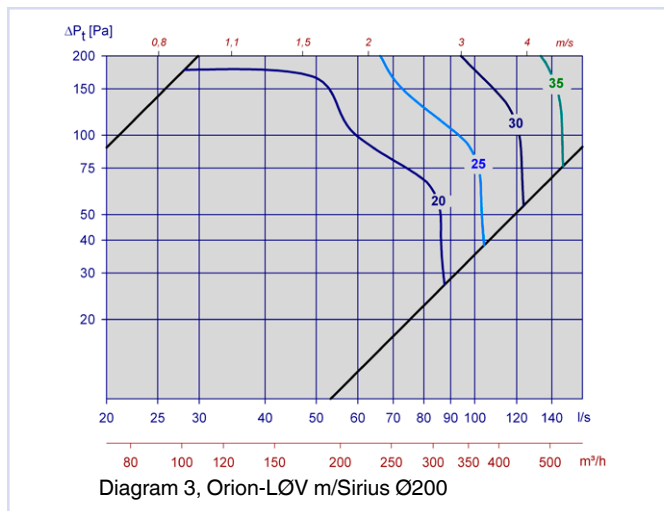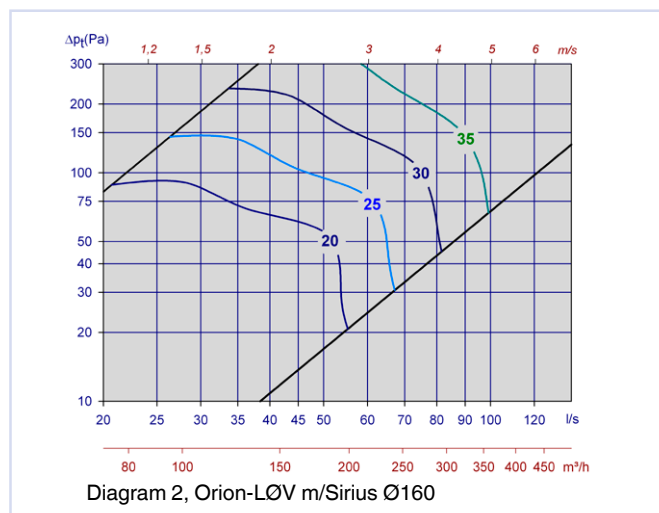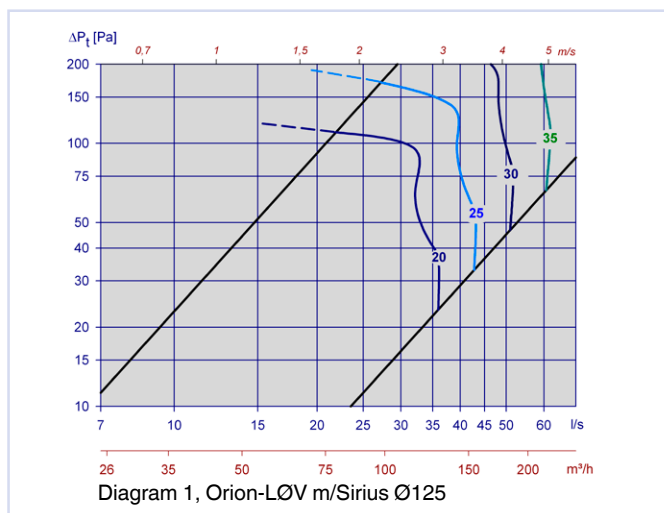
Orion-LØV med Sirius
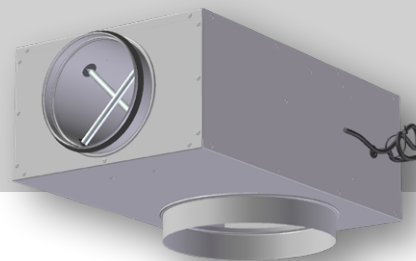
KO [dB]																
	Høyre trykktapslinje (åpent)								Venstre trykktapslinje (mye strupt)							
Sirius dim.	63	125	250	500	1κ	2κ	4κ	8κ	63	125	250	500	1κ	2κ	4κ	8κ
125	4	-1	-2	-1	-6	-11	-15	-11	2	-3	-4	-9	-6	-6	-8	-9
160	2	1	0	-1	-8	-13	-13	-9	1	-1	-3	-6	-4	-11	-11	-9
200	2	1	-2	-1	-6	-12	-14	-10	1	0	-3	-5	-5	-9	-9	-9
250	3	2	-1	-1	-7	-13	-13	-10	2	2	-1	-3	-6	-11	-10	-9

Tabell 5, KO-faktor Orion-LØV med Sirius

KASTELENGDE

Diagram 5, Orion-LØV med Sirius-Kastelengde
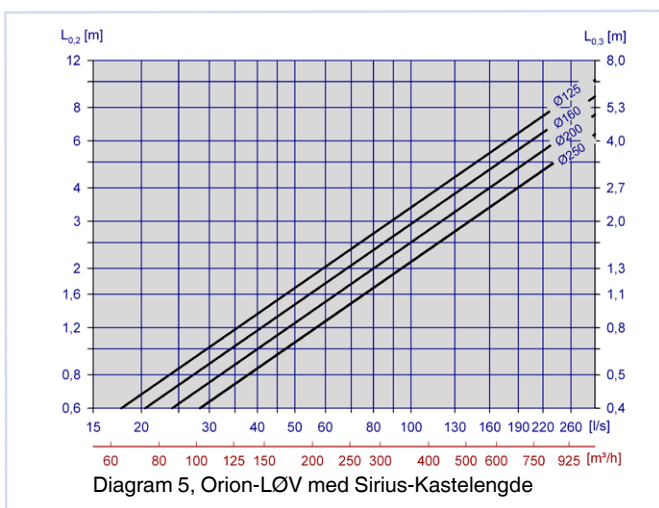
SPREDNINGSMØNSTER
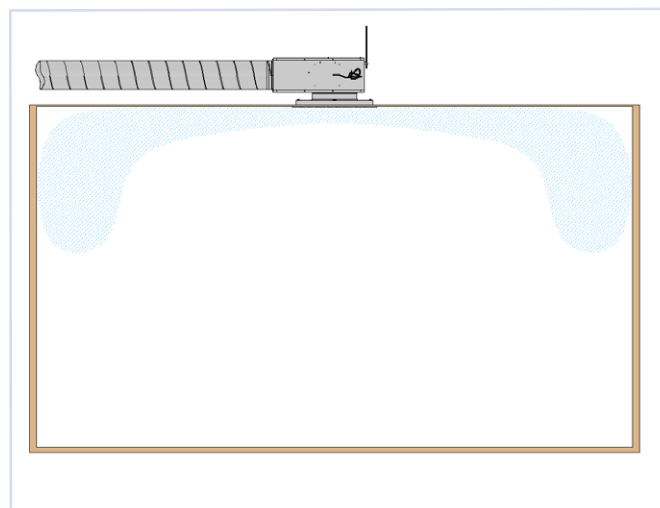
Figur 2, Spredningsbilde Orion LØV

Orion-LØV med Sirius	Demping [dB]							
Dim.	63	125	250	500	1k	2k	4k	8k
125	14	11	12	12	18	11	14	15
160	12	9	12	11	16	10	14	15
200	10	8	11	12	15	12	12	14
250	8	7	11	12	13	13	13	14

Tabell 6, Statisk lyddemping inkl. enderefleksjon, Orion-LØV med Sirius
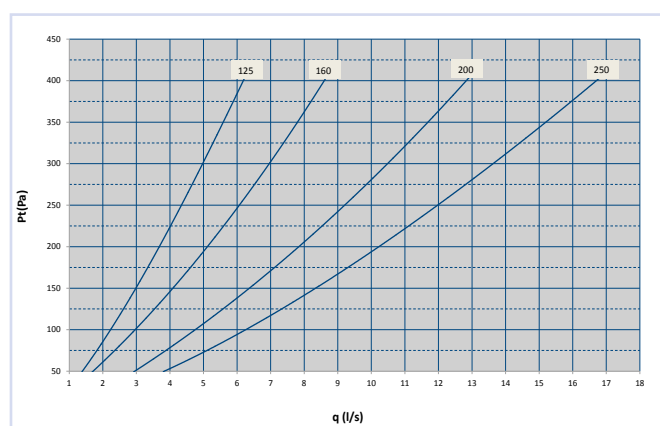
Figur 3, Lekkasjemengde Sirius ved stengtspjeld

Orion-LØV med Sirius

🔥 MONTERING

Ventilen Orion-LØV kan monteres i forskjellige typer systemhimlinger eller i fast himling. På Sirius benyttes opphengsbrakett i bakkant med gjengestang eller bånd, se figur 5. For å opprettholde enhetens målenøyaktighet er det viktig at den monteres med avstander som vist i figur 6.

A-kant | Dampa Clip-In | Dg-kant

Ds-kant | E-kant |

T24/T15 | Fast tak

X-kant
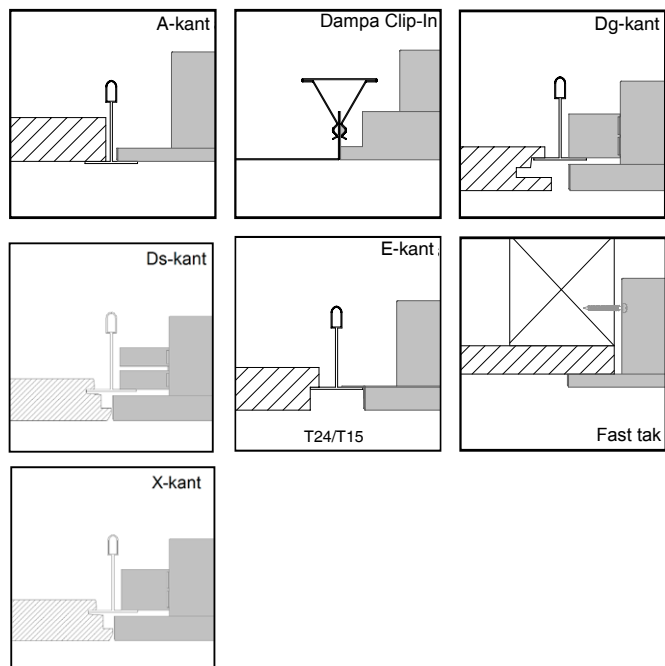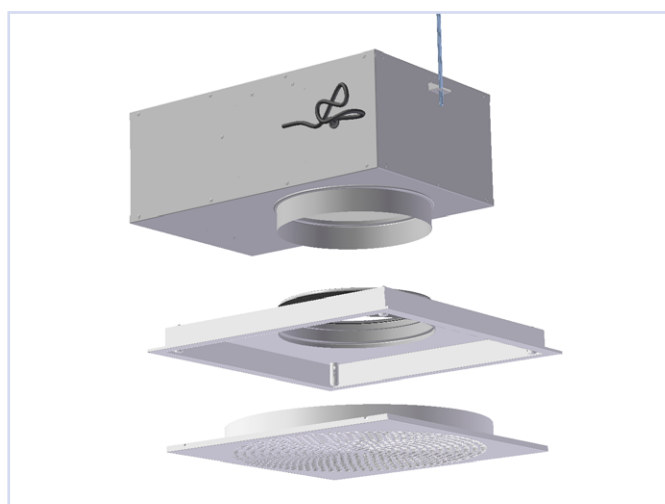
Figur 4, Montasje

🔢 INNREGULERING

Orion LØV med sirius benytter Belimo PC-Tool eller ZTH-GEN for å gjøre de nødvendige innstillingene.

💬 VEDLIKEHOLD

Det er ingen spesielle krav til vedlikehold.

✳ MILJØ

Forespørsel vedrørende byggvaredeklarasjon kan rettes til en av våre selgere, eller finnes på vår hjemmeside: www.trox.no

Figur 5, Montasje

Min 5 x Dia
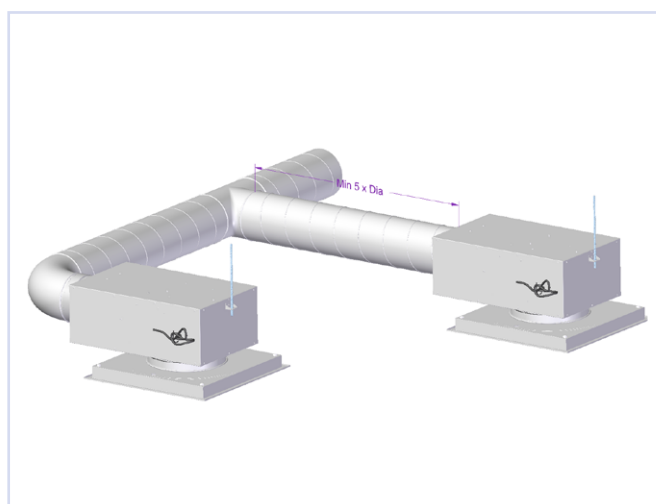
Figur 6, Montasje

Orion-LØV med Sirius er utviklet og produsert av:

Rett til endringer forbeholdes.

C.3 LVC VAV damper

LVC

VAV-regulator
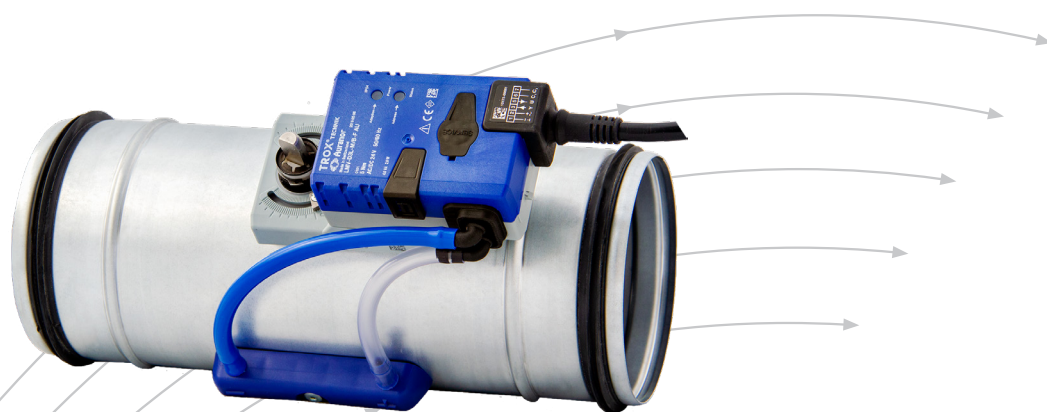
- Reguleringsområde fra 0,4 til 6 m/s
- Dimensjoner fra Ø125 - Ø250.
- Kan monteres direkte i avgrening og bend.
- Kun 310 mm byggelengde for alle dimensjoner
- Muligheter for Belimo MP-Bus, MOD/BACnet og KNX.

TROX® TECHNIK

Auranor

LVC

⊞ ANVENDELSE

LVC er en volumregulator som fungerer uavhengig av kanaltrykket, og som regulerer til ønsket luftmengde på grunnlag av styresignal.
Ønsket luftmengde blir eksempelvis gitt som et 0-10V signal fra romregulator, eller som digitalt buss-signal fra automatikksystem.
Innstilling av ønsket minimum og maksimum luftmengder kan gjøres på fabrikk, eller etter montasje, ved hjelp av serviceverktøy fra Belimo.
LVC er beregnet for komfortventilasjon med temperaturforhold mellom 10°C og 50°C og relativ fuktighet mellom 5 % og 95 % uten kondensering.

✸ UTFØRELSE

LVC er utført som en komplett måle- og reguleringsenhet for behovsstyring av luftmengder i ventilasjonsanlegg.
Målestasjonen måler differansetrykk via en dyse integrert i enheten.
LVC overholder tetthetsklasse 2 med spjeldblad i lukket stilling, og klasse C for lekkasje til omgivelsene, i henhold til EN 1751. Hygienekrav er i samsvar med VDI 6022.
LVC er utstyrt med VAV-regulator fra Belimo, type LMV-D3L-FK.1 AU.
Regulatorenes spesifikasjoner finnes i tabell 1.
Teknisk dokumentasjon for LMV-D3 MP/MOD/KNX kan lastes ned på www.belimo.eu

⊞ FUNKSJON

LVC baserer seg på dynamisk måling av luftmengde, og regulerer spjeldstillingen slik at ønsket luftmengde opprettholdes. Når det skjer en endring i kanaltrykket, for eksempel ved at andre volumregulatorer på grenen åpner eller stenger, vil LVC kompensere ved å justere på spjeldet inntil ønsket mengde igjen er oppnådd.
Siden enheten benytter trykkfall over spjeldblad som måletrykk, vil minimum luftmengde bli påvirket av spjeldbladets posisjon. Ved åpent spjeld er minimum lufthastighet ved 0,6 m/s. Ved nedregulert spjeld kan minimum lufthastighet reduseres til ca. 0,4 m/s

▤ MATERIALE OG OVERFLATEBEHANDLING

LVC sarg er produsert i galvanisert stål. Dyse, spjeldblad og opplagring i ABS plast, UL 90 flammehemmende (V-0)
Spjeldpakning er produsert av TPV (plast). Anslutningen på LVC har EPDM-gummipakning.

🛒 BESTILLINGSKODE, LVC

LVC - 0 - 1 - 160 - 0

Produkt:

Motorvalg:
0 = Belimo MP-Bus
3 = Belimo MOD-Bus
4 = Belimo BACnet
7 = Belimo KNX

MS = Merkeskjema
Dimensjon: Ø125 – Ø250

Plugg:
0 = Uten plugg
1 = Wago 4. Pol Midi, Grå*
2 = Wago 4. Pol Midi, Grønn**

* Kun for motorvalg 0
** Kun for motorvalg 3,4,7

Eksempel:
LVC-0-1-160-0
Forklaring:
LVC, med Belimo MP-Bus, Wago-plugg påmontert, dim Ø160, uten merkeskjema.
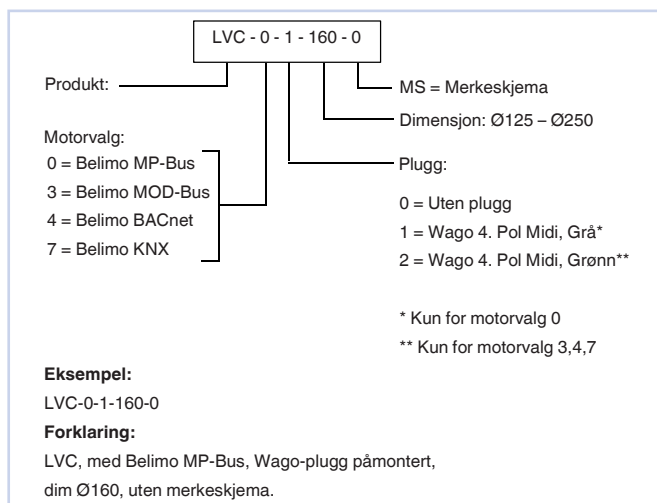
Tekniske data	
Dimensjon	125 - 250 mm
Luftmengdeområde	8 - 300 l/s eller 30 - 1080 m³/h
Luftmengde reguleringsområde	Ca. 10 til 100% av den nominelle luftmengden
Minimum differansetrykk	5 - 30 Pa
Maksimum differansetrykk	600 Pa
Driftstemperatur	10 - 50 ºC

Tabell 1, Teknisk-spesifikasjon, LVC

VAV-regulator	LMV-D3L-MP/MOD/BACnet/KNX
Driftsspenning	AC 24 V 50/60 Hz, DC 24 V
Effektforbruk	2W
Dim. effekt	4 VA (max. 8A @5 ms)

Tabell 2, Teknisk-spesifikasjon, Belimo VAV-regulator

⚖ MÅL OG VEKT

Dim.	ØD	Vekt
	mm	kg
125	124	1,5
160	159	1,9
200	199	2,1
250	249	2,7

Tabell 3, Mål og vekt

LVC
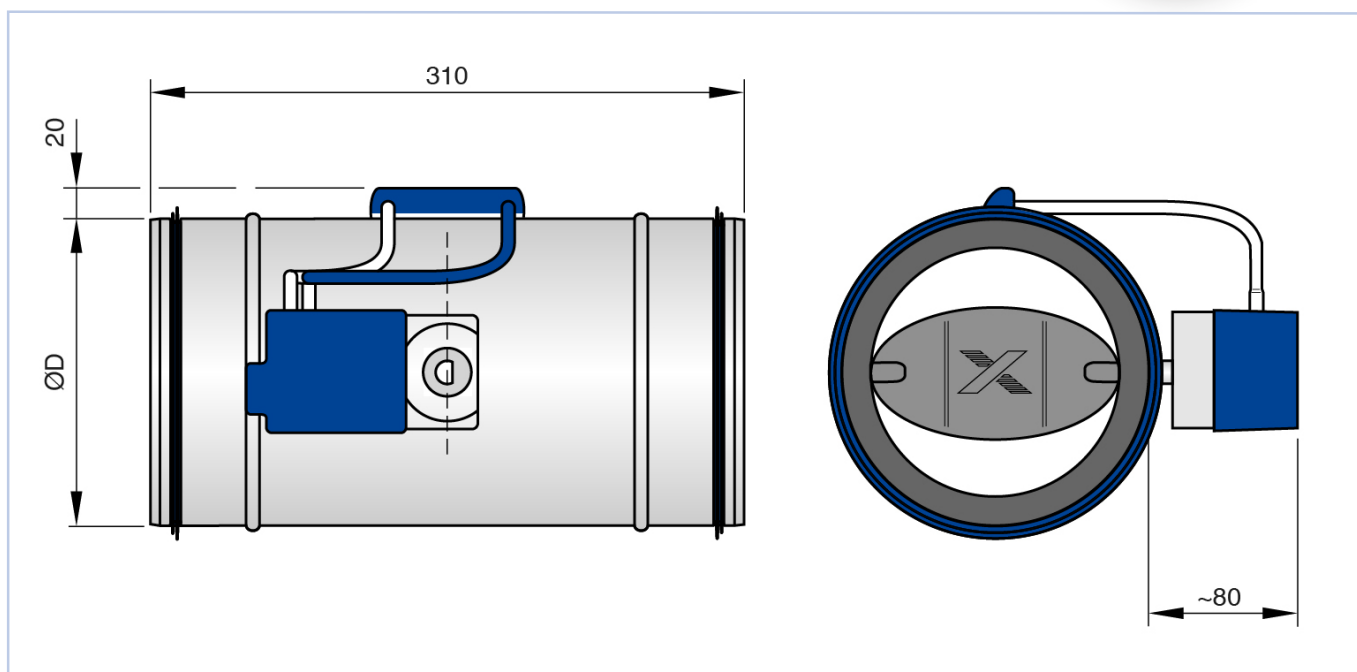
Figur 1, Målskisse

 HURTIGVALG

Dim.	$\dot{V}$		ΔPst min	Δ$\dot{V}$
	l/s	m³/h	Pa	± %
125	8	29	5	15
	30	108	5	12
	55	195	16	8
	75	270	30	5
160	12	43	5	15
	50	180	5	12
	85	306	15	8
	120	432	30	5
200	20	72	5	15
	75	270	5	12
	135	486	15	8
	190	684	30	5
250	30	108	5	15
	120	432	5	12
	210	756	15	8
	300	1080	30	5

Tabell 4. LVC - luftmengdeområde, differansetrykk og målenøyaktighet ved åpent spjeld.

LVC

🔊 AKUSTISK DOKUMENTASJON

LVC, lydtrykknivå ved 50 Pa differansetrykk

Dim.	$\dot{V}$	$\dot{V}$	Generert støy til kanalen			Flankestøy
			1	2	3	
			L_{PA}	L_{PA1}		L_{PA2}
	l/s	m³/h	dB(A)			
125	8	29	27	<15	<15	<15
	30	108	35	24	17	17
	55	198	39	30	24	21
	75	270	42	34	28	23
160	12	43	29	19	<15	<15
	50	180	34	26	23	19
	85	306	36	28	23	22
	120	432	38	31	26	24
200	20	72	31	21	<15	<15
	75	270	35	26	19	19
	135	486	36	28	22	22
	190	684	36	28	23	24
250	30	108	31	24	18	17
	120	432	36	28	22	25
	210	756	36	28	22	28
	300	1080	36	29	23	31

Tabell 5,   *1. LVC*
2. LVC med lyddemper LEV-500
3. LVC Med lyddemper LEV-1000

LVC

MONTERING

Tilstrekkelig serviceavstand må avsettes for igangkjøring og vedlikehold. Ved behov må inspeksjonsluker monteres. Det anbefales å montere LVC med minimum serviceavstand i henhold til figur 4. For best regulering bør spjeldblad/spjeldaksling følge (være parallell med) retningsendring i bend eller avgrening. Se figur 2 og figur 3.
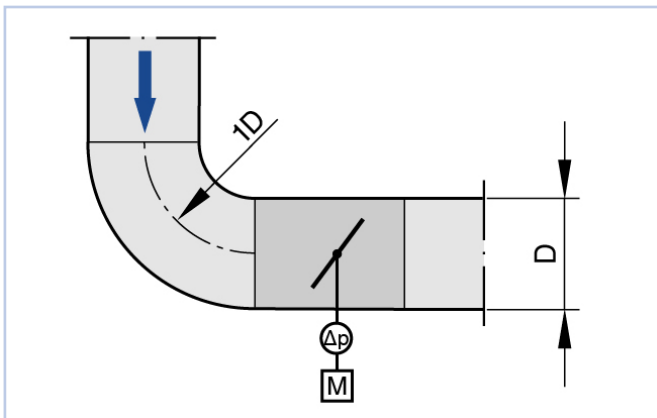
Figur 2, LVC montert direkte i bend.

Figur 3, LVC montert direkte i avgreining.

Serviceavstand min. 100 mm.

Figur 4, montasje

INNREGULERING

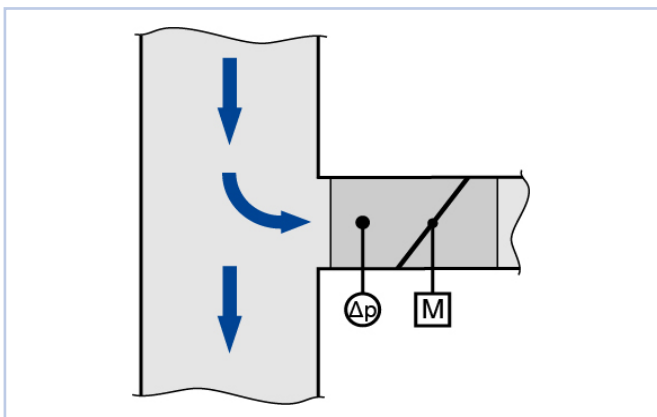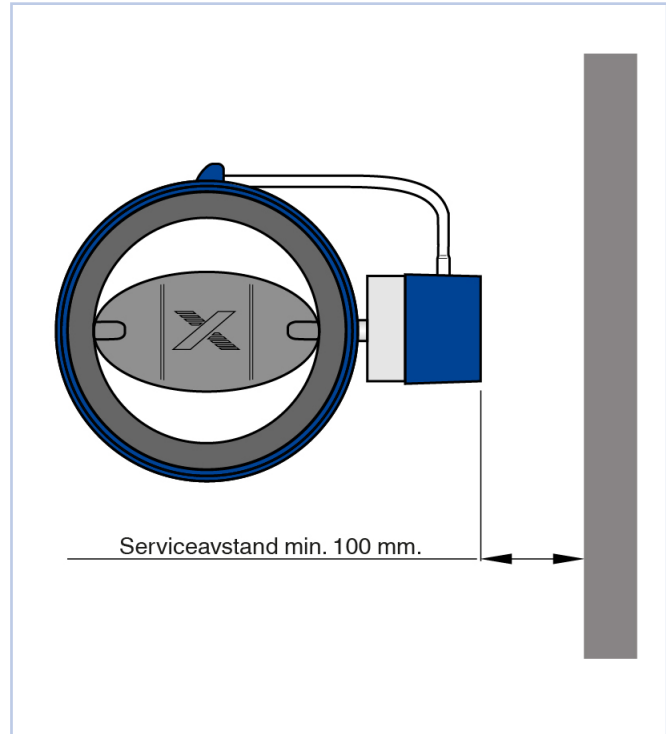Ved innregulering og service benyttes pc-programmet Belimo PC-Tool. Med dette serviceverktøyet kan regulatoren stilles inn til b.l.a. ønskede minimum og maksimum luftmengde, 0-10 V eller 2-10 V styresignal og Open-loop. Det kan også kjøres funksjons tester som kan vises grafisk for dokumentasjon av regulatorens funksjon. Det finnes også service-verktøy som ikke krever PC, Belimo ZTH-VAV.
For mer informasjon, se www.belimo.eu eller kontakt en av våre selgere. Spjeldblad er fabrikkinnstilt til åpen posisjon.

VEDLIKEHOLD

Hvis enheten benyttes som avtrekksspjeld kan det være behov for rengjøring av målestasjon med jevne mellomrom. Dette er avhengig av type rom og rengjøringskvaliteten. Kontroll hvert år eller hvert 2. år er å anbefale

MILJØ

Forespørsel vedrørende byggvaredeklarasjon kan rettes til en av våre selgere, eller finnes på vår hjemmeside: www.trox.no

Leo er utviklet og produsert av:

Rett til endringer forbeholdes.

TROX® TECHNIK

Auranor

Hovedkontor:
TROX Auranor Norge AS, Postboks 100, 2712 Brandbu
Telefon: 61 31 35 00   Telefaks: 61 31 35 10   **www.trox.no**

C.4 Recirculation filter F9

Camfil posefilter 2019

ALLE PRISER ER VEIL.UTSALG EKSKL. MVA, AB LAGER. RETT TIL PRISFORANDRING FORBEHOLDES UTEN VARSEL.

Hi-Flo II XLT

Varenr.	Type	Kvalitet-Dim. (BxHxD)-Poser	ISO16890	Pris
610151	Hi-Flo II XLT 6	HFGX-M6-287/592/370-5	ePM2.5 50%	621
610160	Hi-Flo II XLT 7	HFGX-F7-287/592/370-5	ePM1 60%	651
610158	Hi-Flo II XLT 6	HFGX-M6-287/287/640-5	ePM2.5 50%	657
610167	Hi-Flo II XLT 7	HFGX-F7-287/287/640-5	ePM1 60%	671
610176	Hi-Flo II XLT 9	HFGX-F9-287/287/640-5	ePM1 85%	744
610155	Hi-Flo II XLT 6	HFGX-M6-287/287/520-5	ePM2.5 50%	571
610164	Hi-Flo II XLT 7	HFGX-F7-287/287/520-5	ePM1 60%	547
610173	Hi-Flo II XLT 9	HFGX-F9-287/287/520-5	ePM1 85%	682
610152	Hi-Flo II XLT 6	HFGX-M6-287/287/370-5	ePM2.5 50%	499
610161	Hi-Flo II XLT 7	HFGX-F7-287/287/370-5	ePM1 60%	482
610952	Hi-Flo II XLT 6	HFGX-M6-592/287/640-10	ePM2.5 50%	970
610958	Hi-Flo II XLT 7	HFGX-F7-592/287/640-10	ePM1 60%	1086
610960	Hi-Flo II XLT 9	HFGX-F9-592/287/640-10	ePM1 85%	1143
610951	Hi-Flo II XLT 6	HFGX-M6-592/287/520-10	ePM2.5 50%	867
610957	Hi-Flo II XLT 7	HFGX-F7-592/287/520-10	ePM1 60%	958
610959	Hi-Flo II XLT 9	HFGX-F9-592/287/520-10	ePM1 85%	1005
610950	Hi-Flo II XLT 6	HFGX-M6-592/287/370-10	ePM2.5 50%	744
610956	Hi-Flo II XLT 7	HFGX-F7-592/287/370-10	ePM1 60%	810
612792	Hi-Flo II XLT 6	HFGX-M6-592/490/640-10	ePM2.5 50%	1316
612795	Hi-Flo II XLT 7	HFGX-F7-592/490/640-10	ePM1 60%	1401
612798	Hi-Flo II XLT 9	HFGX-F9-592/490/640-10	ePM1 85%	1613
612793	Hi-Flo II XLT 6	HFGX-M6-592/490/520-10	ePM2.5 50%	1159
612796	Hi-Flo II XLT 7	HFGX-F7-592/490/520-10	ePM1 60%	1226
612799	Hi-Flo II XLT 9	HFGX-F9-592/490/520-10	ePM1 85%	1361
612794	Hi-Flo II XLT 6	HFGX-M6-592/490/370-10	ePM2.5 50%	967
612797	Hi-Flo II XLT 7	HFGX-F7-592/490/370-10	ePM1 60%	1015
612800	Hi-Flo II XLT 6	HFGX-M6-490/490/640-8	ePM2.5 50%	1104
612803	Hi-Flo II XLT 7	HFGX-F7-490/490/640-8	ePM1 60%	1172
612806	Hi-Flo II XLT 9	HFGX-F9-490/490/640-8	ePM1 85%	1348
612801	Hi-Flo II XLT 6	HFGX-M6-490/490/520-8	ePM2.5 50%	977
612804	Hi-Flo II XLT 7	HFGX-F7-490/490/520-8	ePM1 60%	1029
612807	Hi-Flo II XLT 9	HFGX-F9-490/490/520-8	ePM1 85%	1179
612802	Hi-Flo II XLT 6	HFGX-M6-490/490/370-8	ePM2.5 50%	825
612805	Hi-Flo II XLT 7	HFGX-F7-490/490/370-8	ePM1 60%	863

Appendix D

Risk analysis

D.1   Hazardous activity identification proocess

Following is the risk analysis related to the work conducted in the laboratory. The work included installation of ventilation ductwork, and construction of the inner walls in the full-scale laboratory model.

Unit: *Department of Energy and Process Engineering*

Line manager: Morten Grønli

Participants in the identification process (including their function): **Hans Martin Mathisen (supervisor), Jørgen Tonning Buch (student), Maria Justo Alonso (co-supervisor)**

Date: 06.05.2021

Short description of the main activity/main process: Master project for student Jørgen Tonning Buch. "Control and optimization of ventilation in Zero emission buildings using IoT".

Is the project work purely theoretical? (YES/NO): NO

Answer "YES" implies that supervisor is assured that no activities requiring risk assessment are involved in the work. If YES, briefly describe the activities below. The risk assessment form need not be filled out.

Signatures: Responsible supervisor: *[signature]*   Student: *[signature]*

ID nr.	Activity/process	Responsible person	Existing documentation	Existing safety measures	Laws, regulations etc.	Comment
1	Climbing in ladder in the labaratory	Jørgen Tonning Buch		Use a step-ladder if available. Use with caution		
2	Use of power tools	Jørgen Tonning Buch		Use safety googles , hearing protection and gloves		

Risk assessment

	Prepared by	Number	Date
	HSE section	HMSRV2603E	04.02.2011
	Approved by		Replaces
	The Rector		01.12.2006

Date:

Unit: *(Department)*

Line manager:

Participants in the identification process (including their function):

Short description of the main activity/main process: Master project for student Jørgen Tonning Buch. Project title.

Signatures: *Responsible supervisor:* [signature]   *Student:*

Activity from the identification process form	Potential undesirable incident/strain	Likelihood:	Consequence:			Risk Value (human)	Comments/status Suggested measures
		Likelihood (1-5)	Human (A-E)	Environment (A-E)	Economy/ material (A-E)		
Use of power tools	Cut	2	C	A	A	C2	Use with caution. Use safety googles and hearing protection.
Climbing in ladder	Falling	2	B	A	A	B2	Use with caution. Use step-ladder instead leaning ladder into the wall.

Likelihood, e.g.:
1. Minimal
2. Low
3. Medium
4. High
5. Very high

Consequence, e.g.:
A. Safe
B. Relatively safe
C. Dangerous
D. Critical
E. Very critical

Risk value (each one to be estimated separately):
Human = Likelihood x Human Consequence
Environmental = Likelihood x Environmental consequence
Financial/material = Likelihood x Consequence for Economy/materiel

Risk assessment

	Prepared by	Number	Date
	HSE section	HMSRV2603E	04.02.2011
	Approved by	Replaces	
	The Rector		01.12.2006

Potential undesirable incident/strain

Identify possible incidents and conditions that may lead to situations that pose a hazard to people, the environment and any materiel/equipment involved.

Criteria for the assessment of likelihood and consequence in relation to fieldwork

Each activity is assessed according to a worst-case scenario. Likelihood and consequence are to be assessed separately for each potential undesirable incident. Before starting on the quantification, the participants should agree what they understand by the assessment criteria:

Likelihood

Minimal	Low	Medium	High	Very high
1	2	3	4	5
Once every 50 years or less	Once every 10 years or less	Once a year or less	Once a month or less	Once a week

Consequence

Grading	Human	Environment	Financial/material
E Very critical	May produce fatality/ies	Very prolonged, non-reversible damage	Shutdown of work >1 year.
D Critical	Permanent injury, may produce serious serious health damage/sickness	Prolonged damage. Long recovery time.	Shutdown of work 0.5-1 year.
C Dangerous	Serious personal injury	Minor damage. Long recovery time	Shutdown of work < 1 month
B Relatively safe	Injury that requires medical treatment	Minor damage. Short recovery time	Shutdown of work < 1week
A Safe	Injury that requires first aid	Insignificant damage. Short recovery time	Shutdown of work < 1day

The unit makes its own decision as to whether opting to fill in or not consequences for economy/materiel, for example if the unit is going to use particularly valuable equipment. It is up to the individual unit to choose the assessment criteria for this column.

Risk = Likelihood x Consequence

Please calculate the risk value for "Human", "Environment" and, if chosen, "Economy/materiel", separately.

About the column "Comments/status, suggested preventative and corrective measures":

Measures can impact on both likelihood and consequences. Prioritise measures that can prevent the incident from occurring; in other words, likelihood-reducing measures are to be prioritised above greater emergency preparedness, i.e. consequence-reducing measures.

NTNU			Risk matrix	prepared by	Number	Date
				HSE Section	HMSRV2604	8 March 2010
HSE/KS				approved by	Page	Replaces
				Rector	4 of 4	9 February 2010

MATRIX FOR RISK ASSESSMENTS at NTNU

CONSEQUENCE		LIKELIHOOD				
		Very low	Low	Medium	High	Very high
Extremely serious		E1	E2	E3	E4	E5
Serious		D1	D2	D3	D4	D5
Moderate		C1	C2	C3	C4	C5
Minor		B1	B2	B3	B4	B5
Not significant		A1	A2	A3	A4	A5

Principle for acceptance criteria. Explanation of the colours used in the risk matrix.

Colour		Description
Red		Unacceptable risk. Measures must be taken to reduce the risk.
Yellow		Assessment range. Measures must be considered.
Green		Acceptable risk Measures can be considered based on other considerations.